

NONLINEAR STATIC ANALYSIS OF COMPOSITE DRIVE SHAFT OF MEDIUM UTILITY VEHICLE TO EVALUATE EFFECT OF NONLINEAR PARAMETERS

Mr. Jamir A. Mulani¹, Prof. Dr. S.H.Sawant²

*¹PG Student, ²Professor, Department of Mechanical Engineering,
Dr. J.J. Magdum College of Engineering, Jaysingpur (India)*

ABSTRACT

In this paper numerical static analysis of composite drive shaft is carried out to find out effect of nonlinearities. For Linear and Nonlinear Finite Element Analysis ANSYS software is used. Experimental set up is developed in order to find out Torque-Angular Displacement characteristics of Composite drive shaft. Torque-Angular Displacement characteristics are studied in order to find out torsional stiffness of drive shaft and to evaluate nonlinearities present in composite drive shaft. The present work deals with the numerical analysis of composite drive shaft with nonlinear parameters. In this paper Material and Geometric nonlinearities are considered.

Keywords: ANSYS, Composite Drive Shaft, E-Glass/Epoxy, Nonlinearity.

I INTRODUCTION

Drive shafts as power transmission tubing are used in many applications, including cooling towers, pumping sets, aerospace, trucks and automobiles. In metallic shaft design, knowing the torque and the allowable shear stress for the material, the size of the shaft's cross section can be determined. Polymer matrix composites such as carbon/epoxy or glass/epoxy offer better fatigue characteristics because micro cracks in the resin do not freely propagate as in metals, but terminate at the fibers. Generally, composites are less susceptible to the effects of stress concentration, such as are caused by notches and holes, compared with metals [1]. An efficient design of composite drive shaft could be achieved by selecting the proper variables, which are specified to minimize the chance of failure and to meet the performance requirements. In the optimal design of the drive shaft, these variables are constrained by the lateral natural frequency, torsional vibration, torsional strength and torsional buckling of the shaft [2].

Composite materials consist of two or more physically dissimilar and instinctively separable components called reinforcement and matrix. These two components can be mixed in a restricted way to achieve optimum properties, which are superior to the properties of each individual component. Composite materials have

been widely used in automobile industry because of its high strength and modulus to weight ratio, low cost and flexibility in material and structure design.

CAE tools are widely used in the automotive industries. In fact, their use has enabled the automakers to reduce product development cost and time while improving the safety, comfort, and durability of the vehicles they produce. The predictive capability of CAE tools has progressed to the point where much of the design verification is now done using computer simulation rather than physical prototype testing. CAE dependability is based upon all proper assumptions as inputs and must identify critical inputs. Even though there have been many advances in CAE and it is widely used in the engineering field, physical testing is still used as a final confirmation for subsystems due to the fact that CAE cannot predict all variables in complex assemblies, therefore the validation of CAE results is important [2].

In this analysis the material of composite drive shaft is Aluminum-E- Glass Epoxy. There are four layers of material lay up by following way:

The E Glass Epoxy is also type of fiber, SiO₂ 54wt%, Al₂O₃ 14wt%, CaO+MgO 22wt%, B₂O₃ 10wt%, Na₂O+K₂O less than 2wt%. The properties of E-Glass Epoxy material used for the analysis are as follows:

II MATERIAL PROPERTIES E-GLASS EPOXY

Sr. No.	Property	Value
1	Tensile Modulus Along X-Direction	34000MPa
2	Tensile Modulus Along Y-Direction	6530MPa
3	Tensile Modulus Along Z-Direction	6530MPa
4	Tensile Strength of Material	900MPa
5	Compressive Strength of Material	450MPa
6	Shear Modulus Along XY-Direction	2433MPa
7	Shear Modulus Along YZ-Direction	1698MPa
8	Shear Modulus Along ZX-Direction	2433MPa
9	Poisson Ratio Along XY-Direction	0.217
10	Poisson Ratio Along YZ-Direction	0.0366
11	Poisson Ratio Along ZX-Direction	0.217
12	Mass Density	2.6*10 ⁻³ Kg/mm ³
13	Flexural Modulus	40000MPa
14	Flexural Strength	1200MPa

III NUMERICAL ANALYSIS

The Finite Element Method (FEM) is practical application often known as Finite Element Analysis (FEA) is a numerical technique for finding approximate solutions of partial differential equations (PDE) as well as of integral equations. Finite Element Analysis is a simulation technique which evaluates the behavior of components, equipment and structures for various loading conditions including applied forces, pressures and temperatures. Thus, a complex engineering problem with non-standard shape and geometry can be solved using finite element analysis where a closed form solution is not available. The finite element analysis methods result in the stress distribution, displacements and reaction loads at supports etc. for the model. The three dimensional model of spring is drawn in CATIA V5 R16 environment. This geometry is imported to ANSYS environment. 20 node hexahedral element SOLID-95 used for meshing of the geometry. Meshing is done by Hexagonal Sweep. The geometry can be meshed by 10 node tetrahedron element as well but tetrahedron is stiffer as compared to hexahedron element so results in lower accuracy [4]. In this paper linear and nonlinear analysis of composite drive shaft is carried out using ANSYS.

In finite element analysis 3D model of composite drive shaft is developed. After modeling of composite drive shaft the actual supporting boundary conditions are given. i.e. fixed support at one end and torque at other end. In fixed support there is no any degree of freedom i.e. there is no displacement at any direction. Torque is applied on mass 21 element which has negligible mass and which is applied on flange by use of constrained equations.

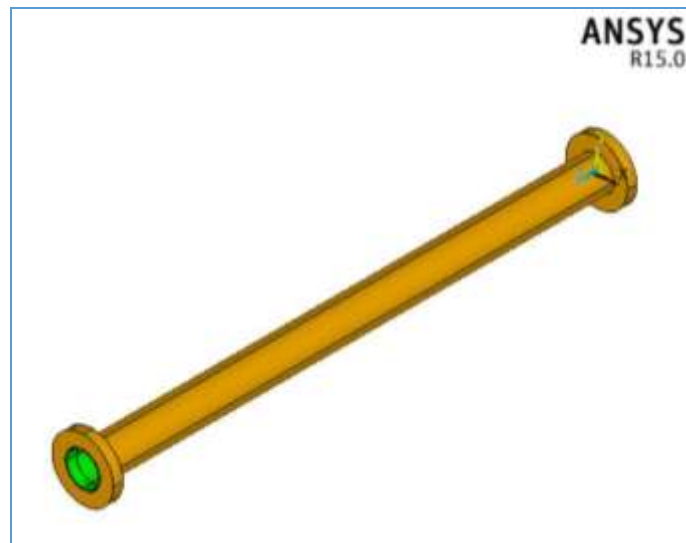


Fig..1 Cad Model of Composite Drive Shaft

In ANSYS the Cad Model of composite drive shaft is imported. After that for analysis the Finite element model is generated. At the point of application of load the fine meshing is done. After meshing we get total 56667 No. of Nodes and 39385 No. of Elements.

Fig..2 Shows meshed model of composite drive shaft spring. Fig..3 shows angular displacement of linear composite Drive Shaft at 2400 Nm.

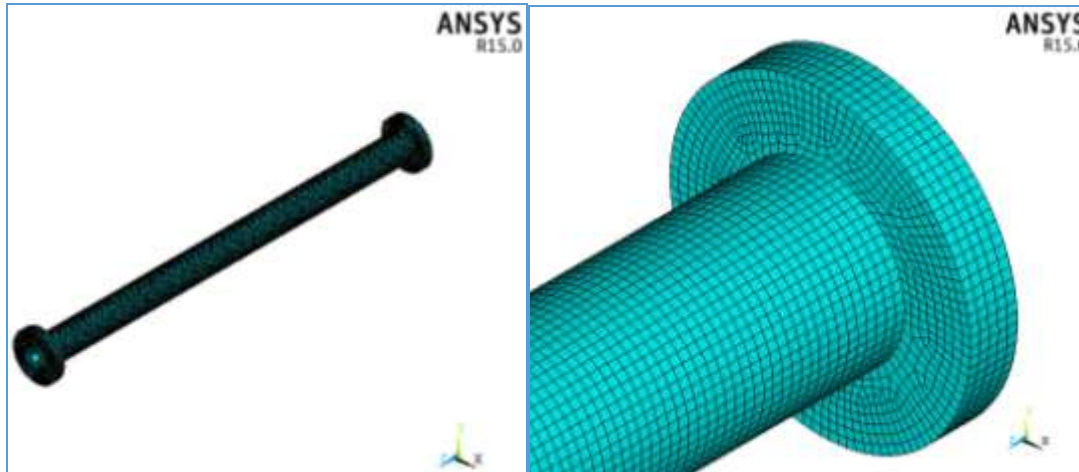


Fig.2 Meshed Model of Composite Drive Shaft

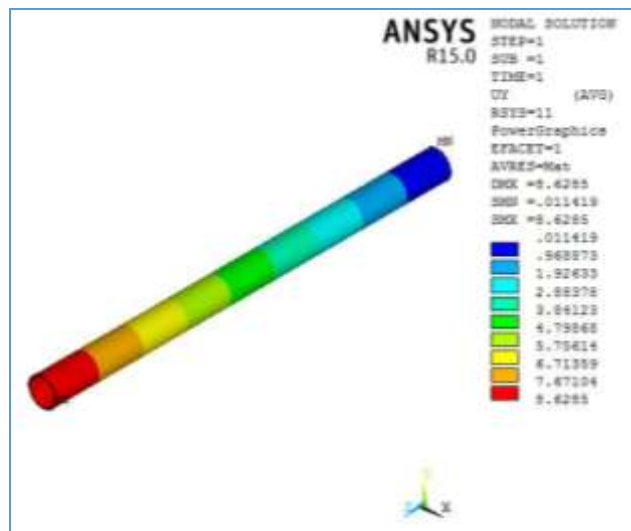


Fig.3 Angular Deformation of Linear Composite Drive Shaft at 2400 Nm .

3.1 Nonlinear Finite Element Analysis

i) Material Non-Linearity: Force (stress) Vs. Displacement (strain) curve is Nonlinear(polynomial).

ii) Geometric Non-Linearity: In real life, the stiffness $[K]$ is a function of Displacement $[d]$. This means in a geometric nonlinear analysis, the stiffness $[K]$ is re-calculated after a certain predefined displacement.

iii) Contact Non-Linearity: In contact analysis, the Stiffness $[K]$ also changes as a function of Displacement (when parts get into contact or separate). Non-linear analysis deals with true stress and strain (unlike engineering stress and strain in linear static analysis) [5].

In this paper Material and Geometric nonlinearities are considered to find out Torque Vs. Angular Deflection characteristics and maximum equivalent stress contours (Von Misses Stress plots).

For maximum load acting on composite drive shaft 66.27 MPa equivalent stress is developed which is far below yield strength of material, hence design of composite drive shaft is also safe. Fig.4a. shows angular Deflection of nonlinear composite drive shaft at 2400 Nm and Fig.4b and 4c shows maximum equivalent stress in nonlinear composite drive shaft.

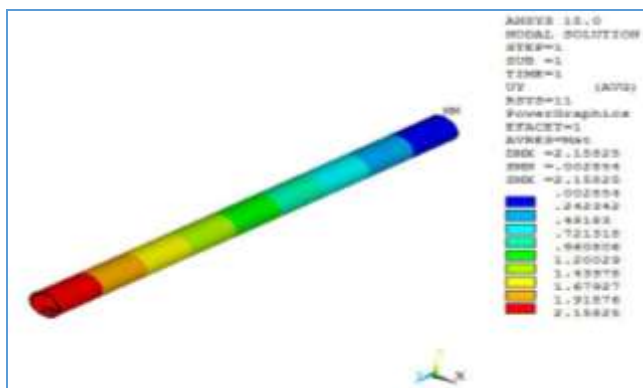


Fig.4a

Fig.4a Angular Deflection of Linear Composite Drive Shaft at 2400 Nm.

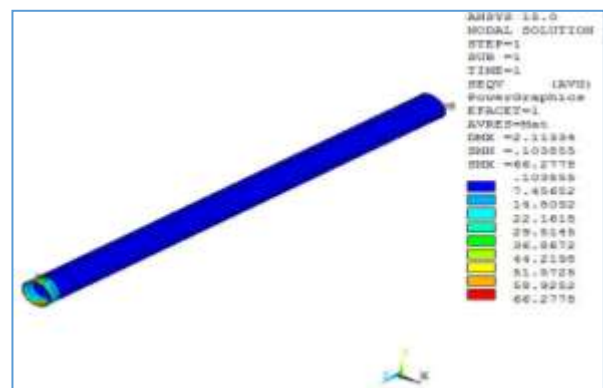


Fig.4b

Fig.4b Maximum Equivalent Stress in Non-Linear Composite Drive Shaft.

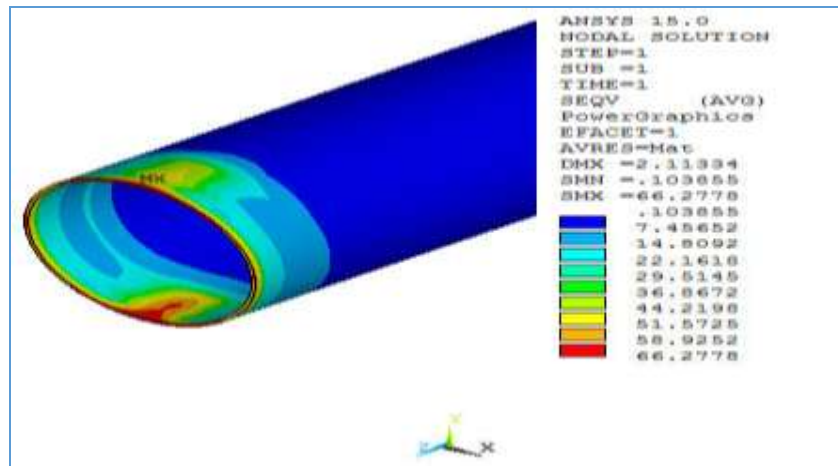


Fig.4c Maximum Equivalent Stress in Non-Linear Composite Drive Shaft.

IV EXPERIMENTAL RESULTS

The experimentation is done by using Torsion Testing Machine. The torque is applied by using the torsion testing machine. At various torque the deflection of composite drive shaft is measured. The following results are obtained during the experimental analysis of composite drive shaft. Experimental results show good agreement with load-deflection characteristics of nonlinear composite drive shaft.



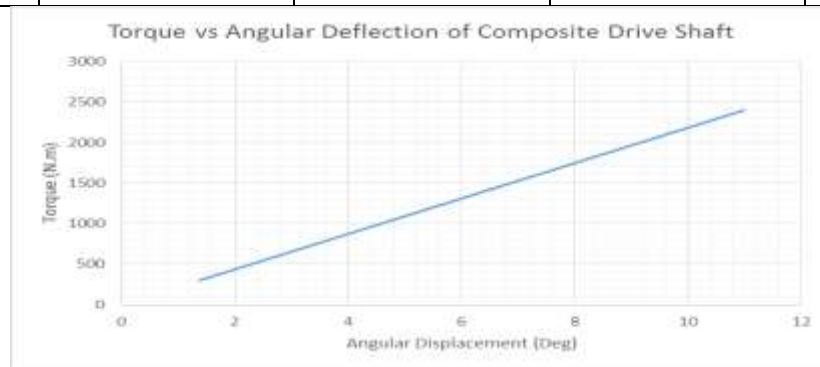
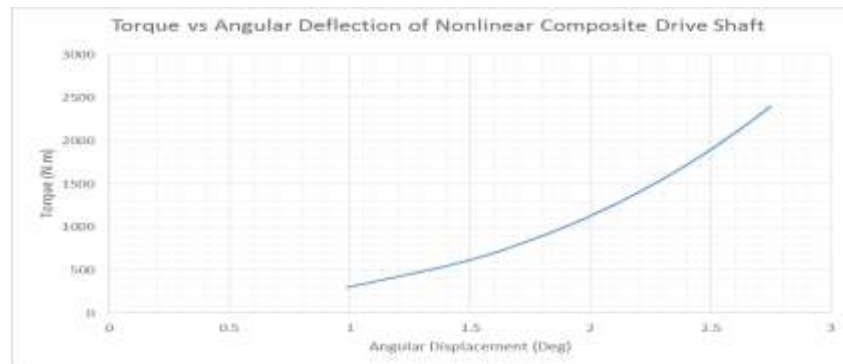
Fig.4 Experimental Setup

V RESULTS AND DISCUSSIONS

Table 1 shows the comparative Torque-Angular deflection characteristics of numerical linear and nonlinear composite drive shaft and experimental analysis.

Table. 1: Torque-Angular Deflection Characteristics

Sr.No.	Torque (Nm)	Angular Deflection of Linear Composite Drive Shaft (rad)	Numerical Angular Deflection of Nonlinear Composite Drive Shaft (rad)	Experimental Angular Deflection of Composite Drive Shaft (rad)
1	300	1.373265243	0.988777459	1
2	600	2.746530487	1.473762041	1.5
3	900	4.119808463	1.800335251	1.6
4	1200	5.493073706	2.053264287	1.98
5	1500	6.866338949	2.262903178	2
6	1800	8.239604193	2.443690461	2.4
7	2100	9.612869436	2.603711207	2.5
8	2400	10.98614741	2.747969247	2.6

**Fig.5a-Torque-Angular Deflection characteristics of Numerical Linear Composite Drive Shaft.****Fig.5b-Torque-Angular Deflection characteristics of Nonlinear Composite Drive Shaft**

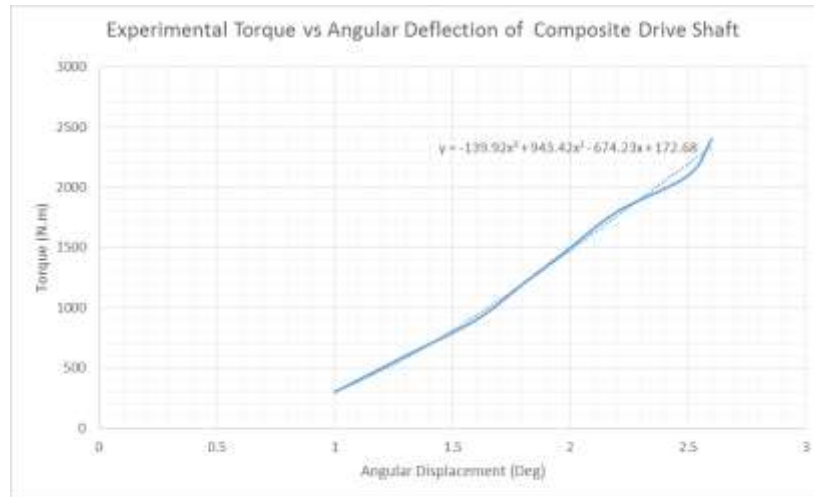


Fig.5c-Experimental Torque-Angular Deflection characteristics of Composite Drive Shaft

From experimental Torque-Angular Deflection characteristics it is observed there is good agreement between Torque-Angular Deflection characteristics of Nonlinear Composite Drive Shaft and experimental Torque-Angular Deflection results, therefore in order to find out non-linear effects included in the torsional Stiffness' t_s' , it is modeled as third order polynomial function as

$$T_s = k_0 + k_1\Delta x + k_2\Delta x^2 + k_3\Delta x^3$$

Where the co-efficients are obtained by fitting the experimental data, which resulted in $k_3 = -139.92 \text{ N/m}^3$, $k_2 = -943.42 \text{ N/m}^2$, $k_1 = -674.23 \text{ N/m}$ and $k_0 = 172.68 \text{ N}$. Hence, in order to model the nonlinearities in composite drive shaft above equation will be used, which includes the nonlinear effects in stiffness,

VI CONCLUSION

Comparative Nonlinear Static Analysis of Composite Drive Shaft used in medium utility vehicle is carried out. Nonlinearities present in drive shaft are found out. The theoretical results from Nonlinear Finite Element Analysis showed in general a good agreement with the experimental values. However, differences appear indicating the necessity to improve the model input data and the experimental procedure. By using nonlinear analysis simulation of real life conditions which were not possible in linear analysis is possible, hence it is essential to carry out nonlinear analysis to get real life results.

Acknowledgements

The authors are grateful to Dr. J.J. Magdum College of Engineering Jaysingpur for supporting this work.

REFERENCES

- [1] Miss PriyaDongare and Dr. SuhasDeshmukh, “Static and Modal Analysis of Composite Drive Shaft and Development of Regression Equations”, International Journal of Engineering Research & Technology (IJERT) 1(10), December- 2012 ISSN: 2278-0181
- [2] M.Arun, K.SomasundaraVinoth, “Design and Development of Laminated Aluminum Glass Fiber Drive Shaft for Light Duty Vehicles”, International Journal of Innovative Technology and Exploring Engineering (IJITEE) 2(6), May 2013
- [3] VinkelArora et al. “A Comparative Study of CAE and Experimental Results of Leaf Springs in Automotive Vehicles”,International Journal of Engineering Science and Technology (IJEST), 3(9) September 2011.
- [4]Mr. Amit A. Hingane, Prof. Dr. S. H. Sawant. “Static Analysis of Helical Compression Spring Used in Vibration Absorber with Nonlinear Parameters.”International Journal for Scientific Research andDevelopment. 2,(4), 2014.
- [5] “Practical Aspects of Finite Element Simulation A Student Guide”,2011 Altair Engineering, Inc

POWER EFFICIENT DATA DISSEMINATION IN UNICASTING OF UNDERWATER SENSOR NETWORK

V.Gayathri¹, A.Vijaya²

¹Department of Computer Science, Sri Krishna Arts & Science College, Coimbatore (India)

²Assistant Professor, Department of Computer Science, Sri Krishna Arts & Science College, Coimbatore (India)

ABSTRACT

Multipath Wireless Sensor networks are envisioned as tiny power constrained devices, which can be scattered over a region of interest, to enable monitoring of that region for an extended period of time. To Preserving coverage and connectivity in underwater sensor network has been a problem that has been addressed in the past. To proposed the use of directional antennas or localization infrastructure. Given that sensors are envisioned to be light-weight energy constrained devices, it may not be desirable to equip them with such additions. This work considers a scheme that ensures coverage and connectivity in a sensor network, without the dependence on external infrastructure or complex hardware.

Keywords: *MANET, Underwater Sensor Network, EERP (Energy Efficient Routing Protocol), GAF (Geographic Adaptive Fidelity).*

I. INTRODUCTION

The wireless sensor networks of the near future are envisioned to consist of hundreds to thousands of inexpensive wireless nodes, each sensing capability and computational power. They are intended for a broad range of environmental sensing applications from vehicle tracking to habitat monitoring. The hardware technologies for these networks – low cost processors, miniature sensing and radio modules – are available today, with further improvements in cost and capabilities expected within the next decade. The applications, networking principles and protocols for these systems are just beginning to be developed.

Sensor networks are quint essentially event-based systems. A sensor network consists of one or more “sinks” which subscribe to specific data streams by expressing interests or queries. The sensors in the network act as “sources” which detect environmental events and push relevant data to the appropriate subscriber sinks. Because of the requirement of unattended operation in remote or even potentially hostile locations, sensor networks are extremely energy-limited. However since various sensor nodes often detect common phenomena, there is likely to be some redundancy in the data the various sources communicate to a particular sink. In-network filtering and processing techniques can help to conserve the scarce energy resources.

II. RELATED WORK

When η identical randomly located nodes, each capable of transmitting at W bits per second and using a fixed range, form a wireless network, the throughput $\lambda(n)$ obtainable by each node for a randomly chosen destination is $\theta(W\sqrt{n\log n})$ bits per second under a noninterference protocol. If the nodes are optimally placed in a disk of unit area, traffic patterns are optimally assigned, and each transmission's range is optimally chosen, the bit-distance product that can be transported by the network per second is $\theta(W\sqrt{An})$ bit-meters per second. Similar results also hold under an alternate physical model where a required signal-to-interference ratio is specified for successful receptions. Splitting the channel into several sub channels does not change any of the results. Since the throughput furnished to each user diminishes to zero as the number of users is increased, perhaps networks connecting smaller numbers of users, or featuring connections mostly with nearby neighbors, may be more likely to be find acceptance [1]. The capacity of ad hoc wireless networks is constrained by the mutual interference of concurrent transmissions between nodes. Study a model of an ad hoc network where nodes communicate in random source–destination pairs. These nodes are assumed to be mobile. Examine the per-session throughput for applications with loose delay constraints, such that the topology changes over the time-scale of packet delivery. Under this assumption, the per-user throughput can increase dramatically when nodes are mobile rather than fixed. This improvement can be achieved by exploiting a form of *multiuserdiversity* via packet relaying. [2]. This work provides a general framework for the analysis of the capacity scaling properties in mobile ad-hoc networks with heterogeneous nodes and spatial in homogeneities. Existing analytical studies strongly rely on the assumption that nodes are identical and uniformly visit the entire network space. Experimental data, however, have shown that the mobility pattern of individual nodes is typically restricted over the area, while the overall node density is often largely inhomogeneous, due to prevailing clustering behavior resulting from hot-spots. Such ubiquitous features of realistic mobility processes demand to reconsider the scaling laws for the per user throughput achievable by the *store-carry-forward* communication paradigm which provides the foundation of many promising applications of delay tolerant networking. We show how the analysis of the asymptotic capacity of dense mobile ad-hoc networks can be transformed, under mild assumptions, into a *Maximum ConcurrentFlow* (MCF) problem over an associated *Generalized RandomGeometric Graph* (GRGG). Our methodology allows to identify the scaling laws for a general class of mobile wireless networks, and to precisely determine under which conditions the mobility of nodes can indeed be exploited to increase the per-node throughput. At last we propose a simple, asymptotically optimal, scheduling and routing scheme that achieves the maximum transport capacity of the network.

This work extended the analysis of the capacity scaling properties in mobile ad-hoc networks by considering heterogeneous nodes and spatial in homogeneities, two common features widely recognized in realistic mobility traces. The main problem onto a *Maximum Concurrent Flow* (MCF) problem over an associated *Generalized Random Geometric Graph* (GRGG). Our methodology allows to identify the scaling laws of a general class of mobile wireless networks, and to precisely determine under which conditions the mobility of nodes can indeed be

exploited to increase the per-node throughput. Finally GRGG and MCF are considering to identifying the scaling laws are using in it [3].

III. PROPOSED SYSTEM

Heterogeneous under water sensor networks with infrastructure support:

3.1 Two-dimensional hybrid random walk model

Consider a unit square which is further divided into $1=B^2$ squares of equal size. Each of the smaller square is called a RW-cell (random walk cell), and indexed by $(U_x; U_y)$ where $U_x; U_y \in \{1; \dots; 1=B\}$. A node which is in one RW-cell at a time slot moves to one of its eight adjacent RW-cells or stays in the same RW-cell in the next time-slot with a same probability. Two RW-cells are said to be adjacent if they share a common point. The node position within the RW-cell is randomly and uniformly selected.

3.2 Mobility Time Scales: Two time scales of mobility are

3.2.1 Fast mobility: The mobility supports high speed IP packet data only. Random way point mobility with 3 speeds of 1m/s, 10m/s, 20m/s. Wireless local area network are using WIFI is IEEE 802.11b MAC (Message Authentication Code) and packet size is 512 bytes. The mobility of nodes is at the same time scale as the transmission of packets, i.e., in each time-slot, only one transmission is allowed. Fast mobility environments, a typical GOOD duration are 0.06 seconds (about 6 packet transmission times).

3.2.2 Slow mobility: The mobility takes low bandwidth and low propagation delay. The packet loss probability (for 1k byte packet) ranging from 0.15 to 0.001. The slow mobility bandwidth ranging from 50 Kbit/s to 1.5 Mbit/s. The GOOD state has low packet loss probability say 10^{-2} . The BAD state has a high packet loss probability, say 1. The mobility of nodes is much slower than the transmission of packets, i.e., multiple transmissions may happen within one time-slot. A slow mobility environment, a typical GOOD duration is 0.12 seconds (or about 128 packet transmission times).

3.3 Scheduling Policies

Assume that there exists a scheduler that has all the information about the current and past status of the network, and can schedule any radio transmission in the current and future time slots, similar. A packet is successfully delivered if and only if all destinations within the multicast session have received the packet. In scheduling policies mainly using protocol is Energy Efficient Routing Protocol (EERP). The Proposed protocol is implemented with the object oriented discrete event simulator. In our simulation, 50 mobile nodes move in a 1200 meter x 1200 meter square region for 50 seconds simulation time. We assume each node moves independently with the same average speed. All nodes have the same transmission range of 250 meters. The simulated traffic is Constant Bit Rate (CBR).

Simulation settings and parameters are summarized in table

No. of Nodes	50
Area Size	1200 x 1200 m^2
MAC	802.11
Radio range	250 m
Simulation Time	50 sec
Traffic Source	Constant Bit Rate(CBR)
Packet Size	512 bytes
Mobility Model	Random Way Point
Maximum & Minimum Speed	10 & 0.5 m/s

3.3.1 Throughput and delay: Throughput is generally measured as the percentage of successfully transmitted radio-link level frames per unit time. Transmission delay is defined as the interval between the frame arrival time at the MAC layer of a transmitter and the time at which the transmitter realizes that the transmitted frame has been successfully received by the receiver.

3.3.2 Data packet delivery ratio: The data packet delivery ratio is the ratio of the number of packets generated at the sources to the number of packets received by the destinations.

3.3.3 End-to-end delay: This metric includes not only the delays of data propagation and transfer, but also all possible delays caused by buffering, queuing, and retransmitting data packets.

3.3.4 Consumption per Packet: It is defined by the total energy consumption divided by the total number of packets received. This metric reflects the energy efficiency for each protocol.

3.3.5 Energy efficiency: Energy efficiency can be defined as

$$\text{Energy Efficiency} = \frac{\text{Total no. of bits transmitted}}{\text{Total Energy Consumed}}$$

In each time slot, for each packet that has not been successfully delivered and each of its unreached destinations, the scheduler needs to perform the following two functions:

3.4 Capture

The scheduler needs to decide whether to deliver packet to destination in the current time slot. If yes, the scheduler then needs to choose one relay node (possibly the source node itself) that has a copy of the packet at the beginning of the time slot, and schedules radio transmissions to forward this packet to destination within the same time slot, using possibly multi-hop transmissions. When this happens successfully, say that the chosen relay node has successfully captured the destination of packet. Call this chosen relay node the last mobile relay for packet and destination. Call the

distance between the last mobile relay and the destination as the capture range is 124 mi is equal to 248 miles. Range is the maximum range possible to receive data at 25% of the typical rate.

3.5 Duplication

For a packet p that has not been successfully delivered, the scheduler needs to decide whether to duplicate packet to other nodes that does not have the packet at the beginning of the time-slot. The scheduler also needs to decide which nodes to relay from and relay to, and how. All transmissions can be carried out either in ad hoc mode or in infrastructure mode. We assume that the base stations have a same transmission bandwidth. The bandwidth for each mobile ad hoc node is denoted by packets. Further, we evenly divide the bandwidth into two parts, one for uplink transmissions and the other for downlink transmissions, so that these different kinds of transmissions will not interfere with each other.

Uplink: A mobile node holding packet is selected, and transmits this packet to the nearest base station. Uplink is using High Speed Packet Access (HSPA) the average upload is 600 kbps to 1.5mbps. WIFI of 802.11a, 802.11b, and 802.11g of uplink is 54 the range is ~30 m and 802.11n of downlink is 600 the range is ~50m.

Infrastructure relay: Once a base station receives a packet from a mobile node, all the other m base stations share this packet immediately, (i.e., the delay is considered to be zero) since all base stations are connected by wires.

Downlink: Each base station searches for all the packets needed in its own sub region, and transmit all of them to their destined mobile nodes. At this step, every base station will adopt TDMA schemes to delivered different packets for different multicast sessions. Finally a rate present is 2 Mbit/s to 200 Kbit/s. WIFI of 802.11a, 802.11b, and 802.11g of downlink is 54 the range is ~30 m and 802.11n of downlink is 600 the range is ~50m.

IV. GAF (GEOGRAPHIC ADAPTIVE FIDELITY) PROTOCOL

In GAF protocol, each node uses location information based on GPS to associate itself with a “*virtual grid*” so that the entire area is divided into several square grids, and the node with the highest residual energy within each grid becomes the master of the grid. Other nodes in the same grid can be regarded as redundant with respect to forwarding packets, and thus they can be safely put to sleep without sacrificing the “*routing fidelity*” (or routing efficiency).

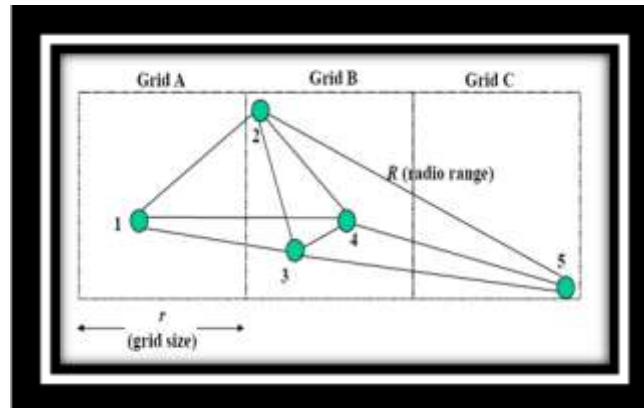


Fig 4.1 Virtual grid structure in the GAF protocol.

Master election rule in GAF is as follows. Nodes are in one of three states as shown in Figure: *sleeping*, *discovering* and *active*. Initially, a node is in the discovery state and exchanges discovery messages including grid IDs to find other nodes within the same grid.

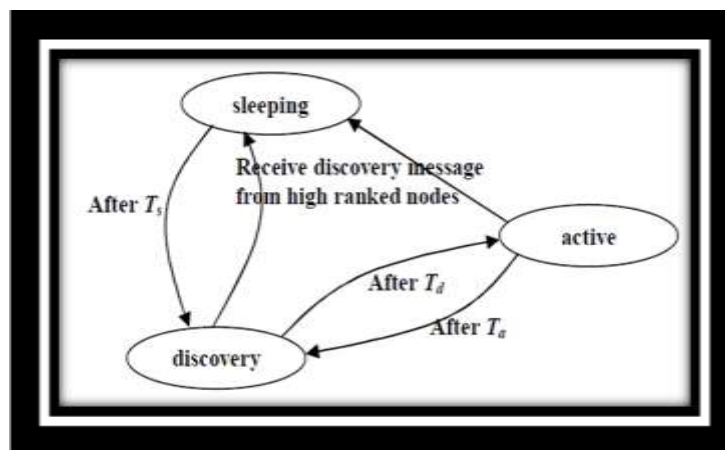


Fig 4.2 State Transition in the GAF Protocol

V RESULT AND DISCUSSION

Optimization ACO due to its distributed nature becomes alternate to GAF, in order to determine the optimal route it needs that the base station already has the required information. For fusion process neural networks are well suited because neural networks can learn and dynamically adaptive to the changing scenarios. Reinforcement learning is fully distributed and it can adapt quickly to network topology change or any node failure. It has been used efficiently for finding the optimal path for aggregation. GAF based distributed approach using sleep state switching numbers and weighted average operators to perform energy efficient flooding-based aggregation has also been proposed and the system outperforms the previous results. In wireless sensor networks many situations demand aggregating data at a central node e.g. monitoring events. For these situations, the centralized approaches like ACO can be used efficiently to know the features of the data are shown in the figures.

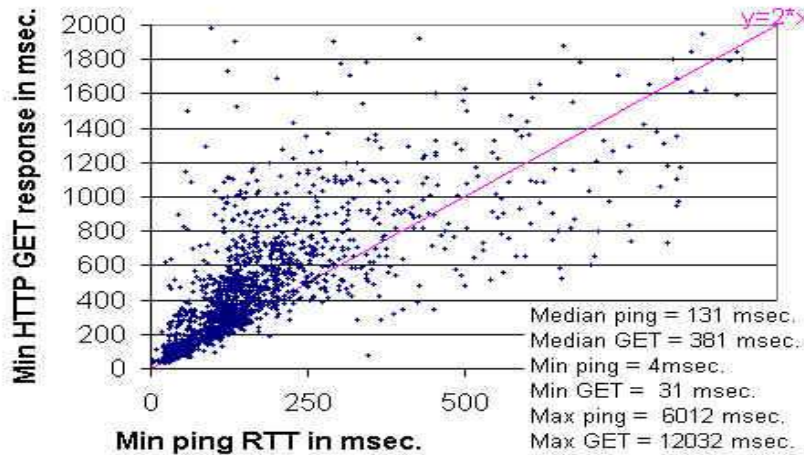


Figure 5.1.Finding distance

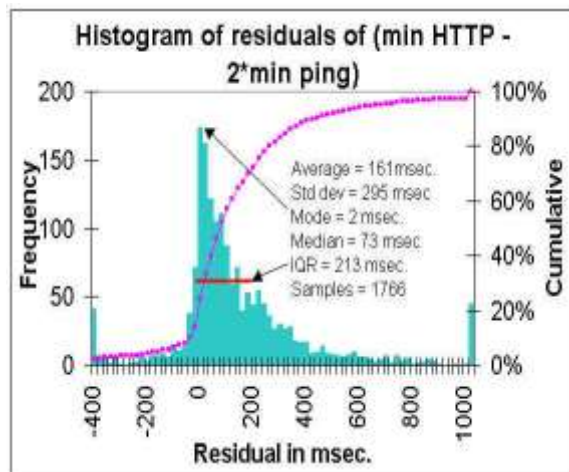


Figure 5.2.Transmission Delay

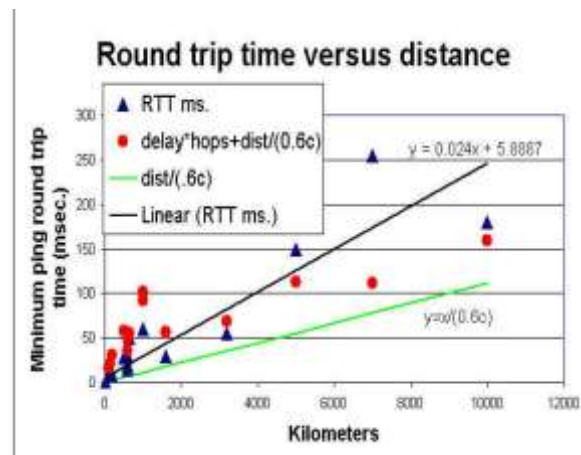


Figure5.3.Data Loss Deduction

This analysis includes calculating percentage of energy conserved in this protocol as well as the previously known protocol. Further time spend by each node in the sense, transmit, off states are calculated for each node. Based on the above results, power consumption of each node in their corresponding state is calculated. Total power consumed by a single sensor node is calculated based on the individual power consumed by the corresponding node in the sense, transmit, off states. Total power consumption of the entire process is calculated based on the total power consumption of the individual nodes. Finally, percentage of energy conserved in this work and previous work is calculated. Theoretical analysis is performed for both static and mobile events.

TABLE 5.1 TIME SPENT BY EACH NODE IN SENSE STATE

NODES	TRANSMISSION TIME IN MINUTE/WAIT
Node 0	49.9273999999 mW
Node 1	49.9273999999 mW
Node 3	49.7204899999 mW
Node 4	49.8765799999 mW
Node 5	50.0 mW
Node 6	50.0 mW
Node 7	50.0 mW
Node 8	49.9165100000 mW
Node 0	49.8765799999 mW

TABLE 5.2 POWER CONSUMED BY EACH NODE IN SENSE STATE

NODES	TRANSMISSION TIME IN MINUTE/SECONDS
Node 0	49.9273999999 ms
Node 1	49.9273999999 ms
Node 3	49.7204899999 ms
Node 4	49.8765799999 ms
Node 5	50.0 ms
Node 6	50.0 ms
Node 7	50.0 ms
Node 8	49.9165100000 ms
Node 0	49.8765799999 ms

TABLE 5.3 POWER CONSUMED BY EACH NODE IN TRANSMIT STATE

NODES	TRANSMISSION TIME IN MINUTE/WAIT
Node 0	0.0725999999 mW
Node 1	0.0725999999 mW
Node 3	0.2795099999 mW
Node 4	0.12342 Mw
Node 5	0 Mw
Node 6	0 mW
Node 7	0 Mw
Node 8	0 mW
Node 0	0.12342 mW

TABLE 5.4 POWER CONSUMED BY EACH NODE IN TRANSMIT STATE

NODES	TRANSMISSION TIME IN MINUTE/WAIT
Node 0	0.0725999999 mW
Node 1	0.0725999999 mW
Node 3	0.2795099999 mW
Node 4	0.12342 Mw
Node 5	0 Mw
Node 6	0 mW
Node 7	0 Mw
Node 8	0 mW
Node 0	0.12342 mW

TABLE 5.5 TOTAL POWER CONSUMPTION BT THE ENTIRE PROCESS

NODES	VALUES
Total power spent in the sense state	499.244959999 mW
Total power spent in the transmit state	0.67154999999 mW
Total power consumed	499.916510002 mW
Percentage of Energy conserved	50.0083489995 %
Percentage of Energy conserved	33.5%(Previous one)

VI. CONCLUSION

Preserving coverage and connectivity in a sensor network has been a problem that has been addressed in the past. However, most of the approaches have assumed the aid of either GPS, or have proposed the use of directional antennas or localization infrastructure. Given that sensors are envisioned to be light-weight energy constrained devices, it may not be desirable to equip them with such additions. This work shows that the power saved in each node outperforms the power saved in any other previously known protocols and this work also shows that it is possible to minimize about 51% of the power and maintain 100% coverage and connectivity. Further, simulation study also proves that it is possible to increase the life time of each sensor network by increasing the number of sensor nodes.

REFERENCES

- [1] Forman G., Zahorjan J. The challenges of mobile computing. IEEE Computer 1994; 27(4):38-47.
 [2] Jubin J, Tornow J. The DARPA Packet Radio Network Protocols. Proceedings of the IEEE 1987; 75(1):21-32.

- [3] Perkins C. Ad Hoc Networking: Addison-Wesley:2001; 1-28.
- [4] Singh S, Woo M, Raghavendra C. Power-Aware Routing in Mobile Ad Hoc Networks. Proceedings of Int'l Conf. on Mobile Computing and Networking (MobiCom'98) 1998.
- [5] Chang J-H, Tassiulas L. Energy Conserving Routing in Wireless Ad-hoc Networks. Proceedings of the Conf. on Computer Communications (IEEE Infocom 2000) 2000; 22-31.
- [6] Li Q, Aslam J, Rus D. Online Power-aware routing in Wireless Ad-hoc Networks. Proceedings of Int'l Conf. on Mobile Computing and Networking (MobiCom'2001) 2001.
- [7] Stojmenovic I, Lin X. Power-Aware Localized Routing in Wireless Networks. IEEE Trans. Parallel and Distributed Systems 2001; 12(11):1122-1133.
- [8] Doshi S, Brown TX. Minimum Energy Routing Schemes for a Wireless Ad Hoc Network. Proceedings of the Conference on Computer Communications (IEEE Infocom 2002) 2002.
- [9] Banerjee S, Misra A. Minimum Energy Paths for Reliable Communication in Multi-hop Wireless Networks. Proceedings of Annual Workshop on Mobile Ad Hoc Networking & Computing (MobiHOC 2002) 2002.
- [10] Narayanaswamy S, Kawadia V, Sreenivas RS, Kumar PR. Power Control in Ad-Hoc Networks: Theory, Architecture, Algorithm and Implementation of the COMPOW Protocol. Proceedings of European Wireless 2002.
- [11] Woo K, Yu C, Youn HY, Lee B. Non-Blocking, Localized Routing Algorithm for Balanced Energy Consumption in Mobile Ad Hoc Networks. Proceedings of Int'l Symp. on Modeling, Analysis and Simulation of Computer and Telecommunication Systems (MASCOTS 2001) 2001; 117-124.
- [12] Toh C-K. Maximum Battery Life Routing to Support Ubiquitous Mobile Computing in Wireless Ad Hoc Networks. IEEE Communications 2001.
- [13] Chen B, Jamieson K, Morris R, Balakrishnan H. Span: An Energy-Efficient Coordination Algorithm for Topology Maintenance in Ad Hoc Wireless Networks. Proceedings of Int'l Conf. on Mobile Computing and Networking (MobiCom'2001) 2001.
- [14] Xu Y, Heidemann J, Estrin D. Geography-informed Energy Conservation for Ad Hoc Routing. Proceedings of Int'l Conf. on Mobile Computing and Networking (MobiCom'2001) 2001.
- [15] Girling G., Wa J, Osborn P, Stefanova R. The Design and Implementation of a Low Power Ad Hoc Protocol Stack. Proceedings of IEEE Wireless Communications and Networking Conference 2000.

Biographical Notes

Ms. V. Gayathri is presently pursuing M.Phil in Computer Science Department from Sri Krishna Arts & Science College, Coimbatore, India.

Mrs. A. Vijaya is working as an Assistant professor in Computer Science Department from Sri Krishna Arts & Science College, Coimbatore, India.

INFLUENCE OF SPUTTERING PARAMETERS ON STRUCTURAL, OPTICAL AND THERMAL PROPERTIES OF COPPER NANOPARTICLES SYNTHESIZED BY DC MAGNETRON SPUTTERING

Jyoti Jaiswal¹, Samta Chauhan², Ramesh Chandra³

^{1, 2, 3} Institute Instrumentation Centre, Indian Institute of Technology Roorkee, (India)

ABSTRACT

We report the synthesis of ultrafine copper nanoparticles (Cu NPs) with very narrow size distribution using DC magnetron sputtering technique. The effect of sputtering pressure and power on the crystal structure, surface morphology, optical and thermal properties of nanoparticles were studied. X-ray diffraction (XRD), Field emission scanning electron microscope (FE-SEM), Energy dispersive X-ray spectroscopy (EDX), Transmission electron microscopy (TEM), UV-VIS diffuse reflectance spectroscopy (DRS) and Thermal gravimetric analysis (TGA) were used to characterize and define the properties of as-synthesized Cu NPs. The XRD pattern confirms FCC phase of copper nanoparticles with preferred orientation along [111] direction. The XRD data reveals that the crystallite size, lattice constant and crystallinity of as-synthesized Cu NPs increases while dislocation density and lattice strain reduces with increase in sputtering pressure and power. The crystallite size and the selected area electron diffraction (SAED) pattern obtained from TEM results are also in agreement with the XRD data. Approximately spherical shape and pure copper nanoparticles were ascertained by TEM, SEM and EDS. With increase in the sputtering pressure and power, a change in the surface plasmon resonance (SPR) wavelength from 548 nm to 550 nm has been observed. The thermal properties of the as-synthesized Cu NPs presented the maximum weight loss of ~2.5 %, which is very low as compared to Cu NPs prepared by chemical method and hence confirm that as-synthesized Cu NPs are thermally more stable.

Keywords- Metal nanoparticles, DC-magnetron sputtering, surface morphology, surface plasmon resonance, thermal properties.

I. INTRODUCTION

In the past two decades, appreciable attention has been dedicated to the synthesis of metal NPs and their diligence in many areas [1-6]. The synthesis of mono-dispersed, ultrafine and pure metal NPs have been continued to capture researcher's interest owing to their useful properties such as the good optical, thermal, electrical and magnetic properties because of their potential application in photonics, catalysis, nanofluids, cooling fluids for electronic systems, plasmonic photovoltaic, antibacterial composite food packaging, optoelectronics devices, fuel cells, pigments, biosensors and so on [7-14]. Among all the metal NPs like gold (Au), silver (Ag), Copper (Cu), palladium (Pd) and platinum (Pt), Cu NPs has always been one of the most preferable material because of its low cost compared with Au or Ag. In addition, Cu NPs plays a significant role

in modern electronic circuits due to its excellent electrical conductivity as well as good antimicrobial efficacy, biocompatibility and SERS [15-17].

The synthesis of pure Cu NPs is often challenging due to the possibility of surface oxidation which can suppress the interesting optical properties such as surface plasmon resonance, as metal oxides generally possess high dielectric constants. Numerous methods have been reported for the synthesis of Cu NPs such as laser ablation [16], one pot [18], chemical reduction [19], photochemical [20], photolytic and radiolytic reduction [21], sonochemical [22], reducing agent [23], thermal decomposition [24, 25] and polyol method [26]. Most of the above mentioned methods are based on chemical vapor deposition (CVD) which employs hazardous chemicals to give irregular shape with broad size distribution and challenges such as contamination of residual precursor material and especially oxidation. Therefore, chemists, physicists and material scientists have expressed keen interest in the evolution of novel methods for the synthesis of smaller, monodispersed and pure metal NPs which are eco-friendly.

Physical vapor deposition (PVD) methods like DC-RF magnetron sputtering method [27, 28] have been used by researchers to synthesize metal NPs. However, the synthesis of Cu nanoparticles by magnetron sputtering process is still lacking in literature. Eco-friendly, uniformity, reproducibility, narrow size distribution, controllable growth, high deposition rate, high purity and almost contamination free effect are some of the advantages of sputtering technique over traditional methods [18-26]. Because of these important advantages, we have synthesized Cu nanoparticles by DC magnetron sputtering at low temperature under highly controlled conditions. During sputtering, various parameters like gas pressure, dc power, substrate temperature, distance between target and substrate are varied to observe the desirable properties of the nanoparticles. Physical methods of deposition of Cu NPs including sputtering can offer a solution to oxidation issues as discussed supra. In this paper, we report the synthesis of Cu NPs of high quality and narrow particle size distribution by using DC magnetron sputtering without using any hazardous chemical.

II. EXPERIMENTAL DETAILS

2.1 Synthesis of Cu NPs

The Cu NPs were synthesized on copper cold finger using DC magnetron sputtering in a custom designed 12 inch-diameter vacuum chamber (Excel Instrument, Mumbai, India). The vacuum chamber consists of windows for sputtering gun and copper finger arrangement. The DC magnetron sputtering was carried out using Cu target of 2 inch-diameter and 5 mm thickness. The distance between the target and the copper cold finger was kept 4.5 cm. Before the deposition, the vacuum chamber was initially evacuated to 2×10^{-6} Torr using a turbo molecular pump backed by rotary pump. Further, the copper cold finger was kept cooled by continuous filling of liquid nitrogen (-185°C) throughout the deposition to maintain the low temperature while NPs are being deposited. The reason for keeping low substrate temperature is to inhibit the grain growth of during deposition of Cu NPs. Also, contamination due to the possible diffusion of atoms from the substrate with the deposited material is minimized at lower temperature. Argon (Ar) gas with purity 99.999% was introduced during the deposition in a vacuum chamber with a flow rate of 20 sccm. Before starting the actual experiment, the Cu target was pre-sputtered for 5 min to clean the surface of the target and controlled uniformity. The Cu atoms were sputtered from the target on the copper cold finger during deposition to form Cu NPs. After the deposition

time was over, the Cu NPs were collected from the copper finger when it reached at room temperature otherwise Cu NPs can form CuO, Cu₂O, Cu(OH)₂. The various sputtering parameters used during the synthesis of Cu NPs are shown in Table 1.

Table. 1 Sputtering parameters for Cu NPs

Target	Copper (Cu)
Base pressure	2×10^{-7} Torr
Working pressure	5-20 mTorr
Deposition time	4 hours
Deposition power	30-60 W
Substrate temperature	-185 °C
Target substrate distance	4.5 cm
Gas used	Ar (20 sccm)

2.2 Characterization Details

The structural, preferred phase orientation identification, crystallite size, lattice strain, lattice constant and dislocation density of the Cu NPs were studied by X-ray diffractometer, (Bruker AXS, D8 advanced, Diffractometer) having CuK α radiation ($\lambda=1.5406\text{\AA}$). The X-ray diffraction (XRD) pattern was carried out at the slow scan rate 0.5°min^{-1} in a Bragg angle range from 10° - 100° with operating current and voltage of 30mA and 40kV respectively. The TEM images, EDX and selected area electron diffraction (SAED) of Cu NPs were obtained with a Transmission electron microscope (TEM TECNAI G² 20 S-TWIN). The morphology and elemental analysis of samples were analyzed using Scanning electron microscope (FE-SEM, Carl Zeiss, Ultra Plus) and an Energy dispersive X-ray spectroscopy (EDX) attached with the FE-SEM operated at EHT from 5-15 kV respectively. The optical properties of the samples were recorded on UV-VIS spectrophotometer (SHIMADZU, UV-2450) in the wavelength range 200-800 nm. The thermal properties of Cu NPs were studied using Thermo gravimetric analyzer (TGA) (SII 6300 EXSTAR).

III. RESULTS AND DISCUSSION

Fig. 1(a) and 1(b) show the XRD pattern of Cu NPs at different sputtering Argon (Ar) pressure and DC power. XRD peaks are observed at $2\theta = 43.298, 50.434, 74.133, 89.934$ and 95.143 corresponding to phase orientation along (111), (200), (220), (311) and (222) direction respectively match with standard data (JCPDS 00-004-0836) of face centred cubic (FCC) phase of Cu NPs. The dominant peak at $2\theta = 43.298$ is the preferred phase (111) orientation. Moreover, the diffracted peaks in the XRD pattern become more intense and sharper as the working pressure and DC power was increased, indicating an enhanced crystallinity of Cu NPs at high working pressure and power. The crystallite size of the Cu NPs was calculated using the Debye-Scherrer formula [29] given by equation (1).

$$t = \frac{0.9\lambda}{\beta \cos \theta} \quad (1)$$

where t is the crystallite size, λ the wavelength of X-ray (1.54056 \AA), β the full width at half maximum (FWHM) of the dominant peak and θ Bragg diffraction angle.

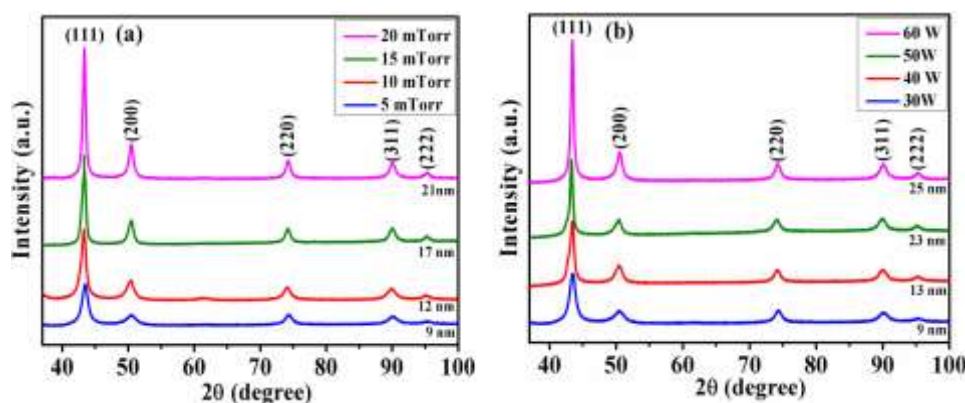


Figure 1 XRD pattern of Cu NPs for various (a) sputtering pressure (5-10 mTorr at 30 W) and (b) sputtering power (30-60 W at 5 mTorr)

The crystallite size and dislocation density of the samples were calculated from the XRD pattern corresponding to the dominant orientation (111) at different sputtering pressure and power. We have also included the instrumental broadening 0.1° for the crystallite size calculation. The crystallite size and dislocation density of Cu NPs as a function of sputtering pressure and power are shown in Fig. 2(a) and 2(b) respectively.

The dislocation density, which indicates the number of crystal defects in NPs was calculated using the following equation (2) [30].

$$\delta = \frac{15\beta \cos \theta}{4a} \quad (2)$$

where δ and a is dislocation density and lattice constant respectively. Fig. 2(a) and Fig. 2(b) depicts that the crystallite size of Cu NPs becomes large (9-25 nm) while dislocation density is reduced as sputtering pressure and power increases. The reduction in lattice imperfection may be due to the movement of interstitial atoms from their grain boundaries towards the crystallites. Moreover, the enhancement in crystallite size with increment in pressure can be explained by comparing the mean free path of a particle (equation (3)) in a sputtering process with the distance from the target to the substrate (4.5 cm in our case) at low temperature with the molecular diameter of the sputtering gas [31].

$$d_m = 2.33 \times 10^{-20} T / P \gamma^2 \quad (3)$$

where d_m is the mean free path of a particle in chamber, T the temperature, P the sputtering pressure and γ the molecular diameter.

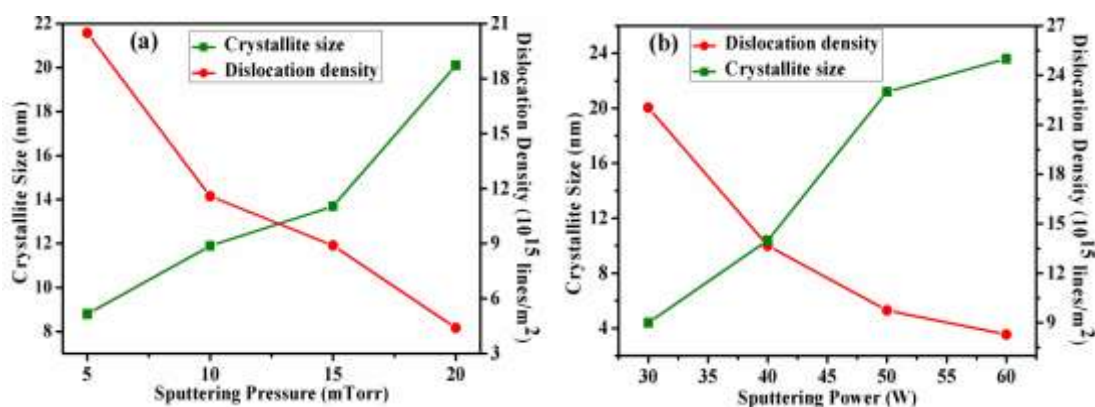


Figure 2. Variation Of Crystallite Size And Dislocation Density Of Cu Nps As A Function Of Sputtering (A) Pressure (5-10 Mtorr At 30 W) And (B) Power (30-60 W At 5 Mtorr).

Fig. 3 depicts that at lower pressure of 5 mTorr the mean free path of a particle is ~ 1.3 cm and it goes through three collisions before reaching the target, therefore, most of its kinetic energy is retained while landing, which is substantial to cause radiation damage and limit the size of the grains [32-35]. At the higher pressure of 20 mTorr, the mean free path is ~0.27 cm so that a particle experiences 13 collisions before reaching the substrate. Consequently, a substantial part of its kinetic energy is thermalized due to this less radiation damages can be fixed in the deposits, allowing larger grains to be formed [32-35].

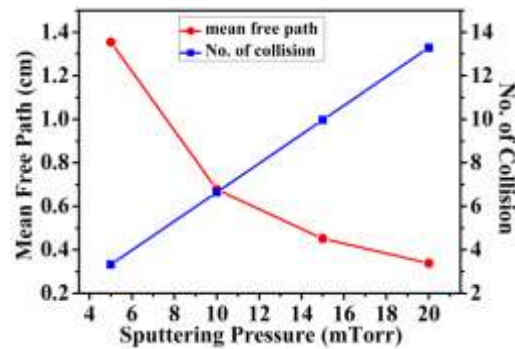


Figure 3 Variations Of Mean Free Path And No. Of Collision With Sputtering Pressure.

The enhancement in crystallite size by an increment in sputtering power is associated with change of kinetic energy of the sputtered particles with the DC power. As the sputtering power increases, the kinetic energy of sputtered particle also increases. Thus, the sputtered particles have sufficient energy to migrate on the substrate and hence results in the higher growth of the crystallite size [36, 37]. Therefore, the crystallinity is improved.

The effect of sputtering pressure at power 30 W and power at pressure 5 mTorr on lattice constant and lattice strain are shown in Fig. 4(a) and 4(b). The lattice constant and strain calculated from XRD data along preferred phase direction ($h k l$) using the following equation (4) and (5) respectively [29, 38].

$$a = d \sqrt{h^2 + k^2 + l^2} \quad (4)$$

$$\varepsilon = \beta \cos \theta / 4 \quad (5)$$

where ($h k l$), d and ε are the Miller indices, interplanar spacing and lattice strain, respectively. From Fig. 4(a) and (b), it is found that the lattice constant increases abruptly at lower pressure and power while slowly at higher values because the lattice constant is directly proportional to the crystallite size [39]. The linearly degradation in lattice strain is observed with increment in sputtering pressure and power. That result can be understood by the enhancement in grain growth of nanoparticles [36, 37].

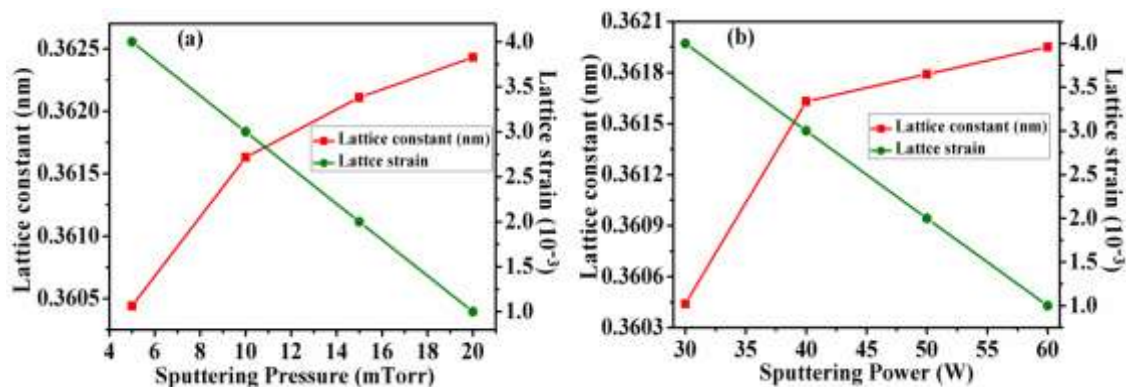


Figure 4. Lattice Constant And Strain With Varying Sputtering (A) Pressure (5-20 Mtorr At 30 W) And (B) Power (30-60 W At 5 Mtorr).

Fig. 5(a), 5(b) and 5(c) represent the transmission electron microscope (TEM) image, selected area electron diffraction (SAED) pattern and energy dispersive X-ray spectroscopy (EDX) spectra of the sample deposited at sputtering pressure 5 mTorr and power 30 W respectively. The TEM image shows that as-deposited Cu NPs are approximately uniform in size and have spherical shape. The observed particle size distribution of the sample is 5-12 nm and average particle size is 8.5 nm. The particle size measured from TEM image is ~8.5 nm which confirms the particle size calculated from XRD pattern (9 nm). It is also clear that the nanoparticles are less dispersed. The SAED pattern shown in Fig. 5(b) has five fringe patterns with planes (111), (200), (220), (311) and (222) of FCC metallic Cu NPs. SAED pattern obtained from TEM are also in accordance with XRD result. The EDX spectra confirms that as deposited Cu NPs are 100% pure. The reason for the presence of carbon in EDX spectra is the carbon grid used to analyses the sample from TEM.

The FE-SEM image and SEM-EDX spectra of the sample deposited at sputtering pressure 5 mTorr and power 30 W are shown in Fig. 6(a) and 6(b) respectively. The FE-SEM image clearly revealed the spherical type of morphology. And the EDX spectra confirms 100% pure deposited Cu NPs. The presence of C in the SEM-EDX spectra comes from double sided carbon tape used to prepare SEM-EDX sample. All the results obtained from the SEM confirm the TEM results.

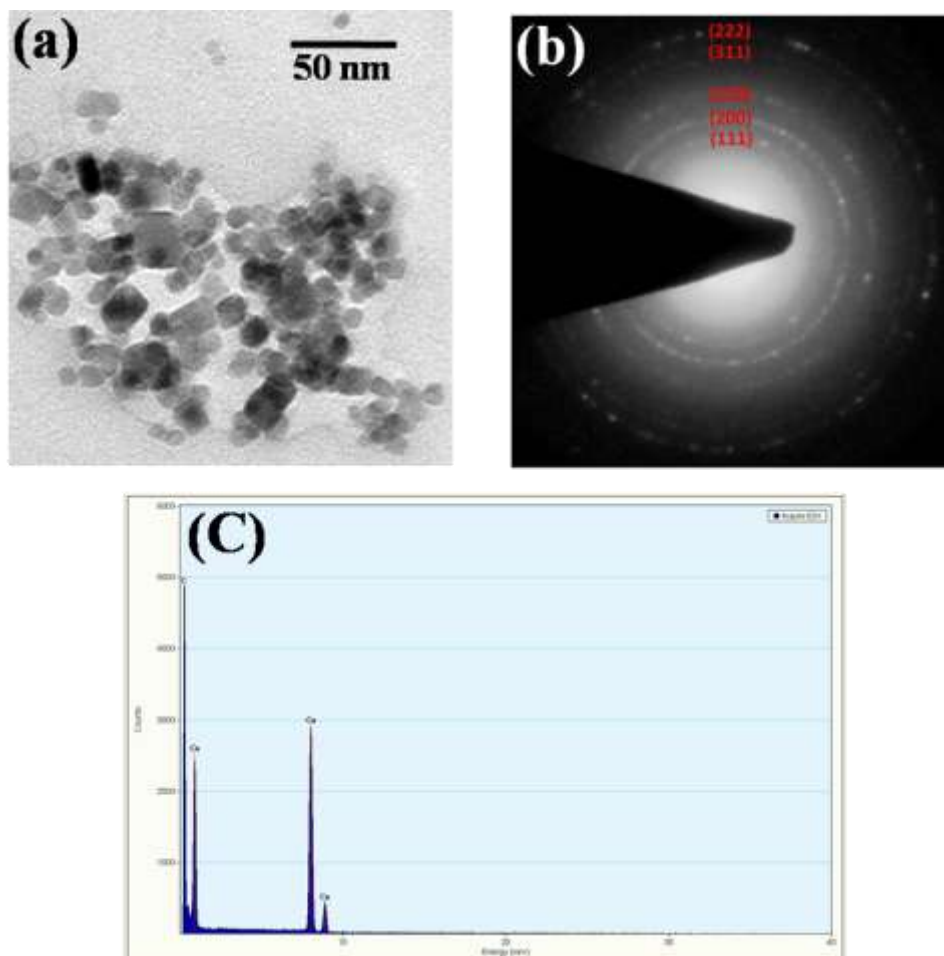


Figure 5. (a) TEM image (b) SAED and (c) EDX of the sample deposited at sputtering pressure 5 mTorr and power 30 W

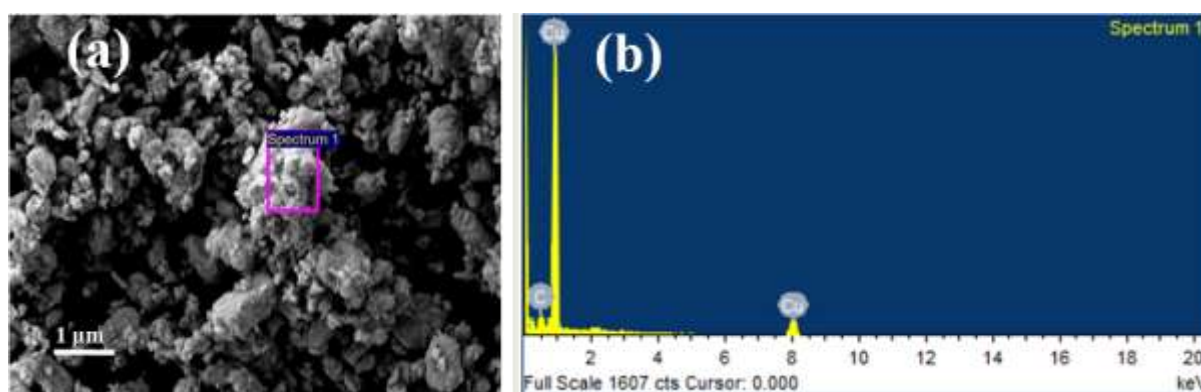


Figure 6. (a) SEM image and (b) EDX of the sample deposited at sputtering pressure 5 mTorr and power 30 W.

The optical properties of metal Cu NPs is determined by using UV-VIS diffuse reflectance spectroscopy (DRS) because DRS is more reliable for solid sample. The DRS was proposed by Kubelka and Munk. This proposed model holds for the particle size smaller or comparable to the incident wavelength. The expression for Kubelka and Munk is given by equation (6) [40-42].

$$\frac{K}{S} = \frac{(1-R_{\infty})^2}{2R_{\infty}} \approx F(R_{\infty}) \quad (6)$$

where K is the absorption coefficient, S the Kubelka-Munk scattering, $F(R_{\infty})$ the Kubelka-Munk function or remission function and $R_{\infty} = R_{\text{sample}}/R_{\text{standard}}$ the absolute reflectance.

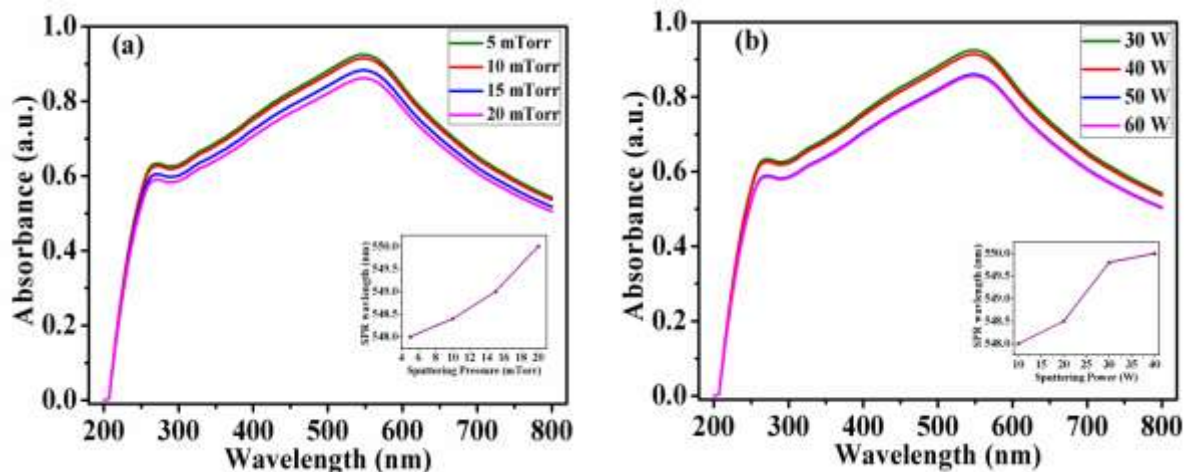


Figure 7. UV-VIS Absorbance Spectra Of All The Samples With Various Sputtering (A) Pressure At 30 W And (B) DC Power At 5mtorr

The UV-VIS absorbance spectra in the wavelength range 200-800 nm of the samples deposited with various sputtering pressures at 30W and sputtering DC power at 5 mTorr are shown in Fig. 7(a) and 7(b). The peaks in the UV-VIS absorption spectra correspond to the true surface plasmon resonance (SPR) wavelength peak because the small metal NPs exhibit the absorption of visible light by collective oscillation of conduction electrons at the surface [27, 43], which is appearing at 548 nm of the sample deposited at sputtering pressure 5mtorr and power 30 W. The least variation in the SPR wavelength peak position (550 nm) towards red shift is observed as sputtering pressure and power increases. Enhanced absorbance of ~0.93 is observed due to SPR of

Cu NPs at lower pressure 5 mTorr and power 30 Watt. Moreover, with the increment in sputtering pressure and power, degradation in absorbance is measured up to 0.85.

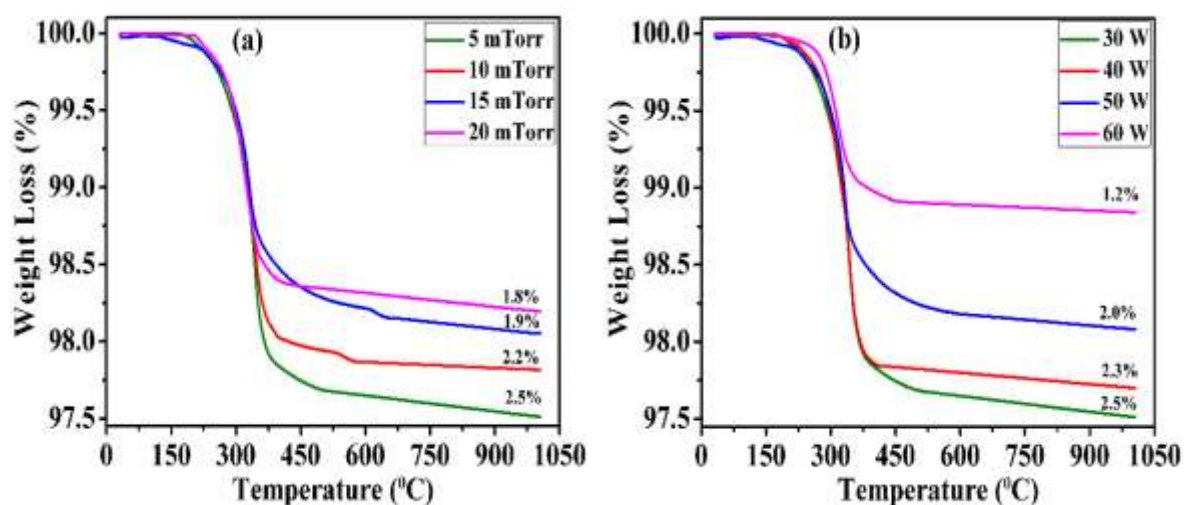


Figure 8. TGA Of All The Samples At Different (A) Sputtering Pressure At 30 W And (B) Sputtering DC Power At 5mTorr

In order to investigate the amount of water content in synthesized Cu NPs, the samples were first dried and then subjected to TGA analysis. The TGA of all the samples in the presence of nitrogen (N_2) gas in the range of 30 °C to 1000 °C with heating rate 10°C/min in non-isothermal conditions are shown in Fig. 8(a) and 8(b). It depicts that thermal decomposition process occurred in one stage for both sputtering pressures and powers. The curve clearly reveal that a continuous weight loss (~ 1.2-2.5%) occur up to 450 °C which may come from the condensation of moisture and hydroxides [44-46]. The reason of amount of water content in samples is that when the synthesized samples exposed to atmosphere after deposition, the moisture get entrapped in samples. No further weight loss occur up to 1000 °C indicating the high purity of Cu NPs. In addition, with increasing sputtering pressure and power a decrease in the mass loss is observed which can be attributed to the increased particle size. It is noted that maximum weight loss of ~2.5% which is very low. Therefore, we can say that crystalline form of Cu NPs are thermally more stable.

IV. CONCLUSION

In summary, highly pure, stable and uniform Cu NPs have been successfully synthesized by DC magnetron sputtering as confirmed by XRD, EDS, SEM and TEM. By varying sputtering pressure and power one can inhibit the particle growth, uniformity, purity and stability of the Cu NPs. Enhancement in crystallite size and lattice constant while reduction in dislocation density and lattice strain is observed as sputtering pressure and power increases. The smallest crystallite size (9 nm) and lattice constant (0.3604 nm) are obtained at lower sputtering pressure and power (5 mTorr, 30 W) while minimum dislocation density and lattice strain are obtained at higher sputtering pressure and power (20 mTorr, 60 W) of as-synthesized Cu NPs which is suitable for future use as a base of conductive ink. With increasing sputtering pressure and power, a little red shift in SPR wavelength (548-550 nm) peak and the reduction in absorbance is observed therefore the presence of non-oxidized metal NPs is also proved by the appearance of the SPR. It is noted that, at lower sputtering pressure and power absorbance is enhanced. Moreover, the effect of sputtering pressure and power on thermal properties

shows degradation in weight loss with increment in sputtering pressure and power. Maximum (2.5 %) and minimum (1.2 %) weight loss prove that as deposited Cu NPs synthesized by sputtering method are highly pure and thermally more stable.

REFERENCES

- [1] Victor I. Klimov, semiconductor and metal nanocrystals (CRC Press, 2003).
- [2] K. Lance Kelly, Eduardo Coronado, Lin Lin Zhao, and George C. Schatz, The optical properties of metal nanoparticles: the influence of size, shape, and dielectric environment, *Journal physical chemistry B*, 107, 2003, 668-677.
- [3] Shuichi Hashimoto, Daniel Werner, Takayuki Uwada, Studies on the interaction of pulsed lasers with plasmonic gold nanoparticles toward light manipulation, heat management, and nanofabrication, *Journal of Photochemistry and Photobiology C: Photochemistry Reviews* 13, 2012, 28-54.
- [4] P.K. Khanna, S. Gaikwad, P.V. Adhyapak, N. Singh, and R. Marimuthu, Synthesis and characterization of copper nanoparticles, *Materials Letters*, 61, 2007, 4711-4714.
- [5] Rafael Luque, and Rajender S. Varma, sustainable preparation of metal nanoparticles: methods and applications (Royal Society of Chemistry, 2013).
- [6] Daniel L. Fedlheim, and Colby A Foss, metal nanoparticles: synthesis, characterization, and applications (CRC Press, 2001).
- [7] Jin Z. Zhang, and Cecilia Noguez, Plasmonic optical properties and applications of metal nanostructures, *Plasmonics*, 3, 2008, 127-150.
- [8] Sabastine C. Ezugwu, *Synthesis and characterization of copper nanoparticles and copper-polymer nanocomposites for plasmonic photovoltaic applications*, Master diss., The University of Western Ontario, London, Ontario, Canada.
- [9] Ravneet Kaur, Cristina Giordano, Michael Gradzielski, and Surinder K. Mehta, Synthesis of highly stable, water-dispersible copper nanoparticles as catalysts for nitrobenzene reduction, *Chemistry-An Asian Journal*, 9, 2014, 189-198.
- [10] Mie and Beyond, optical properties of nanoparticle systems (Wiley-VCH Verlag & Co. KGaA, 2011).
- [11] Prashant K. Jain, Xiaohua Huang, Ivan H. El-Sayed, and Mostafa A. El-Sayed, Noble metals on the nanoscale: optical and photothermal properties and some applications in imaging, sensing, biology, and medicine, *Accounts Of Chemical Research*, 41(12), 2008, 1578-1586.
- [12] Xiao-Feng Tang, Zhen-Guo Yang, and Wei-Jiang Wang, A simple way of preparing high-concentration and high-purity nano copper colloid for conductive ink in inkjet printing technology, *Colloids and Surfaces A: Physicochemical and Engineering Aspects*, 360, 2010, 99-104.
- [13] Byoungyoon Lee, Yoonhyun Kim, Seungnam Yang, Inbum Jeong, and Jooho Moon, A low-cure-temperature copper nano ink for highly conductive printed electrodes, *Current Applied Physics*, 9, 2009, 157-160.
- [14] Stefan A. Maier, plasmonics: fundamentals and applications (Springer, 2007).
- [15] D. Longano, N. Ditaranto, N. Cioffi, F. Di Niso, T. Sibillano, A. Ancona, A. Conte, M. A. Del Nobile, L. Sabbatini, and L. Torsi, Analytical characterization of laser-generated copper nanoparticles for antibacterial composite food packaging, *Analytical and Bioanalytical Chemistry*, 2012.

- [16] Maurizio Muniz-Miranda, Cristina Gellini, and Emilia Giorgetti, Surface-enhanced raman scattering from copper nanoparticles obtained by laser ablation, *Journal of Physical Chemistry C*, 115, 2011, 5021-5027.
- [17] Biswajoy Bagchi, Sumit Dey, Suman Bhandary, Sukhen Das, Alakananda Bhattacharya, Ruma Basu, and Papiya Nandy, Antimicrobial efficacy and biocompatibility study of copper nanoparticle adsorbed mullite aggregates, *Materials Science and Engineering C*, 32, 2012, 1897-1905.
- [18] Nikhil V. Suramwar, Sanjay R. Thakare, and Niraj T. Khaty, One pot synthesis of copper nanoparticles at room temperature and its catalytic activity, *Arabian Journal of Chemistry*, 2012.
- [19] Thi My Dung Dang, Thi Tuyet Thu Le, Eric Fribourg-Blanc, and Mau Chien Dang, Synthesis and optical properties of copper nanoparticles prepared by a chemical reduction method, *Advances in Natural Sciences: Nanoscience and Nanotechnology*, 2, 2011, 015009.
- [20] Sudhir Kapoor, and Tulsi Mukherjee, Photochemical formation of copper nanoparticles in poly (N-vinylpyrrolidone), *Chemical Physics Letters*, 370, 2003, 83-87.
- [21] W. Abidi, and H. Remita, Gold based nanoparticles generated by radiolytic and photolytic methods, *Recent Patents on Engineering*, 4(3), 2010, 170-188.
- [22] Yoshiteru Mizukoshi, Kenji Okitsu, Yasuaki Maeda, Takao A. Yamamoto, Ryuichiro Oshima, and Yoshio Nagata, Sonochemical preparation of bimetallic nanoparticles of gold/palladium in aqueous solution, *Journal of Physical Chemistry B*, 101(36), 1997, 7033-7037.
- [23] Sulekh Chandra, Avdhesh Kumar, and Praveen Kumar Tomar, Synthesis and characterization of copper nanoparticles by reducing agent, *Journal of Saudi Chemical Society*, 18, 2014, 149-153.
- [24] Masoud Salavati-Niasari, Fatemeh Davar, and Noshin Mir, Synthesis and characterization of metallic copper nanoparticles via thermal decomposition, *Polyhedron*, 27, 2008, 3514-3518.
- [25] Masoud Salavati-Niasari, Noshin Mir, and Fatemeh Davar, A novel precursor for synthesis of metallic copper nanocrystals by thermal decomposition approach, *Applied Surface Science*, 256, 2010, 4003-4008.
- [26] Bong Kyun Park, Sunho Jeong, Dongjo Kim, Jooho Moon, Soonkwon Lim, and Jang Sub Kim, Synthesis and size control of monodisperse copper nanoparticles by polyol method, *Journal of Colloid and Interface Science*, 311, 2007, 417-424.
- [27] Praveen Taneja, Pushan Ayyub, and Ramesh Chandra, Size dependence of the optical spectrum in nanocrystalline silver, *Physical Review B*, 65, 2002, 245412-1- 245412-6.
- [28] H. Hahn, and R. S. Averback, The production of nanocrystalline powders by magnetron sputtering, *Journal of Applied Physics* 67, 1990, 1113-1115.
- [29] B. D. Cullity, elements of x-ray diffraction (Addison-Wesley Publishing Company, Inc., 1956).
- [30] Mohd Abdul Majeed Khan, Sushil Kumar, Maqsood Ahamed, Salman A Alrokayan, and Mohammad Saleh AlSalhi, Structural and thermal studies of silver nanoparticles and electrical transport study of their thin films, *Nanoscale Research Letters*, 6, 2011, 434.
- [31] Meng Zhao, Jianxing Huang, and Chung-Wo Ong, Preparation and structure dependence of H₂ sensing properties of palladium-coated tungsten oxide films, *Sensors and Actuators B*, 177, 2013, 1062-1070.
- [32] Dengyuan Song, Armin G. Aberle, and James Xia, Optimisation of ZnO:Al films by change of sputter gas pressure for solar cell application, *Applied Surface Science*, 195, 2002, 291-296.

- [33] Accarat Chaoumead, Youl-moon Sung, and Dong-Joo Kwak, The effects of RF sputtering power and gas pressure on structural and electrical properties of ITIO thin film, *Advances in Condensed Matter Physics*, 651587, 2012, 1-7.
- [34] L.T. Yan, J.K. Rath, and R.E.I. Schropp, Electrical properties of vacuum-annealed titanium-doped indium oxide films, *Applied Surface Science*, 257, 2011, 9461-9465.
- [35] P. Matheswaran, B. Gokul, K.M. Abhirami, and R. Sathyamoorthy, Thickness dependent structural and optical properties of In/Te bilayer thin films, *Materials Science in Semiconductor Processing*, 15, 2012, 486-491.
- [36] Vipin Chawla¹, R. Jayaganthan, and Ramesh Chandra, Influence of sputtering pressure on the structure and mechanical properties of nanocomposite Ti-Si-N thin films, *Journal of Materials Science & Technology*, 26(8), 2010, 673-678.
- [37] N. Martin, A.M.E. Santo, R. Sanjinés, and F. Lévy, Energy distribution of ions bombarding TiO₂ thin films during sputter deposition, *Surface and Coatings Technology*, 138, 2001, 77-83.
- [38] P. Matheswaran, B. Gokul, K.M. Abhirami, and R. Sathyamoorthy, Thickness dependent structural and optical properties of In/Te bilayer thin films, *Materials Science in Semiconductor Processing*, 15, 2012, 486-491.
- [39] W.H. Qi, and M.P. Wang, Size and shape dependent lattice parameters of metallic nanoparticles, *Journal of Nanoparticle Research*, 7, 2005, 51-57.
- [40] A. Escobedo Morales, E. Sanchez Mora, and U. Pal, Use of diffuse reflectance spectroscopy for optical characterization of un-supported nanostructures, *Revista Mexicana De Fisica S*, 53(5), 2007, 18-22.
- [41] M. El Sherif, O.A. Bayoumi, and T.Z.N. Sokkar, Prediction of absorbance from reflectance for an absorbing-scattering fabric, *Color Research & Application*, 22(1), 1997, 32-39.
- [42] Mohammad Mansoob Khan, Sajid Ali Ansari, Jintae Lee, and Moo Hwan Cho, Enhanced optical, visible light catalytic and electrochemical properties of Au@TiO₂ nanocomposites, *Journal of Industrial and Engineering Chemistry*, 19, 2013, 1845-1850.
- [43] Kitsakorn Locharoenrata, Haruyuki Sanoa, and Goro Mizutani, Phenomenological studies of optical properties of Cu nanowires, *Science and Technology of Advanced Materials*, 8, 2007, 277-281.
- [44] T. Vossmeier, L. Katsikas, M. Gienig, I. G. Popovic, K. Diesner, A. Chemseddine, A. Eychmiiller, and H. Weller, CdS nanoclusters: synthesis, characterization, size dependent oscillator strength, temperature shift of the excitonic transition energy, and reversible absorbance shift, *Journal of Physical Chemistry*, 98, 1994, 7665-7673.
- [45] Bing Huang, Min-hua Cao, Fu-de Nie, Hui Huang, and Chang-wen Hu, Construction and properties of structure- and size-controlled micro/nanoenergetic materials, *Defence Technology*, 9, 2013, 59-79.
- [46] Zhen Liu, Yang Liu, Lin Zhang, Selcuk Poyraz, Ning Lu, Moon Kim, James Smith, Xiaolong Wang, Yajiao Yu, and Xinyu Zhang, Controlled synthesis of transition metal/conducting polymer nanocomposites, *Nanotechnology*, 23, 2012, 335603.

CHALLENGES TO SCIENCE: UFOs AND EXTRATERRESTRIAL LIFE

Krishna Kriplani¹, Abhishek Singh², Shailja Singh³

^{1,2,3} Assistant Professor, Department of Applied Chemistry,
Amity University, Greater Noida Campus, U.P.(India)

ABSTRACT

Till now, there are many evidences which are found for the presence of UFO and ALIENS on our planet EARTH. Many sights are observed at the different corners of the earth, which straight away marks the presence of the UFO's and ALIENS. This research examines the evidence, which are showing the rapid growth in our technologies with the help of technological achievements of the ALIENS in their planet. This research also examines the likelihood of extraterrestrial life, and attempts to draw inferences about technological achievements on other worlds and it will also let you know about the secret operations, which is going on different selected research bases on our planet and about the projects which are responsible for control of all information and documents regarding the UFO and ALIEN subjects. It examines the involvement of intelligence agencies and security. It concludes that there is a growing case for the reality of UFOs, and that intelligent extraterrestrial life almost certainly exists. Recommendations involve expanded and more aggressive means of obtaining UFO's and ALIENS evidence, including thoughts on physical seizure.

I INTRODUCTION

Unidentified Flying Objects (UFOs) may constitute one of the most peculiar mysteries, in all the recorded history. The mystery is peculiar because the incidents related to the UFOs and ALIENS are happening repeatedly. To be confident, that there are so many mysteries such as how the species of human emerge on planet earth, how the dinosaur species extinct instantly and the major things are the construction of pyramids, forts and many more monuments which are constructed at the time when the technology is not so developed that they can be able to build tall buildings, forts in or on mountains. So, what do you think that such advanced technology had come from? At the bottom of the mystery, we have found that UFOs are fact, not fiction, they are real not imaginary, they are material object not illusion effect.

The mystery of UFOs and ALIENS are not getting resolved due to the secrecy by the agencies (like MAJESTIC-12, DIA, etc). It has also been said that the president has built a relation with ALIEN visitors according to planetary intelligence group (PI-40).

The president of USA JOHN F. Kennedy was killed by some secret agencies because he is going to tell the facts about their relationship with ALIENS and their presence on our planet. The president is killed by firing guns on him

by his driver who belongs to the group named as MAJESTIC -12 (MJ-12) and the twenty two people who are the witness of this incident died or killed (this is still a mystery) within two years. These are few examples or practices done by the secret agencies (MJ-12, DIA, CIA) because they think that if people know too much about the activities related to UFOs and ALIENS is dangerous and they can disclose the secret projects which can create a big problem to them. Accordingly, the UFO may hold the secret of great technology significance and the technology can be applied to spacecraft and aircraft which can be used for defense purposes and this truth should be faced since, there are sufficient proofs available for the existence of UFOs. For if there is sufficient proof available that UFOs are material object, then again more difficulties arise whether they are secret developments or earthly origin or UFOs are extraterrestrial, then it is a point to be concerned deeply not because of any direct attack but because UFOs on or near our planet means an advance technology in our presence. .

II RESEARCH AND DATA ANALYSIS

The phenomenon of UFOs and ALIENS seems to not to be very new, the proofs of UFO sightings are first observed in 597 BC as also written in BIBLE second solid proof of a UFO sighting is during the WORLD WAR 2nd when there is observation of strange and unidentified objects as seen during flying missions. Earlier these strange observations were taken as religious happenings, but as a matter of illustration they are viewed as comets, meteors, shooting stars etc. to draw the attention as UFO sightings. Today of course, much more is concerned for these unnatural phenomena. Meteors are concerned as a matter of elementary science, but in the early 19th century scientist do not believe in falling stones. Although the rate of UFO sightings kept on increasing from years to years. The attention towards the UFO sightings of scientist and other people increases when the term “FLYING SAUCERS” came into existence as a result of 9 UFO sightings near MOUNT RAINIER in WASHINGTON.

LACES OF UFOs CRASHES	YEAR OF UFOs CRASHES	CAUSE
1. New Mexico, USA	1947-48	Affected by new radar type
2. California, USA	1952	Unknown
3. Mexico, Sonora Desert	1955	Unknown
4. Florida, USA	1969	Affected by radar
5. Texas, Dayton, USA	1968	Unknown
6. Brazil, Metogroso	1968	Unknown
7. Uruguay, Salto	1970	Unknown
8. Brazil, Amazon	1976	Unknown
9. Argentina, Andes	1979	Unknown
10. Alaska, USA	1981	Unknown

III LIST OF SOME MAIN IMPORTANT UFOS SIGHTINGS ALL OVER THE WORLD

These are some of the UFOs crashes which have taken place till now and these activities are continuously increasing day by day in search of new technologies on earth and others planet too.

According to BLUE PLANET PROJECT which is written by some researchers who had worked on the project for the advancement of technology on our planet at the WESTCHESTER CAMP. There are almost 160 species of aliens who has approached or tried to approach our planet. Some species of aliens are stated below:-

1. GREYS, type one – These types of species only concerned about the technologies without caring about human beings. They need special type of secretions for their survivals which they get from EARTH.
2. GREYS, type two – These types of species havethe same appearance as of type one, i.e. almost four feet tall and slanted eyes. They do not require special secretions as of type one and has common sense and passiveness.
3. GREYS, type three – They are same in appearance as of type one and type two, but the only difference is they have thinner lips.
4. NORDICS, BLONDES, SWEDES -- These type of species is similar to human beings in appearance, blonde hair and blue eyes. This specie will only intervene if the GREYS were to affect us.
5. NORDIC CLONES – They are created by GREYS type one and are called controlled drones.
6. INTRADIMENSIONAL – The nature of this species is peaceful and they can assume various shapes.
7. SHORT HUMANOIDS – This specie is seen quite often near MEXICO and they are about two and a half feet tall.
8. HAIRY DWARFS – The nature of this species foundto be neutral and it's believed that they respect technological lives.
9. VERY TALL RACE – This specie is about 8feet tall and similar to human appearance and it's believed that this species are united with SWEDES.
10. MEN IN BLACKS (MIBs) -- These species does not have any relation with the DELTA and NRO government division and are like the agents of their planet. Their appearance is very similar to human beings, they used to wear black and white clothes and their eyes are sensitive to light, that's why they have vertical pupils.

Now, the research will move towards the UFOs technologies that in fact UFO vehicle come from outer space showingthat they have more advanced technology then our earth. The technology of UFOs and ALIENS are of great concern because there have continuously seen cases of UFOs sightings which suggest that they have an advanced propulsion systemwhich is far better than our system. The apparent acceleration system which they have got should be researched because it raises the question that what type of energy source (i.e. Power plants) they have, although the concept of speed and technology can be made illusive since accurate speed can't be judged without knowing the distance and the size of the object. A popular but speculate view suggests that the UFOs are not aerodynamic but are propelled by the force of gravity, but such theory denies the basic law of physics what we study and researched. This theory overcome the inherent difficulty in the way of analogy the NEWTONS Laws of motion are not proven wrong by EINSTIEN rather the letter's merely extended the Newtonian principles, following this it can be said that EINSTIEN theories do not represent the ultimate of physics. So, in short, it's hard to believe that all the basic principles of knowledge fail in the technological development which are made by ALIENS and therefore we have to accept that we have just started in terms of technological developments with the help of technologies which

are developed by ALIENS. The main thing that we have to alter our laws according to the development of technology.

IV CONCLUSION

For many years , the sightings of UFOs and ALIENS has continued in many areas and UFOs are not the artificial objects these are the vehicles used by the ALIENS to travel from one place to another at a greater speed than we can travel.

1. We know that in our solar system, there are not single planets where life can exist (but the research is going on) so the UFOs and the ALIENS must have come from another point of our GALAXY or UNIVERSE.
2. If the ALIENS are from other point of our GALAXY that it is also possible that there are many more planets just like EARTH or more compatible for living.
3. As far as the UFOs sightings are concerned, then if ALIENS can travel from one galaxy to other than just think that how much technology they have developed that we can't think of.
4. In coming years the UFOS sighting going to be increased because as we are curious to know about other compatible planet for living and in search of another living organism just like or unlike us living in this UNIVERSE.
5. As far as this research is concerned, then the most of the area of the USA are acting like base for ALIENS and for them also to exchange the technology in exchange to allow the ALIENS to experiment such as cattle mutilation and the study of human genetics and many more things which are going to harm human species.

V ACKNOWLEDGEMENT

KK, AS and SS are thankful to Amity University, GreaterNoida Campus, U.P. for constant help and support.

REFERENCES

- [1] Adamski, George. "Inside the Space Ships. New York: Schuman, 1955.
- [2] Aime', Michael, "Flying Saucers and the Straight Line Mystery". New York, N.Y.; Criterion Books, 1958.
- [3] Asimov, I. "UFO's--What I Think." Science Digest, Vol. 59, 7 June 1967, P. 44.
- [4] Edwards, Frank. "Flying Saucers-Serious Business", New York, N.Y.: Lyle Stuart, 1966.
- [5] Firsoff, V. A. "Life Beyond the Earth." New York, N.Y.: Basic Books,-Inc., 1963.
- [6] "Flying Saucers from Earth," Science News, Vol. 91.13 May 1967, p. 452.
- [7] Hall, Richard H. "The UFO Evidence." Washington D.C.: NICAP, 1964.
- [8] Hellan, H. "A New Look at the UFO Enigma," Science Digest, Vol. 80, No. 5., November 1967, pp. 9-15.

- [9] Lear, J. "Research in America--What are the Unidentified Aerial Objects?," Saturday Review Vol. 49, 6 August 1966, pp. 41-52.
- [10] Menzel, Donald H. and Boyd, Lyle G. "The World of Flying Saucers: A Scientific Examination of a Major Myth of the Space Age." Garden City, New York: Doubleday, 1963.
- [11] Markowitz, W. "Physics and Metaphysics of Unidentified Flying Objects," Science, Vol. 157, 15 September 1967, pp. 1274-1284.
- [12] "Other Planets, Other Voices?" Advertiser-Journal, Montgomery, Alabama, 5 December 1967, p. 7.
- [13] Ruppelt, Edward J. "The Report on UFO." Garden City, New York: Doubleday, 1956.
- [14] Rodgers, Warren. "Flying Saucers," Look, Vol. 31, No. 6, 21 March 1967, pp. 76-80.
- [15] Sagan, Carl, Dr. "Intelligent Life in the Universe," San Francisco, California: Holden Day, Inc., 1966.
- [16] Sullivan, Walter. "We Are Not Alone." New York, N.Y.: McGraw-Hill Book Co., 1966.
- [17] Unger, George. "Flying Saucers: Physical and Spiritual Aspects." East Grinstead, England: New Knowledge Books, 1958. "UFOs and the Law of Physics," Saturday Review, Vol. 50, 7 October 1967, p. 59.
- [18] "Well Witnessed Invasion by Something," Life, LX, 1 April 1966, pp. 24-31.
- [19] Wilkins, Harold T. "Flying Saucers Uncensored." New York, N.Y.: The Citadel Press, 1955.
- [20] Whitney, David C, "Flying Saucers," Look Special, 1967, pp- 3-67.

UTILIZATION OF TUNGSTEN COPPER ELECTRODE IN MACHINING CHARACTERISTICS ANALYSIS ON EDM FOR INCONEL 718 MATERIAL

Kishor. A¹, J. Arun², Shailja Singh³

^{1,3}Assistant professor, Department of Applied Chemistry, Amity University, Noida, (India)

²Assistant Professor, Angel College of Engineering and Technology, Tirupur, (India)

ABSTRACT

Electrical discharge machining methodology (EDM), the procedure parameters, for example, pulse on time, pulse off time, top present, flushing weight alongside instrument geometry are of incredible criticalness on the grounds that they unfavorably influence the exactness of machined features¹. This paper shows the impact of each one data parameters for exploring the impact of individual parameters on MRR, TWR and SR on Inconel718 on machining with EDM utilizing tungsten copper terminal. The exploratory results demonstrate that the beat on time and crest current are the impacting parameters specifically relative to MRR and conversely corresponding to TWR, SR².

Keywords: *Electrical Discharge Machining (EDM), Material Removal Rate (MRR), Tool Wear Rate (TWR), Surface Roughness (SR)*

I. INTRODUCTION

EDM is the methodology of machining hard metals which are can't be machined utilizing ordinary machining procedure. This system was produced in the late 1940s, has been acknowledged worldwide as a standard process in assembling of structuring apparatuses. EDM discover a wide application in the machining of hard metals¹. EDM is essentially utilized as a part of commercial enterprises like model creation, coinage bite the dust making and in little gap boring. In EDM the principle calculates that impact the machining procedure are crest current and heartbeat on time, which indicates more noteworthy impact in advancing alternate parameters like SR, TWR, MRR however it is hard to clarify the impact of top current and pulse on time on those parameters³. Inconel718 is a high nickel substance combination.. Inconel718 was produced to address the requirement for a nickel-base amalgam suitable for assembling into complex formed segments subject to a blend of high temperature, high push, and high temperature erosion. The inconel718 material is principally utilized as a part of aviation, rocket and marine businesses. In this exploration copper cathode apparatus is made into roundabout, square, rectangle and circle shape which is machined by wire slice EDM to get precise measurements.

II. MATERIALS AND METHODS

Inconel718 material is made into sheets of obliged measurements utilizing wire cut EDM process. At that point the penetrating procedure (through gap operation) is carried out on Inconel718 material utilizing tungsten

copper cathode of distinctive shapes circle, triangle, rectangle and square. The machining is carried out on evaluation EMS 5050 of EDM machine, lamp oil utilized as a dielectric liquid. The info parameters are crest current (4,9,12,17a), beat on time (10,25,40,60 μ s), heartbeat off time (3,5,7,9 μ s) and flushing pressure (23,20,29,18kgf/ cm²) with the device states of circle, triangle, square and rectangle are picked , different parameters are kept steady. In view of the quantity of information parameters and their levels L16 orthogonal show is chosen and the parameters are masterminded by cluster as indicated in table.1.

After the machining methodology both apparatus and work piece ought to be cleaned utilizing compressed air firearm to uproot dust particles and dielectric liquid then both the device and work piece ought to be measured utilizing exact measuring machine. The yield reactions of MRR, TWR and Sr4 are computed after lead the trials according to L16 orthogonal cluster.

Exp.No	Pulse on time		Pulse off time		Current		Flushing pressure		Tool geometry		Output parameters			
	T	O N	T	O F F	A		P		g e o m e t r y	M R R	T W R	S R	Machining time	
	μ	S	μ	S	Ampere		K g f / c m ²		G e o	mm ³ /min	mm ³ /min	μ m	M i n u t e	
1	1	0	3		4		1	8	c i r c l e	0.178	0.003	3.053	1 4 1 2 . 0 8	
2	1	0	5		9		1	9	s q u a r e	8.456	0.022	3.382	2 9 . 9 7	
3	1	0	7		1	2	2	0	r e c t a n g l e	8.514	0.044	3.943	2 9 . 0	
4	1	0	9		1	7	2	3	t r i a n g l e	12.417	0.064	3.885	2 0 . 2 6	
5	2	5	3		9		2	0	t r i a n g l e	12.867	0.000	3.608	1 5 0 . 5 3	
6	2	5	5		4		2	3	r e c t a n g l e	1.695	0.132	5.514	1 9 . 6 4	
7	2	5	7		1	7	1	9	s q u a r e	19.839	0.026	4.849	2 4 . 6 7	
8	2	5	9		1	2	1	9	c i r c l e	10.194	0.102	5.537	1 2 . 7 4	
9	4	0	3		1	2	2	3	s q u a r e	13.308	0.000	3.532	3 8 9 . 6 3	
1 0	4	0	5		1	7	2	0	c i r c l e	14.970	0.034	3.065	1 8 . 9 0	
1 1	4	0	7		4		1	9	t r i a n g l e	0.642	0.038	3.998	1 6 . 8 8	
1 2	4	0	9		9		1	8	r e c t a n g l e	0.681	0.032	5.379	3 6 9 . 5 4	
1 3	6	0	3		9		1	9	r e c t a n g l e	23.168	0.000	3.283	6 1 . 2 0	
1 4	6	0	5		1	7	1	8	t r i a n g l e	22.138	0.017	3.594	3 7 . 6 6	
1 5	6	0	7		9		2	3	c i r c l e	6.776	0.120	3.978	1 0 . 8 6	
1 6	6	0	9		4		2	0	s q u a r e	0.411	0.114	4.009	1 1 . 3 6	

Table 1: Result analysis

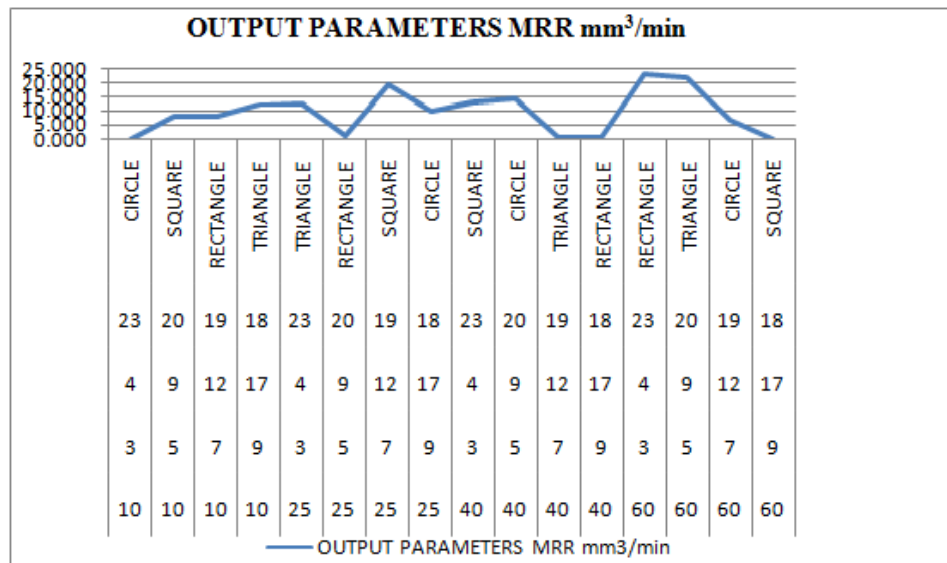


Fig.1 Output Parameters of MRR

III. RESULTS

From table 1, we can comprehend that the material evacuation rate is high when the crest current is at 17a, TON is at 25μs, TOFF is at 7μs with square formed cathode having flushing weight of 20 kgf/cm². Thus the ideal parameters are noted⁷.When we consider TWR it is least when TON is 10μs,toff is 3μs, crest current is at 4a with flushing weight 18 kgf/cm²,with the circle as best shape. On the off chance that we consider surface unpleasantness it is discovered to be least when TON is 10μs, TOFF 3μs which is having a top present of 4a with flushing weight 18kgf/cm², having best shape as circle.

IV. CONCLUSION

At the point when EDM procedure is viewed as the MRR is to be at most extreme, where TWR, SR is to be least. At long last for an ideal machining TON is to be 25μs , TOFF is to be 7μs, with the flushing weight is at 17 kgf/cm², having crest present of 19.

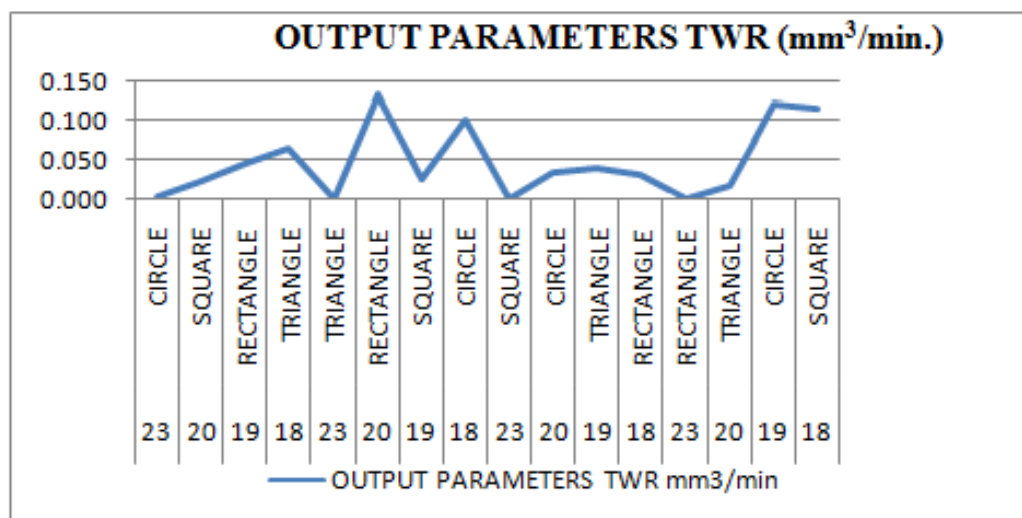


Fig. 2 Output parameters of TWR

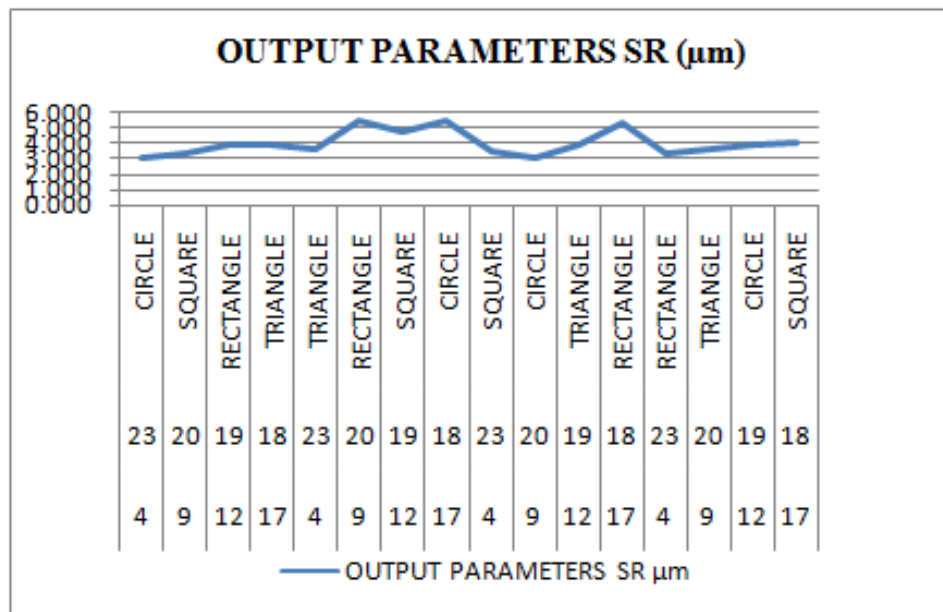


Fig. 3 Output parameters of SR

V. REFERENCES

- [1] Dr. Kumar et-al, “*selection of machining parameters based on the analysis of surface roughness and flank wear in finish turning and facing of inconel 718 using taguchi technique*”
- [2] SanjeevKumar et-al, “*Surface modification by electrical discharge machining*”
- [3] Prof. D.V.Ghewade, Mr. S.R.Nipaniakar “*experimental study of electro discharge machining for inconel material*”
- [4] Krishna Mohan Rao, G.; Satyanarayana, S.; Praveen, M.(2008): “*Influence of machining parameters on electric discharge machining of maraging steels-An experimental investigation, Proceeding of the world congress on Eng., Vol. II*”
- [5] O. Yilmaz et-al, “*A comparative investigation of the effects of single and multi-channel electrodes in EDM fast hole drilling of aerospace alloys*”.

SITES AND SCOPE OF RECYCLING SOLID WASTE IN DELHI AND NCR

Chitra Kumar¹, Rishav Kumar², Shalini Jaiswal³

^{1,2,3} Assistant Professor, Department of Applied Chemistry,
Amity University, Greater Noida Campus, (India)

ABSTRACT

Municipal Solid waste management (MSWM) has become an acute problem due to enhanced economic activities and rapid urbanization. Solid waste, which is an outcome of the day-to-day activity of human kind, needs to be managed appropriately. We face trouble coupled with poorly managed solid waste operation. The irrational management of Solid Waste management has led to serious environmental hazards, which lead to a decline in quality of life in urban areas. Delhi generates about 7000-8000 metric tonnes of solid waste every day, which is likely to be increased to 20,000 metric tonnes/year by 2021. Amount of waste generated by an individual is about 600 gm which is almost 5-6 times the national average. To handle this problem in a safe manner various efforts have been made by the Government. In Delhi city, the waste generated is not collected in a proper manner for its proper disposal. The inappropriate disposal of waste is responsible for depletion of water, air, land and also risks to human health. To solve these problems proper disposal methods like land filling, composting, recycle is required. This paper represents the total amount of waste generated during a year, their impact on the environment along with human beings and solid waste management strategy of highly populated and polluted Delhi city.

Keywords: Composting Plant, Impact Of Solid Waste On Environment And Human Beings, Municipal Solid Waste, 7000-8000T/Day In Delhi City, , Solid Waste Management Strategy In Delhi

I. INTRODUCTION

The waste quantity in India is increasing at a shocking rate due to fast urbanization and a high population growth. The population growth rate in India last decade was 17.6%¹. Municipal Solid Waste management involves the collection, storage, transportation, treatment and efficient disposal of waste scientifically. Municipal Solid Waste management planners face crucial problems due to enhanced economic activities and rapid urbanization. These are the consequence of day-to-day activity of human kind, needs to be managed properly. The irrational management of Solid Waste management has led to serious environmental hazards, which lead to a decline in quality of life in urban area².

II. GENERATION OF SOLID WASTE IN DELHI CITY

Delhi city is facing an imminent disaster due to improper disposal of the waste. The improper disposal of the waste results to various health hazards and environmental problems. The best way to deal with these problems is

to find the alternative site to dump the garbage generated by the city. Another way is to convert it into the energy or any other using byproduct using certain eco-friendly techniques. Delhi generates about 7000-8000 metric tones of solid waste every day, which is likely to be increased to 20,000 metric tones\year by 2021.Amount of waste generated by an individual person in Delhi city is about 600 gm which is almost 5-6 times the national average. Thesolid waste can be combustibile like paper,plastics, yard debris, food waste, wood, textiles, disposable diapers, bones, leather and Non-combustibles like glass, metal, and aluminum³. The composition of waste depends on a broad range of factors like food habits, cultural traditions, lifestyles, climate andincome, etc.⁴The major waste generating sites in Delhi region are commercial markets, hospitals, slaughter houses, industries and construction sites.SWM is disposed off through three landfills located at:

- (a) Bhalswa -nearly 2700 MT/day
- (b) Okhla- nearly 1200 MT/day
- (c) Gazipur - nearly 2100 MT/day

The above mentioned sites are under the category of uncontrolled SWM disposal facility. The generation of methane in the uncovered areas is causing smoldering surface fires.

2.1 Area of Sanitary Land Fill Sites

The existing Sanitary Land Fill Sites in Delhi region is 03-

- 1. Ghazipur (70Acres),
- 2. Okhla (56Acres),
- 3. Bhlasawa (40Acres)

And proposed sites is 02-

- 1. Jaitpur (26 Acres)
- 2. Bawana (150 Acres)

2.2 Sources of Waste Generation

Name	Content	Source
Garbage	produces from cooking of food and domestic work contents	House holds and hotels, etc.
Rubbish	Markets refuse rags cloth and leather	Stores and markets, etc
Ashes	Residue form	Fire
Bulk	Large auto parts, gyres, etc	Service station
Street refuses	Dust and dirt	Street sweepings and litter, etc.
Special waste	Hazardous waste	Hospitals and industry

III. IMPACT OF SOLID WASTE

3.1 Increase Disease Transmission

Incinerator and Landfill sites are responsible for different kind of human health problem like birth defects, cancers and respiratory illnesses which includes asthma.

3.2 Ground and Surface Water Pollution

Municipal solid waste produces harmful materials and micro-organisms into dumps sites and landfills. The harmful materials and micro-organisms after entering into dumps sites and landfills produces leachate (liquid substance) that is composed of rotted organic waste, liquid wastes, infiltrated rainwater and extracts of soluble material. This leach ate can contaminate soil and water when landfill is unlined.

3.3 Global warming and Air Pollution

After disposing organic wastes into dumps sites or landfills, they decomposed in absence of oxygen and generated methane which can trap atmospheric heat 21 times more as compare to CO₂. At the same time burning of garbage generates great amount of smoke that is composed of carbon monoxide, soot and nitrogen oxide, all of them dangerous to human health and air Pollution. Burning of polyvinyl chlorides (PVCs) generates highly carcinogenic dioxins.

3.4 Ecosystems Damage

The solid waste which is into dumped aquatic ecosystem like rivers or streams is responsible for damage of biodiversity because the high nutrient content of organic wastes reduces DO (dissolved oxygen) of rivers or streams that is necessary aquatic life form. Solid waste is also responsible for sedimentation, change stream flow and bottom habitat.

3.5 Damage to people

The slums or shanty towns which are situated close to open dumps or functional landfills can be destroyed or kill the residents. The accumulation of waste along streets may cause physical hazards, clog drains and cause localized flooding.

3.6 Loss of Tourism and Business

The unpleasant smell and uncollected solid waste by the side of streets, fields, forests and other natural areas discourage tourism and the establishment of businesses.

IV. PROBLEMS FOR MANAGEMENT OF MUNICIPAL SOLID WASTE

The key problems for the management of municipal solid waste are:

- -Mixing of waste
- -Collection and storage of waste
- -Transportation of waste
- -Indiscriminate burning of waste
- -Illegal disposal of waste

V. SOLID WASTE MANAGEMENT STRATEGY OF DELHI CITY

5.1 Involved Agencies

For solid waste management in Delhi various agencies were involved, some of which are mentioned below:

MCD (Municipal Corporation of Delhi)

NDMC (New Delhi Municipal Council)

DCB (Delhi Cantonment Board)

MCD single-handedly manage roughly 95 % of the total area of the city. The above authorities are supported by a number of other agencies like DDA, DEDA, DA, DNES, MoEF etc. The Delhi Development Authority (DDA) is responsible for siting and allotment of land to MCD for sanitary land filling. Delhi Energy Development Agency (DEDA) is responsible for generation of bio- gas or energy from solid waste utilization with the help of Department of Non-Conventional Energy Sources (DNES), and Ministry of Environment and Forests (MoEF). The Department of Flood Control of Delhi Administration looks after the supply of soil to be used as cover for sanitary landfills by the MCD.

5.2 Collecting Methodology

The following steps were followed in collection of solid waste:

1. Identification of the site: For the identification of the site various field visits arranged to each to identify, quantify the amount of waste generated.
2. After identifying waste disposal site, the details of site like quantity and quality of waste, age of dump site, site location was recorded. The area and the height of dump site were also recorded.
3. Then these sites were assessed, prioritized and ranked according to the potential of population. Further the waste type, land environment, health issues were recorded and ranked as per Environment Impact Assessment (EIA).
4. To identify the water environment water sampling was carried out. For this, about 0.5km radius of the dumpsite near water bodies were identified and samples were collected. For this purpose, the pre-cleaned PVC (1L capacity) cans were used. Water collected was allowed to flow for 4-6 minutes, before collecting into the cans.
5. The proper labeling of cans were done with some information like date, time, location of collection. For hard metals, 3ml of the nitric acid was used as a preservative to the cans and then the cans were transferred to the laboratory for sampling.
6. For identification of the soil environment, soil sampling was carried out. For this the soil samples from the dumpsites were collected from about the depth of 15-25 cm. The soil was stored in a thick polyethylene covers which were properly labeled with information like the date, time and location, then it was transferred to the laboratory for sampling.

5.3 Waste Collection System

5.3.1 MCD

-Collection from Dhalao

-Improvements in practices

- Door to door Collection
- Segregation from 1.1.2004
- Privatization of collection for collection & transportation in some zones (Karol Bagh Zone, West Zone, Central Zone, South Zone, City Zone and SP Zone).

5.3.2 NDMC

- Segregation and road side collection of sweeping waste
- Mechanization of sweeping at least in VVIP areas
- Door to Door Collection

5.4 Management of Solid Waste

5.4.1 Recycling & Reuse

In this method waste material is collected, reprocessed or remanufactured and are reused. The separation for recycling takes place in households, the public bins, open dumps, etc. The recycling industry is a complex chain of operations and changes from place to place. The recycle and reuse division of waste organization in Delhi city is potentially high.

5.4.2 Sanitaryland-filling

To avoid dangerous effects of abandoned dumping of solid waste Sanitary landfill is used. Sanitary landfill is a specially engineered area of land.⁶ Through appropriate site choice, groundwork and administration, operators, they can minimize the effects of polluted water on landfill and gas production both in the current and in the future. This choice is appropriate when the ground is accessible at a reasonable price. Human and technological assets available are to drive and handle the site. If this possible, then there is no need to produce a great amount of electricity by additional methods. This leads to decrease of generation effluents from power stations.

5.4.3 Composting

Composting is a natural process of breakdown, which worked out in the controlled environment of aeration, temperature, humidity. In composting waste is converted into humus-like matter by the action of microorganism in the presence of air. The ultimate product is stable, odour-free, does not attract flies and is a good soil conditioner, if composting done effectively.⁷ If sufficient skilled manpower and apparatus are accessible, then centralized composting plant for division can be undertaken. So initially at household level and small level composting practices could be successful possible.

5.4.4 Incineration

The restricted burning of waste in a rationale build capability is known as Incineration. Incineration sterilizes, stabilizes and reduce (1/4 of the original) the volume of waste. Most of the combustible material is converted into carbon dioxide and ash. A broad test programme was conducted by Bhide and Sundaresan in 1984 which reveals that the calorific value of most of the waste is 3350 joules/g⁸. Incineration method is used when composition combustible material, paper or plastics is high in solid waste.

Incineration requires a suitable machinery, infrastructure, and expert manpower to function and retain the plant. In most of the Indian cities, Incineration is usually restricted to hospital and other biological wastes.

5.4.5 Anaerobic Digestion (Gasification)

In this process waste is burnt in a reactor at high temperature and absence of oxygen. Due to burning in a reactor the bulk of the organic substance of waste is converted into CO, CH₄, hydrogen.⁹ Lastly the gases are burnt to generate heat, which is generally used to produce electricity. The residual ash can be reused or sent to landfill.

5.5 Composting Plant

5.5.1 MCD Plant at Bhalaswa Sanitary Land Fill site

Capacity 500 MT/day

Composting is being done for 350-400 MT/day¹⁰

5.6 Status of Waste to Energy Plants in Delhi

Authorization is given by DPCC for following 3 new plants for conversion of Solid waste into RDF for generation of power.

- (a) Timarpur: 650 Tons per day MSW giving 225 Tons per day RDF.
- (b) Okhla Plant : 1300 Ton per day MSW giving 450 Tons RDF.
- (c) Ghazipur: 1300 Ton per day MSW giving 450 Tons RDF.

5.7 Status of Power Generation in Waste to Energy Plants in Delhi

- (a) Okhla Plant: 16 MW power generation from 450 Tons per day RDF from Okhla Plant + 225 Tons per day RDF from Timarpur Plant + Biogas from Bio-methanation Plant (100 Tons per day) at Okhla using segregated green waste.
- (b) Ghazipur Plant: 10 MW power generation from 450 Tons RDF production from same plant.

5.8 Status of Waste to Compost Plants in Delhi by ILFS-Eco Smart

Consent to Establish given by DPCC for following two compost plants:

- (a) Okhla Plant: 200 Tons per day MSW.
- (b) APMC Tikri Plant: Upgrading from 125 Tons per day to 200 Tons per day for food and vegetable waste.

IV. CONCLUSION

In the numerous part of the Delhi city and NCR there is a enormous raise of solid wastes and inaccurately disposal of the solid wastes are also observed. The solid wastes are being discarded in the vicinity of human surroundings. Delhi generates about 7000-8000 metric tones of solid waste every day, which is likely to be increased to 20,000 metric tones/year by 2021. Amount of waste generated by an individual is about 600 gm which is almost 5-6 times the national average. The dumped wastes largely had kitchen waste, paper, glass, cloth and construction wastes which includes sand, bricks, concrete blocks, and rock cuttings. Further wastes from the poultry, slaughter house, hospital and vegetable markets were also found dumped. The inappropriate disposal of

waste responsible for depletion of water, air, land and also risks to human health. The key problems for the management of municipal solid waste are, Mixing of waste, Collection and storage of waste, Transportation of waste, Indiscriminate burning of waste, Illegal disposal of waste etc. For solid waste management in Delhi various agencies were involved, some of which are MCD, NDMC, DCB etc. MCD single-handedly manage roughly 95 % of the total area of the city. The Delhi Development Authority (DDA) is responsible for siting and allotment of land to MCD for sanitary land filling. Delhi Energy Development Agency (DEDA) is responsible for generation of bio- gas or energy from solid waste utilization with the help of Department of Non-Conventional Energy Sources (DNES), and Ministry of Environment and Forests (MoEF). To solve these problem proper disposal methods like land filling, composting, recycle is required.

REFERENCES

- [1] Census of India, Ministry of Home Affairs, Government of India, New Delhi, India, 2011.
- [2] N.Abbasi, S.M.Tauseef, and S.A.Abbasi, Anaerobic digestion for global warming control and energy generation-An overview. *Renew,Sustain. Energy Rev.* 16,2012, 3228-3242.
- [3] Denison, R.A. & Ruston, J. 1990. Recycling and Incineration, Island Press, Washington D.C., Dorchester Press, DPR , *Solid waste management*, ISBN: 1-01-502772-5,2009, 1-10.
- [4] S.Gupta,K. Mohan, R.Prasad, S.Gupta, and A. Kansal, Solid waste management in India: options and opportunities Resources,*Conservation and Recycling*, 24 (2),1998, 115 137.
- [5] A.D.Bhide and B.B.Sundaresan, Solid waste management in developing countries, Indian National Scientific Documentation Centre,(New Delhi,India, 1983).
- [6] A.Bagchi , Design of Landfills and Integrated Solid Waste Managemen,(Wiley, Hoboken, 2007),
- [7] G.Finnveden,Solid wastetreatment within the framework of life-cycle assessment- Metals inmunicipal solid waste landfills, *Journal of Life Cycle Assessment*, 1, 1996,74-78.
- [8] G.Hamer, Solid waste treatment and disposal-effects on public health and environmental safety, *Biotechnology Advance*; 22, 2003,71-79.
- [9] J.Jin,Z. Wang ,S. Ran, Solid waste management in Macao: practices and challenges, *Journal of Waste Management*, 26,2006 ,1045-1051.
- [10] A .M.Schiopu, I.Apostol , M.Hodoreanu and M.Gavrilescu, Solid waste in Romania-management, treatment and pollution prevention practices, *Environmental Engineering and Management Journal*, 6, 2007, 451-465.

RIDE PERFORMANCE ANALYSIS OF HALF CAR VEHICLE DYNAMIC SYSTEM SUBJECTED TO DIFFERENT ROAD PROFILES WITH WHEEL BASE DELAY AND NONLINEAR PARAMETERS

Mr. Sushant S. Patole¹, Prof. Dr. S. H. Sawant²

¹*P.G. Student, Department of Mechanical Engineering, Dr. J.J.M.C.OE., Jaysingpur, (India)*

²*Professor, Department of Mechanical Engineering, Dr. J.J.M.C.OE., Jaysingpur, (India)*

ABSTRACT

The purpose of a vehicle suspension system is to improve ride comfort and road handling. Vehicle dynamic analysis has been a hot research topic due to its important role in ride comfort, vehicle safety and overall vehicle performance. For proper designing of suspension system, nonlinearities in suspension system parameters must be considered. In this paper, nonlinearities of spring and damper are considered while preparing half car model. The current article is simulated and analyzed the handling and ride performance of a vehicle with passive suspension system Half Car Model with Four Degree of Freedom. Since, the equations of the system cannot be solved mathematically has developed a scheme in MATLAB/Simulink that allows analyzing the behavior of the suspension system for different road profiles.

Keywords: *4 DoF, Half Car Model, MATLAB /Simulink, Passive Suspension System.*

I. INTRODUCTION

The vibration of vehicle and seat leads to fatigue of driver and decreases driver safety and operation stability of vehicle. Hence developing improved suspension system to achieve high ride quality is one of the important ride challenges in automotive industry. Therefore the goal of vehicle suspension systems is to decrease the acceleration of car body as well as the passenger seat. In reality, some of the vehicle parameters are with uncertainties, so that it is an important issue to deal with vehicle suspension subjected to uncertain parameters in engineering application [1].

The vehicle suspension system differs depending on the manufacturer which ensures a wide range of models. Whichever solution is adapted to design, a suspension system has the primary role to ensuring the safety function. It is known that road unevenness produce oscillations of the vehicle wheels which will transmitted to their axles. It becomes clear that the role of the suspension system which connect the axles to the car body is to reduce as much vibrations and shocks occurring in the operation. This causes the necessity to use a suspension of a better quality. A quality suspension must achieve a good behavior of the vehicle and a degree of comfort depending on the interaction with uneven road surface [2, 3].

When the vehicle is requested by uneven road profile, it should not be too large oscillations, and if this occurs, they must be removed as quickly. The design of a vehicle suspension is an issue that requires a series of

calculations based on the purpose. Suspension systems are classified in the well-known terms of passive, semi-active, active and various in between systems[4]. Passive systems are the most common. Suspension is subjected to various road conditions like a single step road profile, brake and release maneuver, sinusoidal road profile with pitching, heaving and mixed model excitation, broad band road profile etc. at constant or variable speed[5]. The measurement of road surface qualities is one of the important opportunities of vehicle manufactures all over the world. The operations of the measuring devices depend mainly on the use of displacement transducers [6]. This paper deals with the analysis of the vibrational effect when the vehicle is subjected to different road profiles. For this purpose half car vehicle model with linear and nonlinear parameters is developed. For analysis Hyundai Elantra 1992 half car model with front suspension is experimented for different road profiles.

II. THE MATHEMATICAL MODEL OF HALF CAR SUSPENSION SYSTEM

The system shown in Fig.1 is half car system where m_s - Sprung Mass, m_{uf} - Front Unsprung Mass, m_{ur} - Rear Unsprung Mass, k_f - Front Suspension Stiffness, k_r - Rear Suspension Stiffness, c_f - Front Suspension Damping Coefficient, c_r -Rear Suspension Damping Coefficient, k_t -Tyre (195/65R15) Stiffness, c_t -Tyre (195/65R15) Damping Coefficient, r - Radius of Gyration, b -Wheel Base.The model comprises of sprung mass and two unsprung masses. The x_s denotes the vertical displacement (bounce) at the center of gravity and θ is the pitch of the sprung mass. The front and rear displacements of the unsprung masses are denoted by x_{uf} and x_{ur} . In this model, the disturbances q_f and q_r are caused by road irregularities.

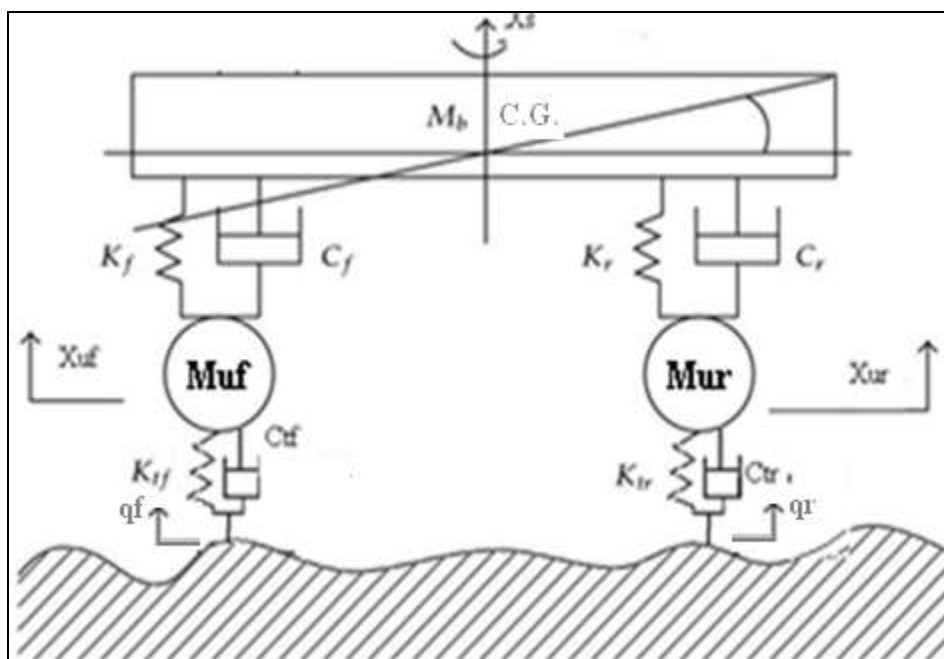


Fig.1: 4DoF Half Car Vehicle Model

The equations of motion can be obtained using the Newton's second law for each of the two masses in motion. These will be:

$$m_s \ddot{x}_s + k_f (x_s - l_f \theta - x_{uf}) + c_f (\dot{x}_s + l_f \dot{\theta} - \dot{x}_{uf}) + k_r (x_s + l_r \theta - x_{ur}) + c_r (\dot{x}_s + l_r \dot{\theta} - \dot{x}_{ur}) = 0 \quad \dots (1)$$

$$I\ddot{\theta} - k_f(x_s - l_f\theta - x_{uf})l_f - c_f(\dot{x}_s - l_f\dot{\theta} - \dot{x}_{uf})l_f + k_r(x_s + l_r\theta - \dot{x}_{ur})l_r + c_r(\dot{x}_s - l_r\dot{\theta} - \dot{x}_{ur})l_r = 0 \quad \dots (2)$$

$$m_{uf}\ddot{x}_{uf} + k_{tf}(x_{uf} - q_f) + c_{tf}(\dot{x}_{ur} - \dot{q}_f) + k_f(-x_s + l_f\theta + x_{uf}) + c_f(-\dot{x}_s + l_f\dot{\theta} + \dot{x}_{uf}) = 0 \quad \dots (3)$$

$$m_{ur}\ddot{x}_{ur} + k_{tr}(x_{ur} - q_r) + c_{tr}(\dot{x}_{ur} - \dot{q}_r) + k_r(-x_s - l_r\theta + x_{ur}) + c_r(-\dot{x}_s - l_r\dot{\theta} + \dot{x}_{ur}) = 0 \quad \dots (4)$$

Where,

$$q_f(t) = q_r(t + \tau_w)$$

$$\text{and, } \tau_w = \text{Time Delay} = \frac{\text{wheel base (b)}}{\text{vehicle velocity (v)}} = \frac{2.5 \times 3600}{1000 \times 40} = 0.225$$

By introducing nonlinearities in mass, suspension spring, damper and tyre, the equations of motion for body bouncing motion for nonlinear passive model are,

$$f_{Is} = -f_{sf} - f_{df} - f_{sr} - f_{dr} - m_{sg}$$

$$t_{Is} = t_{sf} + t_{df} - t_{sr} - t_{dr}$$

$$f_{Iuf} = -f_{stf} - f_{dtf} + f_{sf} + f_{df}$$

$$f_{Iur} = -f_{str} - f_{dtr} + f_{sr} + f_{dr}$$

In order to analyze the behavior of the half car suspension system model is simulated in MATLAB/Simulink.

The input parameters are as follows,

Table 1: Suspension Parameters for Hyundai Elantra 1992 Half Car Model

Sprung Mass (m_s)	515.45 Kg
Front Unsprung Mass (m_{uf})	23.61 Kg
Rear Unsprung Mass (m_{ur})	28 Kg
Front Suspension Stiffness (k_f)	12.394 kN/m
Rear Suspension Stiffness (k_r)	14.662 N/m
Front Suspension Damping Coefficient (c_f)	1.3854 kN-sec/m
Rear Suspension Damping Coefficient (c_r)	1.6352 kN-Sec/m
Tyre (195/65R15) Stiffness (k_t)	181.81888 kN/m
Tyre (195/65R15) Damping Coefficient (c_t)	0.0138 kN-sec/m
Radius of Gyration (r)	1.55 m
Wheel Base (b)	M

Vehicle is assumed to be traveling over a road with velocity of 40km/hr, during this travel the excitation frequency is calculated as

$$f = \frac{2\pi V}{\lambda} = \frac{2 \times \pi \times 40 \times 1000}{6 \times 2600} = 11.6 \text{ rad/sec} = 1.85 \text{ Hz}$$

III. NON-LINEARITY IN SUSPENSION SPRING

The non-linear effects included in the spring force f_s are due to two parts. One is bump stop which restricts the wheel travel within the given range and prevents the tire from contacting the vehicle body. And the other is strut bushing which connects the strut with the body structure and reduces the harshness from the road input. This non-linear effect can be included in spring force f_s with non-linear characteristic versus suspension rattle space from the measured data on SPMD (Suspension Parameter Measurement Device) shown in Fig.2.

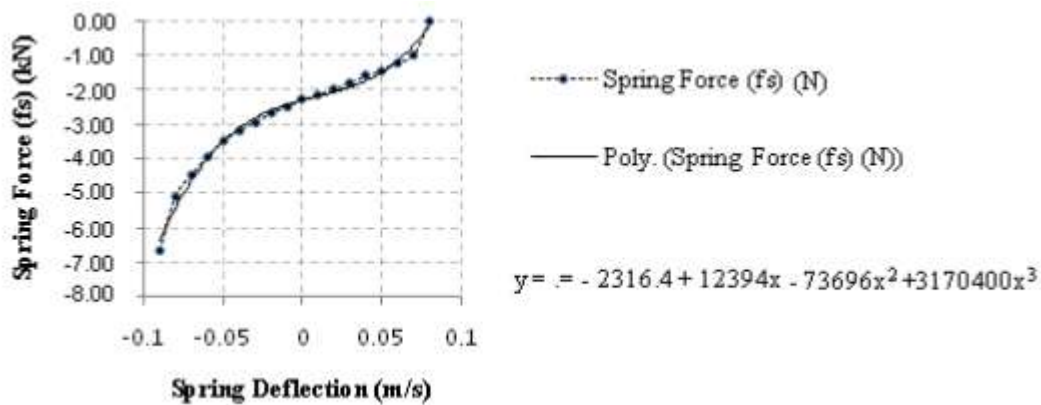


Fig2. Non-linear Spring Force Property of Hyundai Elantra 1992 Model Suspension Spring

The spring force f_s is modeled as third order polynomial function.

$$f_s = k_0 + k_1 \Delta x + k_2 \Delta x^2 + k_3 \Delta x^3 \tag{5}$$

Where the co-efficient are $k_0 = -2.31 \text{ kN}$, $k_1 = 12.39 \text{ kN/m}$, $k_2 = -73.69 \text{ kN/m}^2$ and $k_3 = 3170.40 \text{ kN/m}^3$ (The SPMD data from the 1992 Model Hyundai Elantra front suspension were used).

IV. NON-LINEARITY IN SUSPENSION DAMPER

Generally, the damping force is asymmetric with respect to speed of the rattle space: Damping force during bump is bigger than that during rebound in order to reduce the harshness from the road during bump while dissipating sufficient energy of oscillation during rebound at the same time. Measured data for the damping force versus relative velocity of upper and lower struts, shows the asymmetric property which is shown in Fig.3

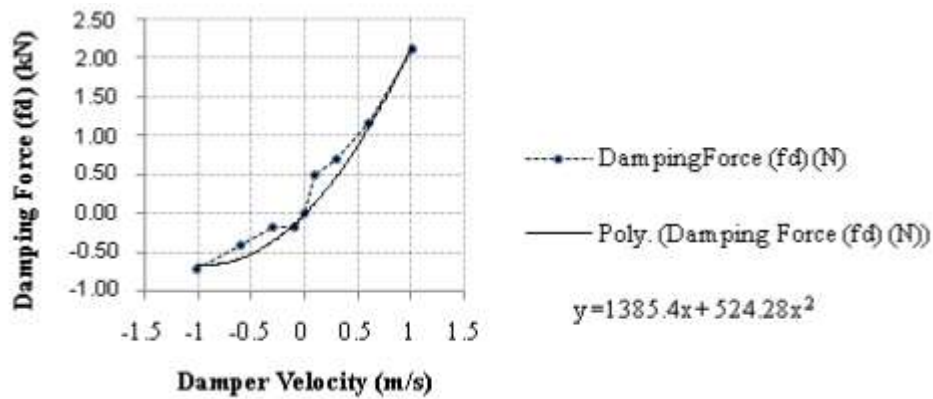


Fig.3.Non-linear Damping Force Property of Hyundai Elantra 1992 Model Suspension Damper

From the measured data the damping force f_d is modeled as second order polynomial function. The mathematical model for this is given by,

$$f_d = c_1 \Delta \dot{x} + c_2 \Delta \dot{x}^2 \quad \dots\dots\dots (6)$$

Where the coefficient are obtained from fitting the experimental data, which resulted in

$$c_1 = 1385.4 \text{ N-s/m,}$$

$$c_2 = 524.28 \text{ N-s/mand (The SPMD data from the 1992 model Hyundai Elantra front suspension were used).}$$

V. MATLAB ANALYSIS

The MATLAB/Simulink model is prepared and the sprung mass displacement and pitch for different road profiles were obtained in time domain. The sprung mass displacement and pitch for linear and non-linear passive suspension system for different road profiles are as below,

5.1 Bumpy (sinusoidal) Road Input

A single bump road input, y is described by (Jung-Shan Lin 1997), is used to simulate the road to verify the developed control system. The road input described by Eq. (7) is shown in Fig.4.

$$y = a(1 - \cos \omega t) \quad \text{for } 0.4 < t < 0.9 \quad \dots\dots\dots (7)$$

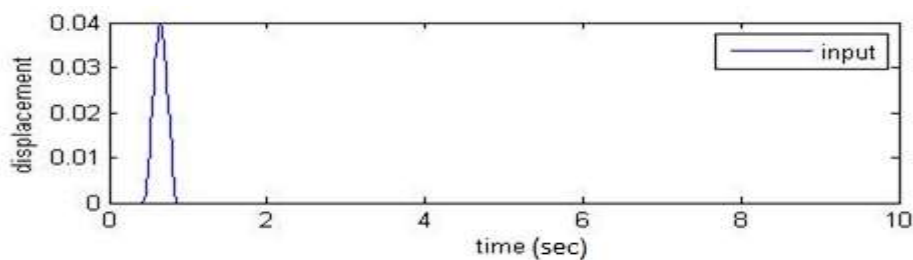


Fig.4 Bumpy Road Input

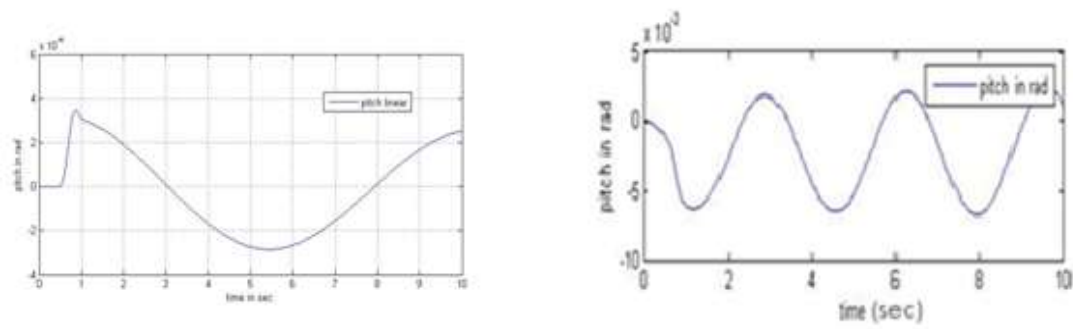


Fig.5. Pitch of Sprung Mass for Linear and Non-Linear Half Car Model

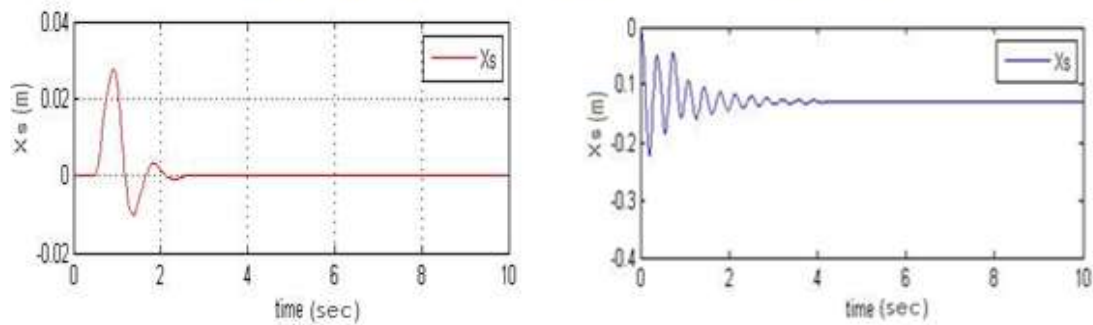


Fig.6. Sprung Mass Displacement (X_s) for Linear and Non-Linear Half Car Model

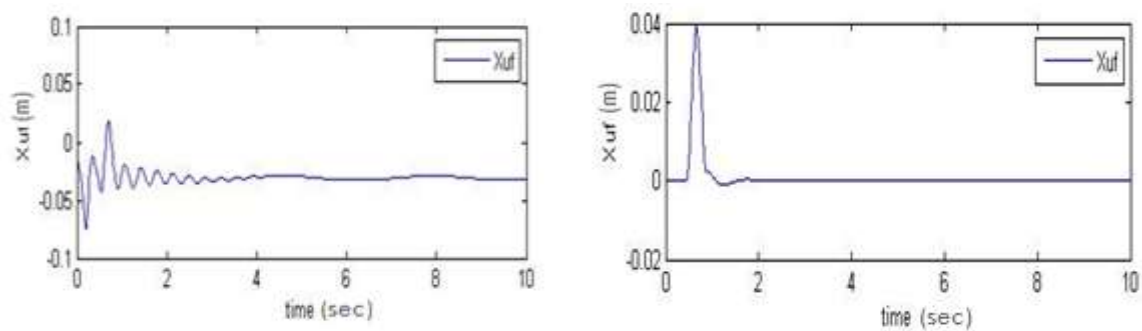


Fig.7. Unsprung Mass Displacement (X_{uf}) for Linear and Non-Linear Half Car Model

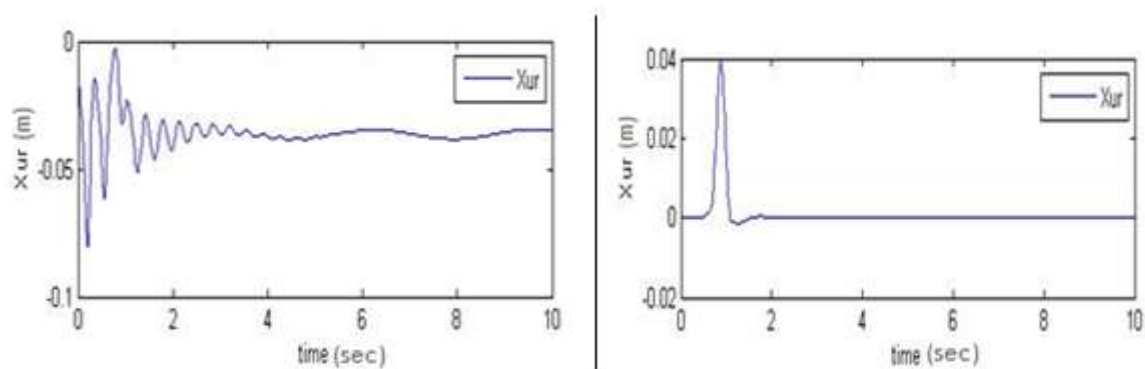


Fig.8. Unsprung Mass Displacement (X_{ur}) for Linear and Non-Linear Half Car Model

5.2 Rectangular Input

The Rectangular Pulse is represented by equation (8)

$y = -0.04$ for $0.42 < t < 0.88$,

0.00 for otherwise

.....(8)

Here also the height of the road disturbance is maintained at 4 cm. The road input is described by Eq. (8) is shown in

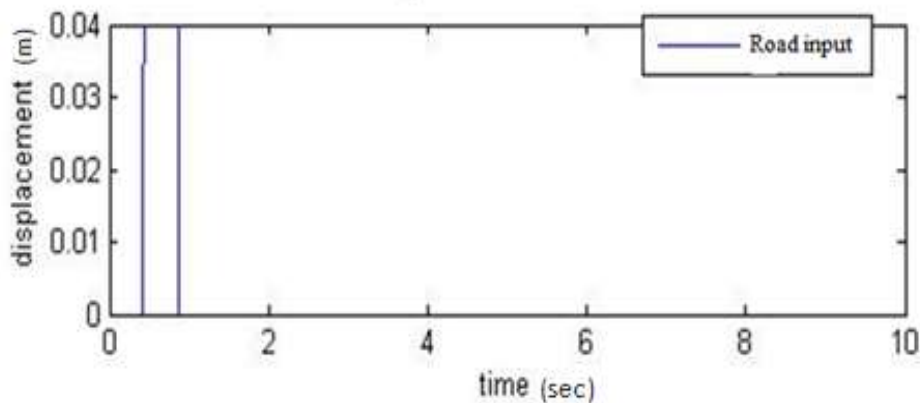


Fig.9.

Fig. 9.Rectangular Input

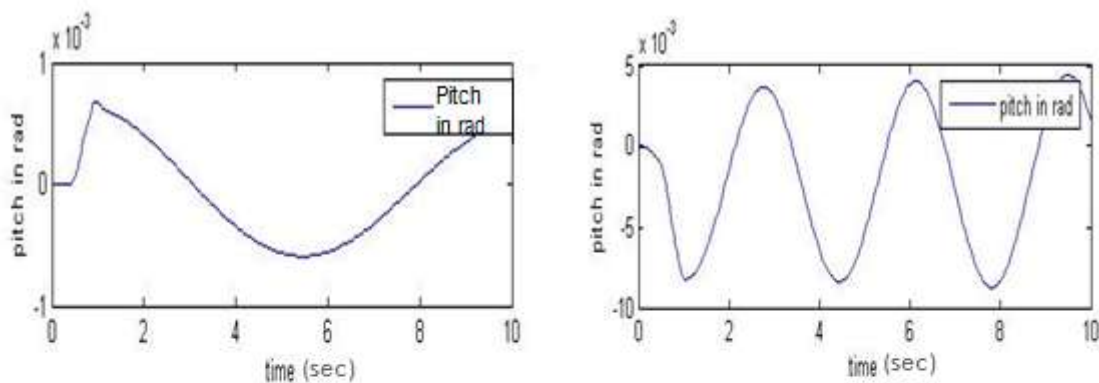


Fig.10. Pitch of Sprung Mass for Linear and Non-Linear Half Car Model

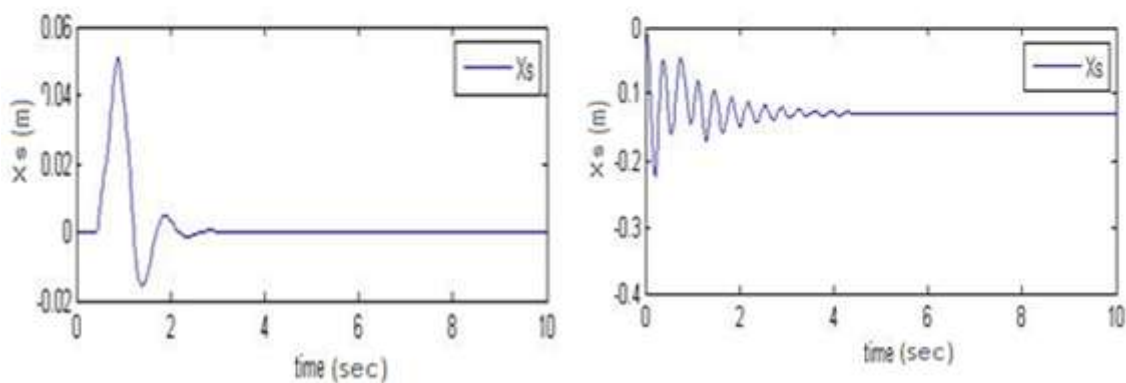


Fig.11.Sprung Mass Displacement (Xs) for Linear and Non-Linear Half Car Model

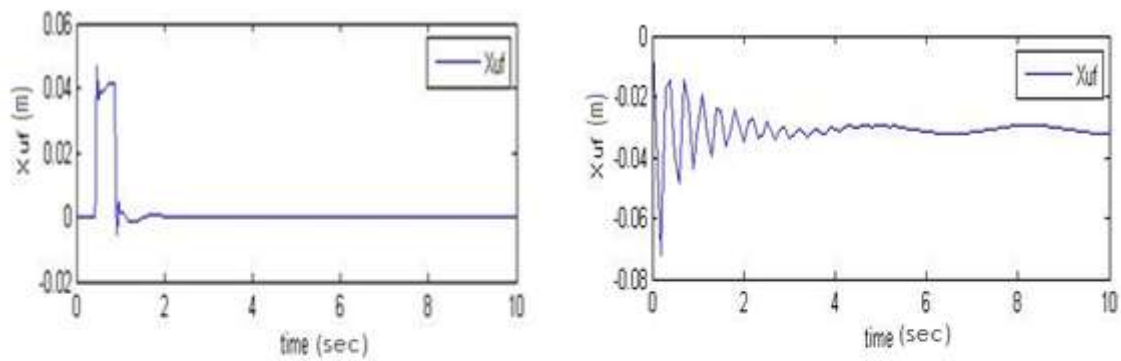


Fig.12. Unsprung Mass Displacement (Xur) for Linear and Non-Linear Half Car Model

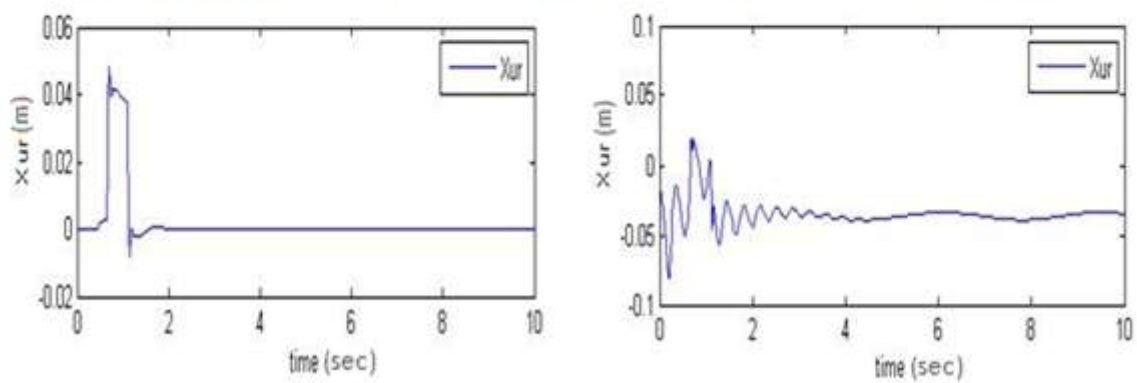


Fig.13. Unsprung Mass Displacement (Xur) for Linear and Non-Linear Half Car Model

5.3. Step Input

The Step excitation is represented by equation (9)

$$y = -0.04 \text{ for } 0.42 < t < 0.88,$$

$$0.00 \text{ for otherwise}$$

.....(9)

The road input is described by Eq. (9) is shown in Fig.14.

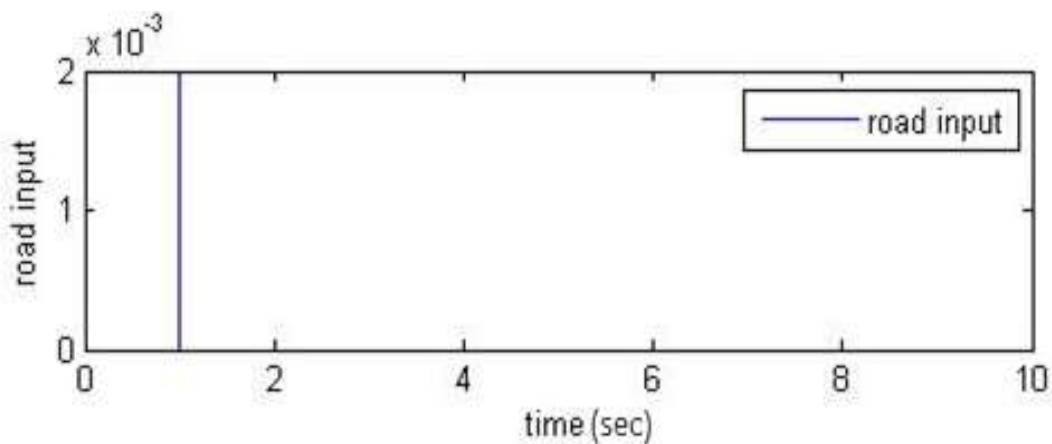


Fig.14. Step Input

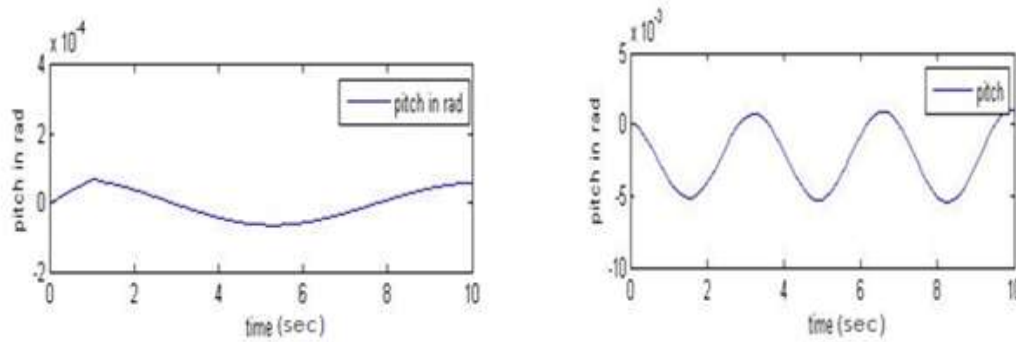


Fig.15.Pitch of Sprung Mass for Linear and Non-Linear Half Car Model

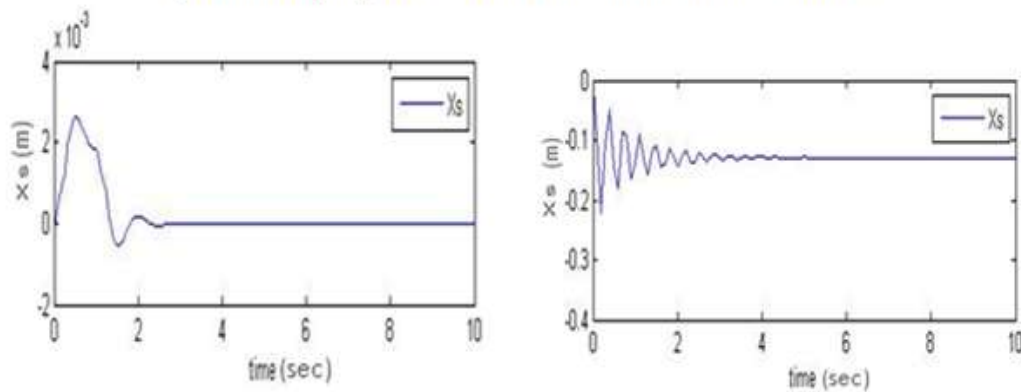


Fig.16.Sprung Mass Displacement (X_s) for Linear and Non-Linear Half Car Model

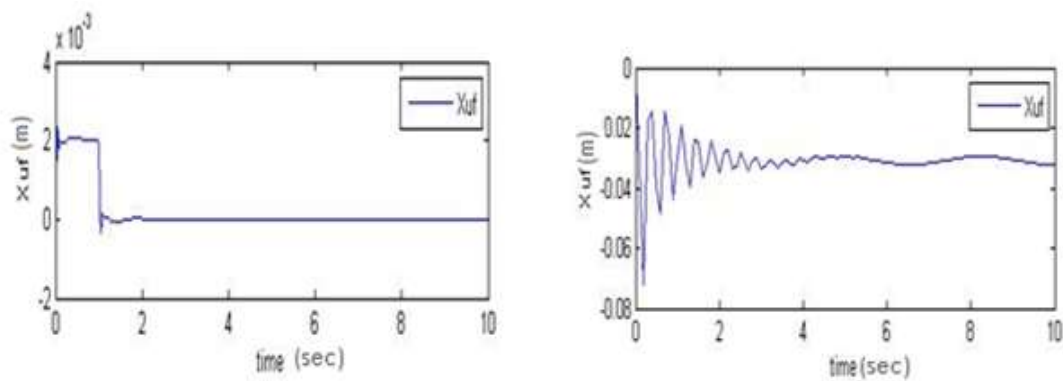


Fig.17.Unsprung Mass Displacement (X_{uf}) for Linear and Non-Linear Half Car Model

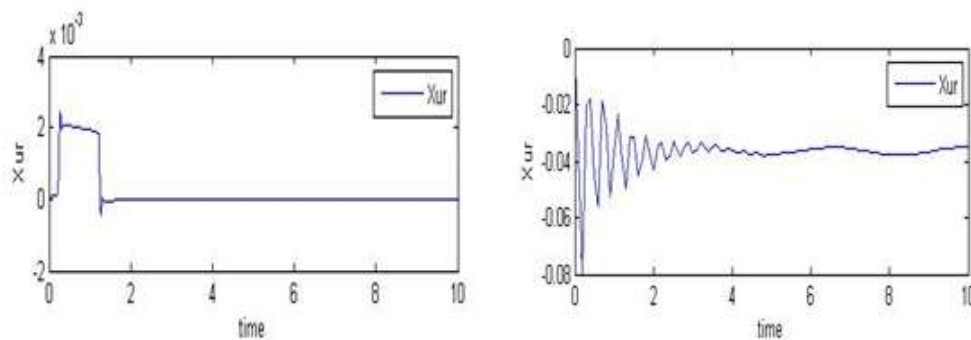


Fig.18.Unsprung Mass Displacement (X_{ur}) for Linear and Non-Linear Half Car Model

VI. CONCLUSION

From the results obtained from simulation, it is seen that in the analysis of vehicle dynamic system consideration of nonlinear parameters is important. When graph of nonlinear passive suspension system is compared to linear suspension system for different road profiles, it is seen that behavior of nonlinear passive suspension system tends to move towards the actual behavior of the system. Comfort to the passengers can be achieved by choosing proper spring and damper of the sprung mass which effects on its natural frequency. For Linear half car model Sprung mass displacement is less than for Non Linear half car model for all types of road profiles under consideration.

VII. ACKNOWLEDGEMENTS

The authors are grateful to Dr. J.J. Magdum College of Engineering, Jaysingpur for supporting this work.

REFERENCES

- [1]. Ali Mohammadzadeh, Salim Haider, "Analysis and Design of Vehicle Suspension System Using MATLAB and SIMULINK", American Society for Engineering Education, 2006.
- [2]. M. Silveira, B.R. Pontes., J. M. Balthazar, "Use of Nonlinear Asymmetrical Shock Absorber to Improve Comfort on Passenger Vehicles", Journal of Sound and Vibration 333, 2114–2129, 2014.
- [3]. Md. Zahid Hossain and Md. Nurul Absar Chowdhury, "Ride Comfort of 4 DoF Nonlinear Heavy Vehicle Suspension", ISSCO Journal of Science and Technology Volume 8-No. 13, 80-85, 2012.
- [4]. C.B. Patel, P.P. Gohil and Borhade, "Modeling and Vibration Analysis of Road Profile Measuring System", International Journal of Automotive and Mechanical Engineering (IJAME) Volume 1, pp.13-28, 2010.
- [5]. A. Mitra, N. Benerjee, H. A. Khalane, M. A. Sonawane, D. R. Joshi, "Simulation and Analysis of Full Car Model for Various Road profile on a Analytically Validated MATLAB/SIMULINK Model", IOSR Journal of Mechanical and Civil Engineering (IOSR-JMCE) ISSN(e) : 2278-1684, ISSN(p) : 2320–334X, PP : 22-33.
- [6]. Andronic Florin, Manolache-Rusuioan-Cozmin, Patuleanuliliana, "Passive Suspension Modeling using MATLAB, Quarter Car Model, Input Signal Step Type", TEHNOMUS - New Technologies and Products in Machine Manufacturing Technologies, 2013.
- [7]. Javad Marzbanrad, Masoud Mohammadi Saeed Mostaani, "Optimization of a Passive Vehicle Suspension System for Ride Comfort Enhancement with Different Speeds Based on Design of Experiment (DoE) Method", Journal of Mechanical Engineering Research, ISSN 2141-2383 © 2013 Academic Journals, DOI 10.5897/JMER10.061, Vol. 5(3), pp. 50-59, 2013.
- [8]. Prof. S. P. Chavan, Prof. S. H. Sawant, Dr. J. A. Tamboli, "Experimental Verification of Passive Quarter Car Vehicle Dynamic System Subjected to Harmonic Road Excitation with Nonlinear Parameters", IOSR Journal of Mechanical and Civil Engineering (IOSR-JMCE), ISSN: 2278-1684, PP: 39-45, 2013.

STRUCTURAL ANALYSIS OF MOTORCYCLE CHAIN BY USING C.A.E. SOFTWARE

Mr. Nikhil S. Pisal¹, Prof. V.J. Khot²

¹P.G. Student, ²Associate Professor

Mechanical Department, Dr. J. J. Magdum College of Engineering, Jaysingpur, (India)

ABSTRACT

Any catastrophic failure in the chain used in power transmission of a motorcycle could lead to a safety hazard. Determining safe load for the chain and the ability of the same to withstand the using Finite Element Modeling would be the core objective of this work. An existing chain link would be used for benchmarking the research work. Finite Element Analysis tools like HyperMesh and ANSYS are suitable to find the performance of the link under tensile loads. Recommendation over the best suited geometry or material would be presented to conclude the work.

Keyword: Chain, Chain link, Finite Element Analysis, HyperMesh, Tensile loads.

I. INTRODUCTION

A chain is a reliable machine component, which transmits power by means of tensile forces, and it used primarily for power transmission. The function and uses of chain are similar to a belt, Roller chain or bush roller chain is the type of chain drive most commonly used for transmission of mechanical power on many kinds of domestic, industrial and agricultural machinery, including conveyors, cars, motorcycles, and bicycles. It consists of a series of short cylindrical rollers held together by side links. It is driven by a toothed wheel called a sprocket. It is a simple, reliable, and efficient means of power transmission. Two different sizes of roller chain, showing construction. There are actually two types of links alternating in the bush roller chain. The first type is inner links, having two inner plates held together by two sleeves or bushings upon which rotate two rollers. Inner links alternate with the second type, the outer links, consisting of two outer plates held together by pins passing through the bushings of the inner links. The "bushing less" roller chain is similar in operation though not in construction; instead of separate bushings or sleeves holding the inner plates together, the plate has a tube stamped into it protruding from the hole which serves the same purpose. This has the advantage of removing one step in assembly of the chain [1]. The roller chain design reduces friction compared to simpler designs, resulting in higher efficiency and less wear. The original power transmission chain varieties lacked rollers and bushings, with both the inner and outer plates held by pins which directly contacts with the sprocket teeth; however this configuration exhibited extremely rapid wear of both the sprocket teeth, and the plates where they pivoted on the pins. This problem was partially solved by the development of bushed chains, with the pins holding the outer plates passing through bushings or sleeves connecting the inner plates [2]. The addition of rollers surrounding the bushing sleeves of the chain and provided rolling contact with the teeth of the sprockets resulting in excellent resistance to wear of both sprockets and chain. Roller chains are of primary importance for efficient operation as well as correct tensioning [2].

II. DESIGN CONSIDERATIONS

Roller chains are used in a wide variety of applications, but most roller chain is used in drives. The shaft speeds of the drives range from less than 50 rpm to nearly 10,000 rpm, and the amount of power transmitted ranges from a 1 kW to 1000 kW. The main design considerations for a roller chain to be used on a drive are the various tensile loads [3].

2.1 Ultimate Tensile Strength

The ultimate tensile strength of a chain is the highest load that the chain can withstand in a single application before breaking. It is not a major consideration in designing roller chains. It is only important because yield strength and fatigue strength depend on ultimate tensile strength. Minimum ultimate tensile strength (MUTS) is a requirement in the ASME standards that govern roller chains. A well-made roller chain almost always meets the standard [3].

2.2 Yield Strength

The yield strength of a chain is the maximum load from which the chain will return to its original state (length). For many standard chains, the yield strength is approximately 40% to 60% of the minimum ultimate tensile strength [3].

III. MATHEMATICAL TREATMENT

Table 1 Inputs Data for TVS 250CC Motorcycle.

Specifications of TVS 250CC	
Engine Type	Single Cylinder, 4 Stroke
Engine Displacement (CC)	250CC
Maximum Power	22kW
Speed of smaller sprocket, n_1	5000 rpm
No. of Teeth on smaller sprocket, Z_1	15
No. of Teeth on smaller sprocket, Z_2	44
Chain Pitch, p	12.7 mm
Roller diameter, d	8.51 mm
Mass of chain per meter length, m	0.7 Kg
Breaking strength of chain, WB	22 kN

Velocity of chain,

$$\begin{aligned} V &= (Z_1 \times p \times n_1)/60 \\ &= (15 \times 0.0127 \times 5000)/60 \\ V &= 15.88 \text{ m/s} \end{aligned}$$

Design Power = Rated Power $\times f_1 \times f_2 \times f_3 \times f_4$.

Service Factors:

Effect of the number of teeth of the small chain wheel (f_1) $z = 15, f_1 = 1.27$

Effect of ratio (f_2) $i = 2.93, f_2 = 1$

Effect of Shock factor (f_3) $= 1.59$

Effect of ratio of Centre distance (f_4) $= 1$

$$P = 22 \times 1.27 \times 1 \times 1.59 \times 1$$

$$P = 44.42 \text{ kW}$$

Tangential drive force on chain,

$$F_T = P/V$$

$$= 44420/15.88$$

$$F_T = 2797.23 \text{ N}$$

Centrifugal tension in chain,

$$F_C = m \times V$$

$$= 0.7 \times 15.882$$

$$F_C = 176.52 \text{ N}$$

Total tension in chain,

$$W = F_T + F_C$$

$$= 2797.23 + 176.52$$

$$W = 2973.75 \text{ N} = 3000 \text{ N (Approx.)}$$

IV. CHAIN LINK SPECIFICATIONS

Table 2 Dimensions of Chain Parts

Sr. No	Parameter	Length (mm)
1	Chain Pitch	12.7
2	Width of Inner Plate	7.75
3	Pin Height	17
4	Pin Diameter	4.45
5	Roller Outer Diameter	8.51

V. THREE DIMENSIONAL CAD MODEL

Fig. 1 shows structure of roller chain as per chain specification of chain part.

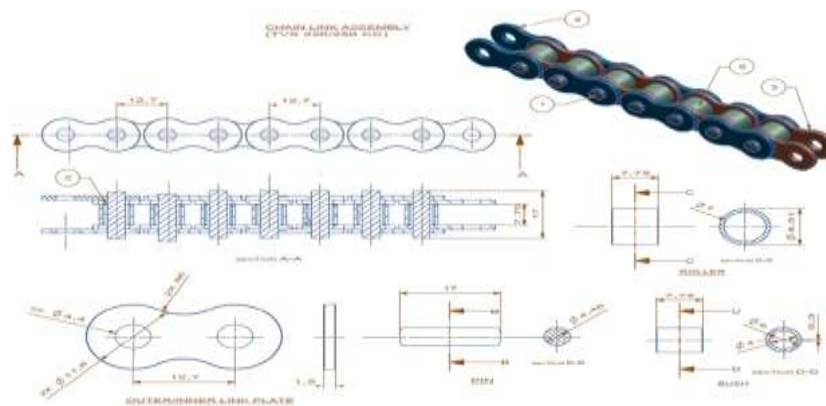


Fig. 1 Three Dimensional Model

VI. FINITE ELEMENT ANALYSIS

Numerical techniques consist of three basic steps: “pre-processor, processor and post-processor”. The pre-processing stage consists of the procedures as constituting creating the model as per dimension. In ANSYS the Cad Model of Chain link is developed. After that for analysis the Finite element model is generated In engineering data define defining material properties. In that entering the physical and material properties of the model to the software, defining the element type meshing criteria, Mesh body consisting of total solid body is created. After modeling the chain link meshing is done in ANSYS Workbench. Meshing involves converting of geometry into nodes and elements. 3D Hex Dominant mesh type is used for meshing. It has compatible displacement shapes and well suited to model curved boundaries. Chain links is done by giving element size 0.5 mm for better results. Here the number of time meshing was done i.e. at 2 mm element size, 1.5 mm element size, 1mm element size, 0.8 mm element size, 0.6 mm element size but at 0.4 mm and 0.5 mm element size the result that is stresses are does not change. Therefore element size taken as 0.5 mm for better results. At the point of application of load the fine meshing is done. After meshing total 305600 No. of Nodes and 159126 No. of Elements are obtained for chain link having inner and outer link plate thickness is 1.5 mm.

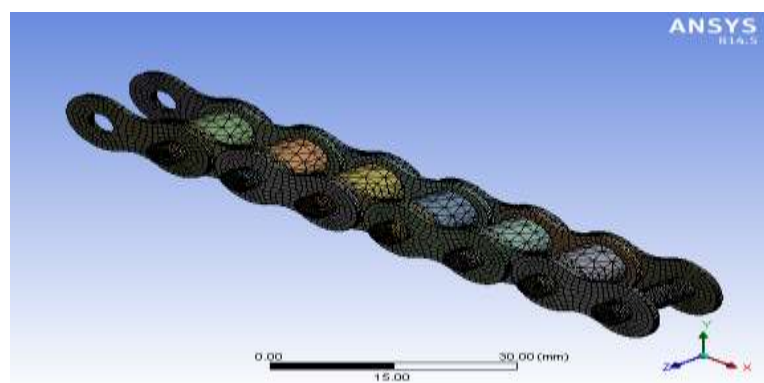


Fig. 2 Meshing of Model

After modeling of chain links then give the actual supporting boundary conditions are applied i.e. fixed support and horizontal support. In fixed support there is no any degree of freedom i.e. there is no displacement at any direction. But in horizontal support only horizontal motion is present and vertical motion is restricted. While modeling link, imprint faces are created which are useful for selecting particular faces at the time of applying

boundary condition. As shown in Fig. 3 the blue face indicates the fixed support and tensile force of 3000 N is applied to red face in X direction.

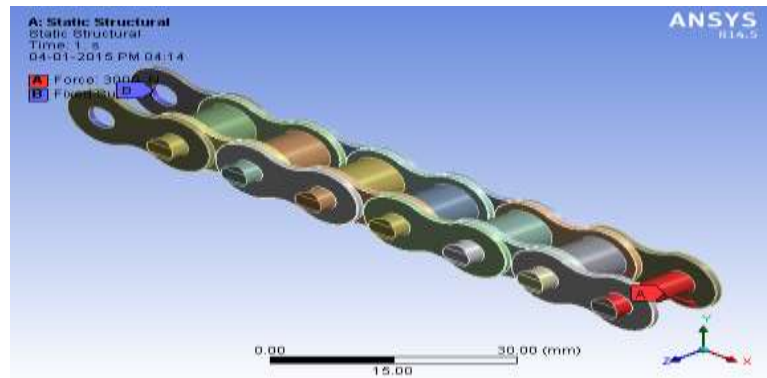


Fig. 3 Applying Boundary Condition

The FEA results of Chain link for Directional deformation, Equivalent Elastic Strain and Equivalent (von-Mises) Stress as calculated by using C.A.E. In Fig. 4 red face indicate maximum deformation occurs on pin which is 0.053343 mm and blue face indicate minimum deformation.

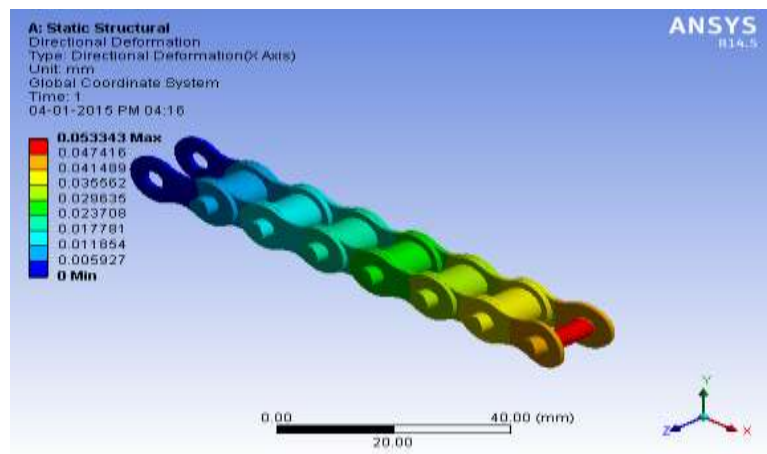


Fig. 4 Deformation in Model

The FEA results of Chain link for Equivalent Elastic Strain is maximum at roller which is 3.2184×10^{-3} mm/mm and minimum at pin 2.6212×10^{-6} mm/mm this result as shown in Fig. 5.

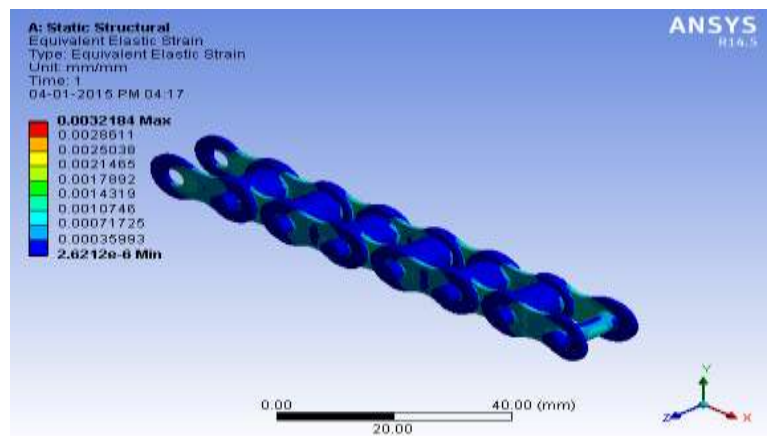


Fig. 5 Equivalent Elastic Strain in Model

The stress distribution in chain link having maximum value of stress that is 643.1 MPa at Roller and minimum value of stress that is 0.2913 MPa at Pin.

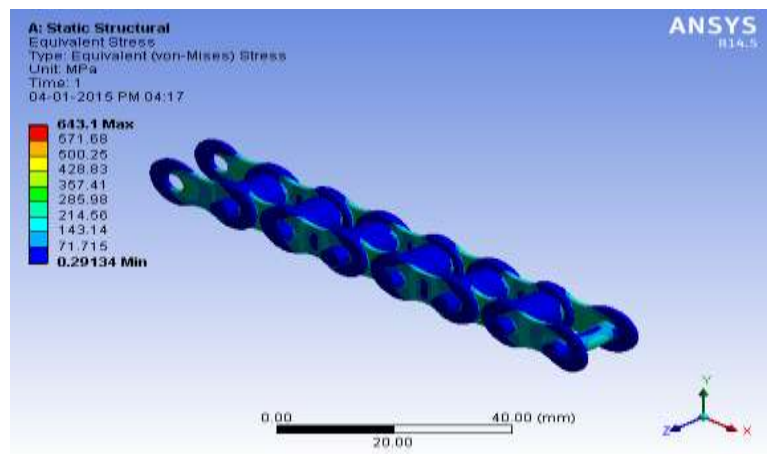


Fig. 6 Stress Distribution in Model

If the thickness were changed, other dimension would remain constant. Therefore effective weight saving would be realized. Thus stress analyzed with change in thickness of 1 mm for inner and outer link plate. The Model for thickness of 1 mm to be analyzed. Calculate result for maximum deformation occurs on pin which is 0.1162 mm and -1.1038e-002 mm minimum deformation.

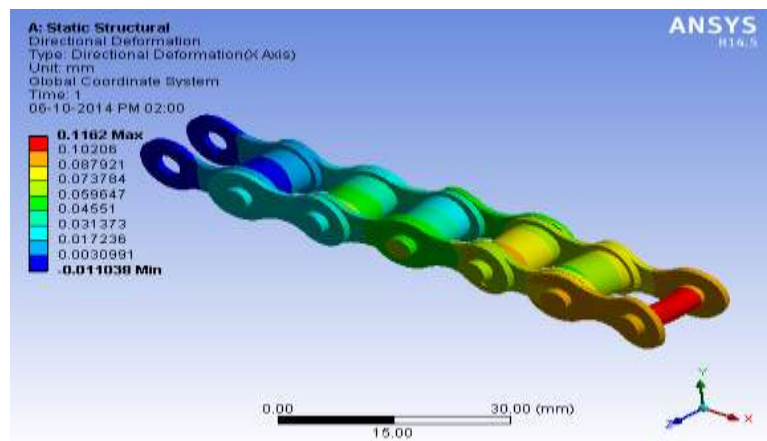


Fig. 7 Deformation in Model

The stress distribution in chain links shown in Fig. 8. Position of stress concentration is the same and maximum value of stress that is 777.25 MPa at Roller and minimum value of stress that is 1.9722e-003 MPa at Pin. The FEA results of Chain link for Equivalent Elastic Strain is maximum at Roller which is 4.0484e-003 mm/mm and minimum at Pin 9.8611e-009 mm/mm.

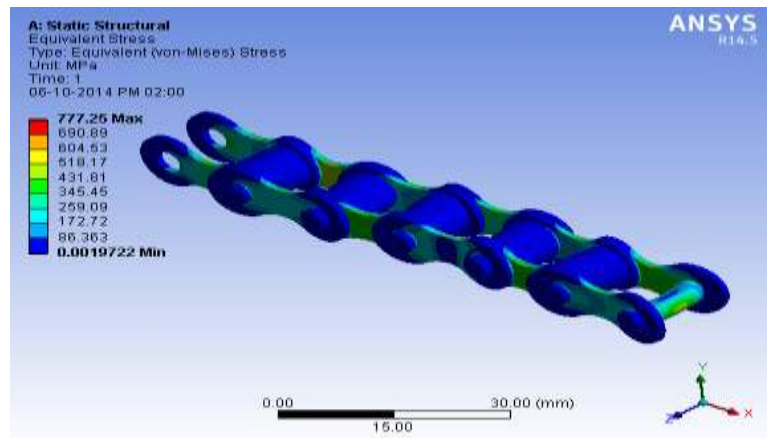


Fig. 8 Stress Distribution in Model

Table 3 Results of F.E Analysis

Thickness of Plate, mm	Maximum Tensile stress, MPa	Maximum compressive Stress, MPa	Maximum deformation	Maximum Equivalent Elastic Strain mm/mm	Minimum Equivalent Elastic Strain mm/mm
1.5	643.1	291.3e-003	0.053343	3.2184e-003	2.6212e-006
1	777.25	1.9722e-003	0.1162	4.0484e-003	9.8611e-009

VII. CONCLUSION

The design for the chain would be subjected to F.E Analysis to find the effect of loads (tension) on the link. The proposed method utilizes software in the FEA domain for analyzing the effects of the variation in the values of the design parameters influencing the performance criterion. As the thickness decreases, other dimension would remain constant. Therefore effective weight saving would be realized. If the thickness of link plate decreases to the rate of increase in tensile stress. Consequently weight saving with a decrease in the thickness of the link plate can be realized using a higher strength of material. The FEM method is used to analyze the stress state of an elastic body with a given geometry, such as chain link.

VIII. ACKNOWLEDGEMENTS

The authors are grateful to Dr. J.J.Magdum College of Engineering, Jaysingpur for supporting this work

REFERENCES

- [1] U.S. Tsubaki, *The Complete Guide to Chain* by Inc. First English-Language Edition, 1997
- [2] Fujiwara, Tanimura, Testsuo, *Bearing Roller chain*, U.S.Patent US7, 972,233, B2, Jul 2011.

- [3] Tushar D. Bhoite, Prashant M. Pawar, *Finite Element Analysis based Study of Effect of Radial Variation of Outer Link in A Typical Roller Chain Link Assembly*, *International Journal of Mechanical and Industrial Engineering (IJMIE)*, ISSN No. 2231 –6477, Vol 1, Issue4, (2012) 65-70.
- [4] M. Koray, M. Cuneýt M, Erdem C. *Stress Distribution of the Chain Link by Means of Boundary Method*”, *Journal of Engineering and Natural Sciences, Sigma 04.11.2004* 255-263.
- [5] Noguchi S., Nagasaki K., Nakayama S., Kanda T., Nishino T. and Ohtani T., *Static Stress Analysis of Link Plate Of Roller Chain using Finite Element Method and Some Design Proposals for Weight Saving*, *Journal of Advanced Mechanical Design, Systems, and Manufacturing, Vol 3.No2*, 2009, 159-170.
- [6] James C. Conwell and G.E.Johnson, *Experimental Investigation of Chain Tension and Roller Sprocket Impact Forces in Roller Sprocket Impact in Roller Chain Drive*, 1989.

Biographical Notes

Mr. Nikhil S. Pisal is presently pursuing M.E. final year in Mechanical Engineering Department (Specialization in Machine Design) from Dr. J. J. Magdum College of Engineering, Jaysingpur, India.

Mr. V. J. Khot is working as a Assistant Professor in Mechanical Engineering Department, Dr. J. J. Magdum College of Engineering, Jaysingpur, India.

SECURED DATA STORAGE ENVIRONMENT IN CLOUD COMPUTING

Naresh Sammeta¹, Dr. Latha Parthiban²

¹ *Research Scholar, Dept of Computer Science & Engg, RMKCET, Chennai, Tamilnadu, (India)*

² *Dept of CSE, Community College, Pondicherry University, Laws Pet, Pondicherry, (India)*

ABSTRACT

Cloud computing is one of today's most energizing innovations, in light of the fact that it can diminish the expense and intricacy of uses, and it is adaptable and versatile. These profits changed Cloud computing from a dreamy thought into one of the quickest developing innovations today. Really, virtualization technology is based on virtualization innovation which is an old innovation and had security issues that must be tended to before cloud technology is influenced by them. Moreover, the virtualization technology has limit security abilities so as to secure wide range environment, for example, the cloud. Consequently, the improvement of a vigorous security framework obliges changes in customary virtualization building design. This paper proposes new security building design in a hypervisor based virtualization technology so as to secure the cloud environment.

Keywords: *Cloud Computing, Hypervisor, Security, Virtualization*

I. INTRODUCTION

Cloud computing is a system built environment that centers with respect to offering processing's and assets. Really, distributed computing is characterized as a pool of virtualized machine assets. For the most part, Cloud suppliers use virtualization advances consolidated with organization toward oneself capacities for figuring assets through system frameworks, particularly the Web and different virtual machines are facilitated on the same physical server. Taking into account virtualization, the distributed computing ideal model permits workloads to be conveyed and scaled-out rapidly through the fast provisioning of Virtual Machines or physical machines. A distributed computing stage helps excess, recovering toward oneself, exceedingly adaptable programming models that permit workloads to recuperate from numerous certain fittings/programming disappointments. Subsequently, in mists, costumers pay for what they utilize and don't pay for nearby assets, for example, stockpiling or foundation. A virtual machine assuages a percentage of the eminent administration issues in light of the fact that the vast majority of the support, programming overhauls, design and other administration undertakings are computerized and brought together at the server farm by the cloud supplier in charge of them. Since virtualization is not technology and it has insufficient security abilities for wide system, for example, cloud. This paper is composed as following. Section 2 describes the virtualization approaches. Section 3 depicts connection in the middle of security and dependability in virtual situations. Section 4 present issues and assaults in security and unwavering quality of virtualization. Section 5 exhibits a novel approach with a specific end goal to secure virtualization innovation for Cloud computing. At long last, Section 6 displays the conclusions.

II. VIRTUALIZATION APPROACHES

In a conventional environment comprising of physical servers joined by a physical switch, IT associations can get definite administration data about the movement that goes between the servers from that switch. Lamentably, that level of data administration is not regularly given from a virtual switch. Essentially, the virtual switch has joins from the physical switch by means of the physical NIC that connects to Virtual Machines. The ensuing absence of oversight of the movement streams between and among the Virtual Machines on the same physical level influences security and execution studying. There are a few regular methodologies to virtualization with contrasts between how each one controls the virtual machines.

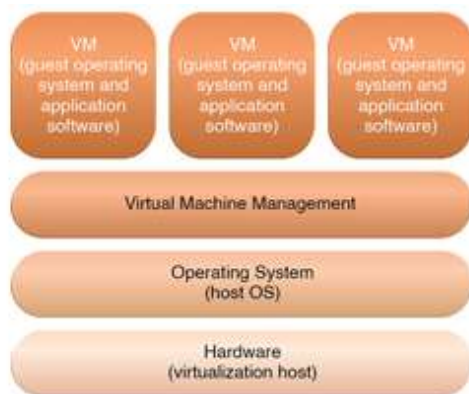


Fig. 1 Operating system-based Virtualization

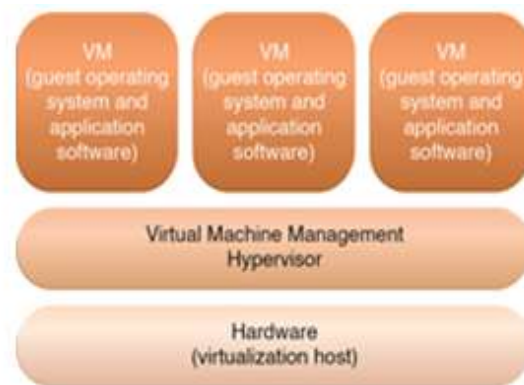


Fig. 2 Hardware-based Virtualization

2.1 Operating System-Based Virtualization

In this methodology (Fig 1), Operating system based virtualization is the establishment of virtualization programming in a prior operating system, which is known as the host operating system. Case in point, a client whose workstation has a particular rendition of Windows introduced chooses it needs to create virtual machines. It introduces the virtualization programming into its have operating system like whatever other program and uses this application to create and work one or more virtual machine. This client needs to utilize its virtualization programming to empower immediate access to any of the produced virtual machines. Since the host operating system can give equipment gadgets the vital help, operating system virtualization can correct hardware similarity issues regardless of the possibility that the equipment driver is inaccessible to the virtualization programming.

Operating system based virtualization can acquaint requests and issues related with execution overhead, for example,

- the host operating system devours CPU, memory, and other hardware IT assets.
- hardware-related calls from visitor operating systems need to navigate a few layers to and from the hardware, which diminishes general execution.
- licenses are typically needed for host operating systems, notwithstanding individual licenses for each of their visitor operating systems.

2.2 Hardware-Based Virtualization

This choice speaks to the establishment of virtualization programming specifically on the virtualization host hardware in order to sidestep the host operating system, which would probably be locked in with operating system based virtualization (Fig 2).

Permitting the virtual machines to connect with hardware without obliging mediator activity from the host operating system for the most part makes equipment based virtualization more effective. The diverse coherent layers of hardware based virtualization, which does not oblige an alternate host operating system.

2.3 Application-Based Virtualization

An application-based virtualization is facilitated on top of the facilitating working framework (Fig 3). This virtualization application then copies every VM containing its own visitor working framework and related applications. This virtualization building design is not usually utilized as a part of business situations. Security issues of this methodology are like Working framework based.

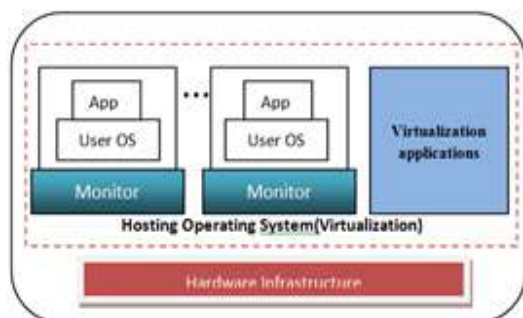


Fig. 3 Application-based Virtualization

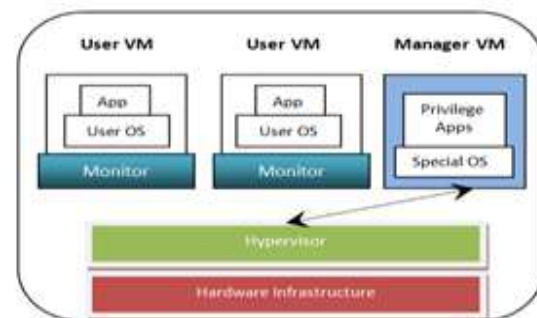


Fig. 4 Hypervisor-based Virtualization

2.4 Hypervisor-Based Virtualization

The hypervisor is accessible at the boot time of machine so as to control the imparting of framework assets crosswise over different VMs. Some of these VMs are advantaged allotments which deal with the virtualization stage and facilitated Virtual Machines. In this structural planning, the special parcels view and control the Virtual Machines.

This methodology creates the most controllable environment and can use extra security instruments, for example, interruption location frameworks [1]. Nonetheless, it is defenseless in light of the fact that the hypervisor has a solitary purpose of disappointment. On the off chance that the hypervisor crashes or the assailant additions control over it, then all VMs are under the aggressor's control. Be that as it may, taking control over the hypervisor from the virtual machine level is troublesome, however not outlandish. As indicated by this trademark, this layer picked for actualizing proposed security structural planning.

III. VIRTUAL MACHINES SECURITY

As specified in the recent past, there are no less than two levels of virtualization, Virtual Machines and the hypervisor. Virtualization is not as new an technology as cloud, however it contains a few security issues that have now moved to cloud innovation. Additionally, there are different vulnerabilities and security issues which are interesting to cloud environment or may have a more discriminating part in cloud.

3.1 Hypervisor Security

In a virtualization environment, there are a few Virtual Machines that may have free security zones which are not open from other virtual machines that have their own zones. A hypervisor has its own security zone, and it is the controlling operators for everything inside the virtualization host. Hypervisor can touch and influence all demonstrations of the virtual machines running inside the virtualization host [3]. there are various security zones, however these security zones exist inside the same physical base that, in a more customary sense, just exists inside a solitary security zone. This can result in a security issue when an aggressor takes control over the hypervisor. At that point the aggressor has full control over all information inside the hypervisor's region. An alternate real virtualization security concern is "getting away from the Virtual Machine" or the capacity to achieve the hypervisor from inside the Virtual Machine level. This will be significantly to a greater degree a worry as more Apis are made for virtualization stages [4]. As more Apis are made, so are controls to handicap the usefulness inside a Virtual Machine that can decrease execution and accessibility.

3.2 Benefits and Weakness of Hypervisor-Based Systems

The hypervisor, separated from its capacity to oversee assets, can possibly secure the foundation of cloud. Hypervisor-based virtualization innovation is the best decision of actualizing routines to attain to a safe cloud environment. The explanations behind picking this innovation:

- hypervisor controls the fittings, and it is best way to get to it. This ability permits hypervisor-based virtualization to have a protected framework. Hypervisor can go about as a firewall and will have the capacity to keep malignant clients to from trading off the fittings base.
- hypervisor is executed underneath the visitor OS in the distributed computing chain of importance, which implies that if an assault passes the security frameworks in the visitor OS, the hypervisor can recognize it.
- the hypervisor is utilized as a layer of reflection to detach the virtual environment from the equipment underneath.
- the hypervisor-level of virtualization controls all the right to gain entrance between the visitors' Oss and the imparted fittings underside. In this way, hypervisor has the capacity improve the exchange observing process in the cloud environment.

3.3 Security Management in Hypervisor-Based Virtualization

As specified in the recent past, hypervisor is administration instruments and the fundamental objective of making this zone is fabricating a trust zone around fittings and the VMs. Other accessible Virtual Machines are under the probation of the hypervisor, and they can depend on it, as clients are assuming that chairmen will do what they can to do give security. There are three noteworthy levels in security administration of hypervisor as said beneath:

- **Authentication:** clients must confirm their record legitimately, utilizing the fitting, standard, and accessible components.
- **Authorization:** clients must secure approval and must have consent to do all that they attempt to do.
- **Networking:** the system must be composed utilizing instruments that guarantee secure associations with the administration application, which is probably found in an alternate security zone than the common client.

IV. THREATS AND ATTACKS IN VIRTUALIZATION

4.1 Threats

In the hypervisor, all clients see their frameworks as independent machines detached from different clients, despite the fact that each client is served by the same machine. In this connection, a Virtual Machine is a working framework that is overseen by a basic control program.

virtual machine level assaults: Potential vulnerabilities are the hypervisor or Virtual machine technology utilized by cloud sellers are a potential issue in multi-occupant building design [8]. These innovations include "virtual Machines" remote variants of conventional on location machine frameworks, including the equipment and working framework.

4.2 Attacks

These days, there are a few assaults in the IT world. Fundamentally, as the cloud can offer administration to lawful clients it can likewise administration to clients that have pernicious purposes. A programmer can utilize a cloud to have a malignant application for accomplish his article which may be a DDOS assaults against cloud itself or orchestrating an alternate client in the cloud. For instance an assailant realized that his exploited person is utilizing cloud seller with name X, now aggressor by utilizing comparable cloud supplier can portray an assault against his victim(s). This circumstance is like this situation that both aggressor and victimized person are in same system however with this distinction that they utilize virtual machines rather than physical system (Fig 5) [9].

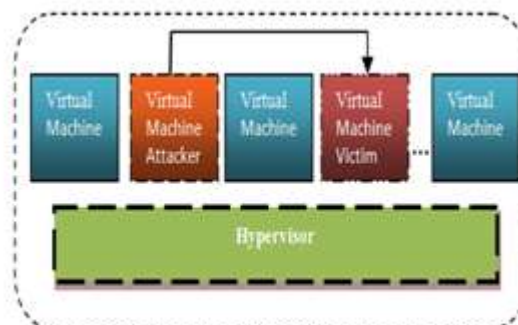


Fig. 5 Attack Scenario within Cloud

4.3 DDOS Attacks

Distributed Denial of Service (DDOS) assaults regularly concentrate high amount of IP bundles at particular system passage components; generally any type of equipment that works on a Blacklist example is rapidly invaded. In distributed computing where base is imparted by expansive number of VM customers, DDOS assaults make have the capability of having much more prominent effect than against single tenanted architectures. On the off chance that cloud has not sufficient asset to give administrations to its VMs then perhaps cause undesirable DDOS assaults. Answer for this occasion is a conventional arrangement that is increment number of such basic assets. In any case genuine issue is the point at which a noxious client deliberately done a DDOS assaults utilizing bot-nets. It might be more exact to say that DDOS security is a piece of the Network Virtualization layer as opposed to Server Virtualization. For instance, cloud frameworks use virtual machines can be overcome by ARP satirizing at the system layer and it is truly about how to layer

security crosswise over multivendor systems, firewalls and burden parities.

4.4 Client To Client Attacks

One malevolent virtual machine could contaminate all Virtual Machines that exist in physical server. An assault on one customer VM can escape to other VM's that facilitated in the same physical, this is the greatest security chance in a virtualized environment. At the point when vindictive client puts the spotlight on virtual machines get to be not difficult to get to, the assailant needs to invest time assaulting one virtual machine, which can prompt contaminating different VMs, and along these lines getting away from the hypervisor and getting to nature level that formally it can't open from VM level. Subsequently, the real security chance in virtualization situations is "customer to customer assaults". In this assault an aggressor gets the executive benefits on the foundation level of virtualization environment and after that can get to all VMs. On the off chance that the programmer could likewise get control of the hypervisor and he possesses all information transmitting between the hypervisor and VMs and he can perform assaults, for example, a parodying assault.

V. PROPOSED ARCHITECTURE

In this paper, a few peculiarities are added to virtualization structural technology to enhance security for cloud environment. Also two fundamental units of proposed building design are focused around this truth."At the point when the workload of the VM increments strangely, the VM may be a victimized person or an aggressor". In this manner, in the structural technology, extra units were included for observing the occasions and exercises in VMs, while attempting to counteract assaults without recognizing what sort of information is being transmitted between VMs or VMs and hypervisor.

5.1 Description of Proposed Architecture

For the most part, encryption is utilized by a large portion of clients and it is impractical to ask clients not to scramble their information. In the proposed building design, there are not any necessities to uncover client information or encryption key to cloud suppliers. Some new gimmicks are added to build security execution in virtualization innovation, for example, security and unwavering quality checking units (VSEM and VREM).

HSEM and HREM are the principle parts of the security framework, and the various parts of the security framework correspond with them, yet HSEM chooses if the VM is an aggressor or an exploited person. Really, HSEM gets behavioral data from VSEM and HREM and never gathers any data itself. Moreover, HSEM informs the hypervisor about which VM is under Level-2 checking with a specific end goal to set administration limits until the status is dead set. Fig 6 shows the new secure construction modeling and the new units in VMs level, VSEM and VREM, which is accessible for all VMs (furthermore in Management VM) also, There are two other new units, HSEM and HREM, which is accessible in the hypervisor level. VSEM and VREM devour low assets of the VM, yet they help to secure VMs against assaults.

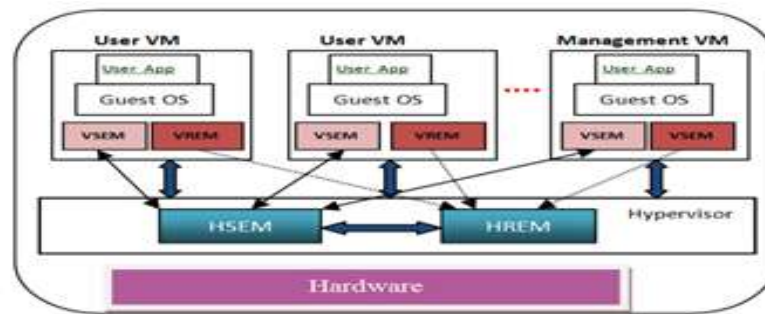


Fig. 6 Architecture of Secured Virtualization

5.2 VM Security Monitor (VSEM)

There is a VSEM inside every VM that is running in a virtual environment. These screens go about as sensors, yet are not the same as sensors. Indeed, VSEM is a two-level controller and conduct recorder in the cloud framework that helps HSEM recognize assaults and vindictive conduct with less handling. VSEM screens the security-related practices of VMs and reports them to HSEM. Since there are countless in cloud, and sending every one of them to HSEM expends a ton of data transmission and preparing assets, which can influence general hypervisor movement, a few errands were carried out by VSEMs in VMs, for example, gathering data that is asked by HSEM. Furthermore, on the grounds that clients would prefer not to expend their assets, which they paid for it, VSEMs have two levels of checking that devour more asset just when it is fundamental. Really, each one level of VSEM is checked just about the same occasions yet at diverse subtle element levels.

1) Level 1

In this level, the VSEMs screen their own VMs. In this level VSEM gathers of the source and objective locations which are in head of information, number of unsuccessful and fruitful tries in sending information, and number of demands that were sent to the hypervisor. At this level, VSEM, as per the concise history of the VM which gave by HSEM, looks for oddity conduct (HSEM has had history of VMs in more points of interest). Case in point, the framework recognizes the VM as a potential assailant or exploited person if the quantity of administration solicitations from the hypervisor is higher than normal focused around the historical backdrop of appeals of the VM. In the event that anomalous conduct is located, or the sort of sending information and unsuccessful tries increment over that limit (as per history of the VM), then VSEM changes to Level 2 furthermore advise HSEM about this exchanging keeping in mind the end goal to HSEM researches the VM for discovering malevolent exercises.

2) Level 2

In this level, the VSEM screens and catches the movement of the VM in more detail, for example, VM's exceptional solicitation from the hypervisor, points of interest of asked for assets (e.g. the quantity of solicitations), and the end of the line transmitted bundles (to perceive on the off chance that it is in the same supplier's surroundings or outside). In this mode VSEM advises HSEM about the level of checking in the VM. As per this notice, the hypervisor set movement restrains in sorts of exercises until HSEM discovers that the VM is not an assailant or victimized person. At this level, HSEM makes an appeal from VREM about the unwavering quality status of the VM, including the workload status and how often the VM workload was near to the most extreme limit of the VM.

5.3 VM Reliability Monitor (VREM)

VREM screens dependability related parameters, for example, workload, and tells the heap balancer (inside the hypervisor) about the parameter results. VREM is additionally utilized for security purposes. The VREM will send helpful data, for example, workload status to HREM and solicitations the status of the VM from HSEM, and after that it chooses whether to give the VM more assets. Really, if the VM asks for the greatest number of assets as it can (that is distinctive conduct as indicated by its utilization history), it may mean a flood assault exploited person. In this way, proposed HREM can distinguish flood assaults and tell the HSEM about it.

VI. CONCLUSION

In this paper, the proposed virtualization structural technology is utilized to secure cloud and attempt to diminish the workload, decentralize security-related undertakings in the middle of hypervisor and VMs, and proselyte the brought together security framework to a dispersed one. The disseminated security framework is a decent approach to decrease the workload from hypervisor-based virtualization, yet this circulation may infuse vulnerabilities to cloud. Moreover, appropriated security frameworks have more many-sided quality than unified ones. As a result of a few advantages, for example, the flaw tolerant capacity, of appropriated security administration, it is unrealistic to disregard it and continue on unified overseeing, however it is imperative to utilize a disseminated administration unit with consideration carefully. Really, in cloud there are part clients and their application that are running however security is essential for every one of them. The cloud must work legitimately and makes an insusceptible environment against assaults, regardless of what application is running on the cloud. In the machine world, anything makeable is fragile, on the other hand. What's more, cloud is an Internet-based innovation, and however building base of -trust cloud frameworks appeared incomprehensible. Along these lines, it appears principle territory of concern in cloud is security and cloud suppliers will confront multitudinous changes when their cloud get to be greater than now. In any case, thusly to decentralize applications and permit general access to information makes its own set of difficulties and security issues that must considered before exchanging information to a cloud. Moving to distributed computing requires the thought of a few vital elements, and the most critical of them is security.

REFERENCES

- [1] Z. Pervez, Sungyoung Lee, Young-Koo Lee. Multi-Tenant, Secure, Load Disseminated SaaS Architecture. In proceedings of the *12th Advanced Communication Technology (ICACT) International Conference*. Phoenix, USA, 2010, pp. 214 – 219.
- [2] M. P. Rad, A. S. Badashian, G. Meydanipour, M. A. Delcheg, M. Alipour, and H. Afzali, "A Survey of Cloud Platforms and Their Future," in *Lecture Notes in Computer Science*, 2009, pp. 788-796.
- [3] Sun Microsystems, Inc. Introduction to Cloud Computing Architecture. White Paper, 1st edition, June 2009.
- [4] G. Gruman and E. Knorr. What cloud computing really means. InfoWorld, April 2008. Electronic Magazine, available at http://www.infoworld.com/article/08/04/07/15FE-cloud-computin_greality1.html.
- [5] Cloud Computing, <http://www.ibm.com/ibm/cloud/>
- [6] L. Litty, "Hypervisor-based Intrusion Detection," M.S. thesis, Dept. Computer Science, University of

Toronto, 2005.

- [7] G. Rowel, "Virtualization: The next generation of application delivery challenges," 2009.
- [8] G. Texiwill, "Is Network Security the Major Component of Virtualization Security?", 2009.
- [9] D. E. Y. Sarna, *Implementing and Developing Cloud Computing Applications*: Taylor and Francis Group, LLC, 2011.
- [10] T. Ristenpart and e. al, "Hey, you, get off of my cloud: exploring information leakage in third-party compute clouds," presented at the 16th ACM conference on Computer and communications security, Chicago, IL, November 9-13, 2009.
- [11] C. Almond, "A Practical Guide to Cloud Computing Security," 2009.
- [12] F. Sabahi, "Security of Virtualization Level in Cloud Computing," in *Proc. 4th Intl. Conf. on Computer Science and Information Technology*, Chengdu, China, 2011, pp. 197-201.
- [13] P. R. Gallagher, *A Guide to Understanding Data Remanence in Automated Information Systems*: The Rainbow Books, ch.3 & ch.4, 1991.
- [14] Software Technology Institute reports, N. Mead, E. Hough, and T. Sehny, "Security quality requirements technology (SQUARE) methodology," Carnegie Mellon Software Technology Institute, 2005.
- [15] K. K. Fletcher, "Cloud Security requirements analysis and security policy development using a high-order object-oriented modeling," M.S. thesis, Dept. Computer Science, Missouri Univ. of Science and Technology, Rolla, MS, 2010.

A REPORT ON THE INCIDENCE OF MULTI DRUG RESISTANT STRAINS IN THE PROKARYOTES FROM CLINICAL SAMPLES

S. Subramani¹, M. Vigneswari²

¹ Asst. Professor, Department of Microbiology, Sourashtra College, Madurai, Tamil Nadu, (India)

² Department of Microbiology, Sourashtra College, Madurai, Tamil Nadu, (India)

ABSTRACT

This case study involved the analysis of clinical samples that were received in a commercial clinical lab over a period of two months from January 2014 to March 2014. The various samples received and processed included Urine, Stools, Pus, Endotracheal Tips, Blood and Cervical swabs. A total of 159 bacterial strains belonging to 7 different Genera namely Escherichia, Klebsiella, Staphylococcus, Pseudomonas, Proteus, Citrobacter and Acinetobacter were isolated. The prevalence of Multi Drug Resistant strains among the isolates were analysed by subjecting the isolates to antimicrobial susceptibility testing using 17 different antibiotics belonging to three different antibiotic classes namely β -lactams, Aminoglycosides and Quinolones/Fluoroquinolones. The study showed that among the test isolates the Staphylococcus sp. was recorded with maximum MDR percentage (44.44%). The other Genera in the decreasing order of count of MDR strains were E. coli (29.62%), Klebsiella (18.51%), Citrobacter sp. (3.70%), Proteus sp., (3.70%), Acinetobacter sp., (0%) and Pseudomonas sp., (0%).

Keywords: Antibiotics, Antimicrobial Susceptibility Testing, Clinical Samples, Multi Drug Resistance, Prokaryotes.

I. INTRODUCTION

Beginning around the middle of the 20th century, major advances in antibacterial drug development and other means of infection control helped humans to combat microbial diseases. With respect to bacterial infections, the situation dramatically improved when penicillin became available for use in the early 1940s. However, the euphoria over the potential conquest of infectious diseases was short lived. Almost as soon as antibacterial drugs were deployed, bacteria responded by manifesting various forms of resistance. As antimicrobial usage increased, so did the level and complexity of the resistance mechanisms exhibited by bacterial pathogens. The struggle to gain the upper hand against infections continues to this day, although the number of scientists who are developing new antibacterial agents is beginning to dwindle, even as bacteria evolve ever more clever mechanisms of resistance. One among the many reasons for why bacterial resistance should be of a concern in attempting to treat infections by antimicrobial chemotherapy is that, resistant bacteria, particularly *Staphylococci*, *Enterococci*, *Klebsiella pneumoniae*, and *Pseudomonas* sp. are becoming commonplace dwellers in healthcare institutions. [1].

II. MATERIALS AND METHODS

2.1 Isolation of Clinical Isolates

The residual clinical samples from a commercial Clinical Lab at Madurai, India, were used to screen for the presence of prokaryotic pathogens for a period of two months from January to March 2014. A total of 330 clinical samples were processed that included Urine, Stools, Pus, Blood, Endotracheal (ET) tips, Sputum and Cervical swab. The samples that resulted in no growth or had non-bacterial infectious agents' growth were not considered for the study.

Aliquots of the samples were plated on Nutrient agar (HI Media), MacConkey agar and Blood agar. The bacterial strains were identified up to generic level by employing the standard morphological and biochemical characteristics described in Bergey's manual of systematic bacteriology [2].

2.2 Antimicrobial Assay

The broth cultures of the isolates were adjusted to 0.5 McFarland standards by standard procedure and used to seed Muller Hinton agar (HI Media) plates. In order to meet the objective of the study, antibiotics that showed 'intermediately sensitive' as per CLSI standards were included in the resistant category. [3 Modified]. The antibiogram pattern of all the isolated bacterial pathogens were assayed by subjecting them to 17 different antibiotics belonging to three different antibiotic classes namely β -lactams, Aminoglycosides and Quinolones/Fluoroquinolones. The antibiotic discs used were Imipenem(10 μ g), Meropenem(10 μ g), Cefdinir(5 μ g), Cefoperazone(75 μ g), Ceftriaxone (30 μ g), Cefotaxime (30 μ g) Ceftazidime (30 μ g), Ceftrizoxime (30 μ g) and Piperacillin/Tazobactam(100 μ g/10 μ g) which belong to the β -lactam group of antibiotics, Amikacin (30 μ g), Gentamicin (10 μ g), Tobramycin(10 μ g) and Netillin (30 μ g) which belong to the aminoglycoside group of antibiotics Nitrofurantoin(300 μ g), Norfloxacin (10 μ g), Ciprofloxacin (5 μ g) and Ofloxacin (5 μ g) which belong to the Quinolone / Fluoroquinolones group of antibiotics.

2.3 MAR Index Calculation:

MAR Index values for each isolates were calculated as (a/b), where 'a' is the number of antibiotics to which the isolate is resistant and 'b' is the total number of antibiotics to which the isolate is subjected [3].

2.4 Identification of Multi Drug Resistant (MDR) Strains

Multidrug resistance is defined as resistance to all of the drugs used in at least two of the following three classes: beta lactams, aminoglycosides, and quinolones [4].

III. DISCUSSION

E. coli strains recorded the maximum number of strains that was incident in all the clinical samples (Fig. 1), but members of *Staphylococcus* recorded the maximum number of strains (44.4%) with Multi Drug Resistant (MDR) character. (Fig. 2).

An interesting feature that was observed in the study was that among the various isolates *Pseudomonas* sp. constituted only 3.77% of the total (Fig. 1). Also not a single strain among the isolates was Multi Drug Resistant strain (Fig. 2). This observation is in black and white contrast with the reports of [5], who had commented that

Pseudomonas strains are known for its intrinsic resistance to a variety of antimicrobial agents and its ability to develop multidrug resistance (MDR) [5].

A study on the Multiple Antibiotic Resistance (MAR) Index value of the isolates revealed that all the 159 bacterial strains isolated had an MAR index > 0.2 (Table I-Table VII). An MAR Index value > 0.2 is an amount of antibiotic resistance considered characteristic of point-source pollution [6].

IV. CONCLUSION

The results of two-month study concludes that among the seven different bacterial genera isolated from various clinical samples, *E. coli* was the greatest in number (40.8%) to be isolated from all the samples. The other genera that were isolated in the decreasing order of incidence were *Staphylococcus sp.* (28.3%), *Klebsiella sp.* (14.6%), *Proteus sp.* (7.5%), *Pseudomonas sp.* (3.7%), *Acinetobacter sp.* (3.1%) and *Citrobacter sp.* (2.5%). Analysis of the Multi Drug Resistant character in the isolates revealed that the *Staphylococcus* isolates ranked the top of the list with maximum percentage of MDR strains (44.44%). *Acinetobacter sp.* and *Pseudomonas sp.* had no MDR strains. All the isolated strains had an MAR index > 0.2 which flashes light on the prevalence of bacterial strains that would have originated due to severe antibiotic abuse.

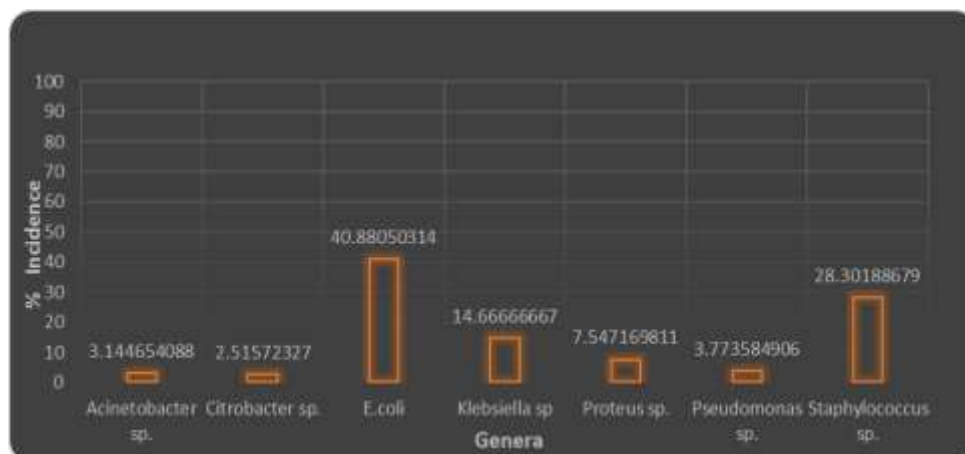


Fig.1. Percentage Incidence of the Various Bacterial Genera from the Clinical Samples

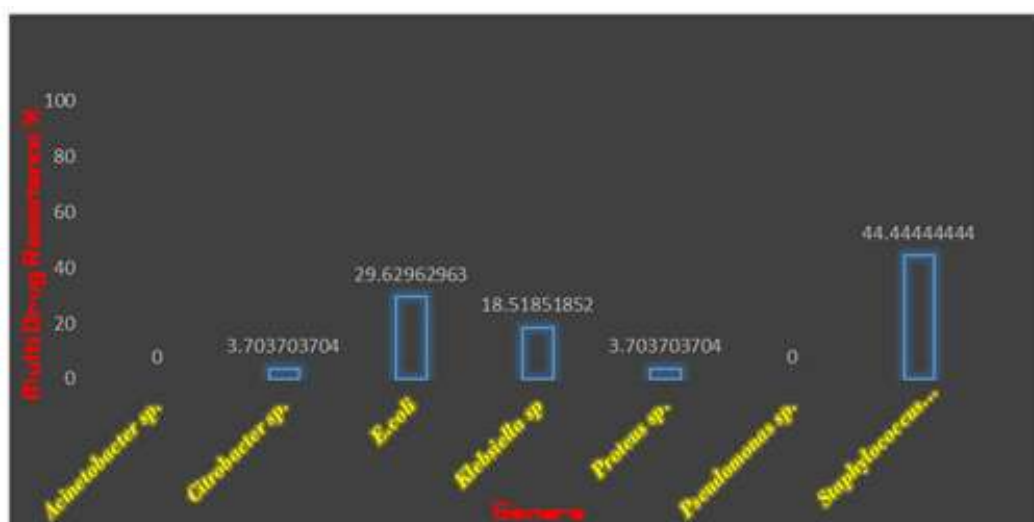


Fig.2. Percentage Occurrence of MDR Strains among the Isolated Genera

Fig.2. Percentage Occurrence of Mult Drug Resistant (MDR) strains among the isolates



Table I. Antibiogram And MAR Index Of The Various *E. coli* Isolates. The Blue Band Indicate MDR Strains

Isolate	BETA-LACTAMS								AMINOGLYCOSIDES				QUINOLONES				MAR Index	
	IPM	MHP	CDR	CPZ	CTR	CTX	CST	CDM	PIT	AK	GEN	TOR	NET	NA	NR	CP		CX
1	S	R	R	S	R	S	R	R	S	S	R	S	S	R	R	S	R	0.58
2	S	R	R	S	R	R	R	R	S	S	S	S	S	R	R	S	R	0.52
3	R	R	R	S	R	S	R	R	S	S	S	S	S	R	R	S	R	0.52
4	S	R	R	S	R	R	R	R	S	S	S	S	S	R	R	S	R	0.52
5	R	S	R	R	R	S	S	R	R	R	S	S	R	R	R	S	R	0.64
6	R	S	R	R	R	S	S	R	R	R	S	S	R	R	R	S	R	0.64

Table II. Antibiogram and MAR Index of the various *Pseudomonas* isolates.

Isolate	BETA-LACTAMS								AMINOGLYCOSIDES				QUINOLONES				MAR Index	
	IPM	MHP	CDR	CPZ	CTR	CTX	CST	CDM	PIT	AK	GEN	TOR	NET	NA	NR	CP		CX
1	S	R	R	S	R	S	R	R	S	S	S	S	R	R	R	S	S	0.47
2	S	R	R	S	R	R	R	R	S	S	S	S	S	R	R	S	R	0.52
3	S	R	R	S	R	R	R	R	S	S	S	S	S	R	R	S	R	0.58
4	S	R	R	S	R	R	R	R	S	S	S	S	S	R	R	S	R	0.47
5	S	R	R	S	R	R	R	R	S	S	S	S	S	R	R	S	R	0.64
6	R	R	R	S	R	R	R	R	S	S	S	S	S	R	R	S	R	0.7
7	R	R	R	S	R	R	R	R	S	S	S	S	S	R	R	S	R	0.7
8	S	S	R	S	R	S	S	R	S	S	S	S	S	R	R	S	S	0.29
9	S	S	R	S	R	S	R	R	S	S	S	S	S	R	R	S	S	0.52
10	S	R	R	S	R	R	R	R	S	S	S	S	S	R	R	S	S	0.52
11	S	R	R	S	R	R	R	R	S	R	S	S	S	R	R	S	R	0.7
12	S	R	R	S	R	R	R	R	S	R	S	S	S	R	R	S	R	0.76

Table III. Antibiogram and MAR Index of the various *Proteus* Isolates. The Blue band indicates MDR Strain.

Isolate	B-LACTAMS									AMINOGLYCOSIDES				QUINOLONES				MAR Index
	IPM	MRP	CDR	OPZ	CTR	CTX	CTZ	CZX	PII	AK	GEN	TOB	NET	NA	NX	OP	OX	
1	S	R	R	S	R	S	R	R	S	S	S	R	R	R	R	R	R	0.64
2	S	R	R	R	S	R	R	R	S	S	S	S	S	S	S	S	S	0.41
3	R	R	R	S	R	R	R	R	R	S	S	S	R	R	R	R	R	0.82
4	R	S	R	S	R	S	R	S	S	R	R	R	R	R	R	R	R	0.7

Table IV. Antibigram and MAR Index of the various *Citrobacter* Isolates. The Blue band indicates MDR Strain.

Isolate	B-LACTAMS									AMINOGLYCOSIDES				QUINOLONES				MAR Index
	IPM	MRP	CDR	OPZ	CTR	CTX	CTZ	CZX	PII	AK	GEN	TOB	NET	NA	NX	OP	OX	
1	R	R	S	S	R	R	R	R	S	S	R	S	S	R	R	R	S	0.58
2	S	R	R	R	R	R	R	R	S	S	R	S	S	R	R	R	R	0.7
3	R	R	R	S	R	R	R	R	S	S	S	S	S	S	R	S	R	0.52
4	S	S	R	R	R	R	R	R	R	S	S	R	S	R	R	R	R	0.7
5	R	R	R	S	R	R	R	R	S	S	S	S	S	S	R	S	R	0.52

Table V. Antibigram and MAR Index of the various *Klebsiella* Isolates. The Blue band indicates MDR Strains.

Isolate	B-LACTAMS									AMINOGLYCOSIDES				QUINOLONES				MAR Index
	IPM	MRP	CDR	OPZ	CTR	CTX	CTZ	CZX	PII	AK	GEN	TOB	NET	NA	NX	OP	OX	
1	R	R	R	R	R	R	R	R	R	R	R	R	R	R	R	R	R	0.4
2	R	R	R	R	R	R	R	R	R	R	R	R	R	R	R	R	R	0.94
3	R	R	R	R	R	R	R	R	R	R	R	R	R	R	R	R	R	0.82
4	R	R	R	R	R	R	R	R	R	R	R	R	R	R	R	R	R	0.64
5	R	R	R	R	R	R	R	R	R	R	R	R	R	R	R	R	R	0.7
6	R	R	R	R	R	R	R	R	R	R	R	R	R	R	R	R	R	0.7
7	R	R	R	R	R	R	R	R	R	R	R	R	R	R	R	R	R	0.76
8	R	R	R	R	R	R	R	R	R	R	R	R	R	R	R	R	R	0.7
9	R	R	R	R	R	R	R	R	R	R	R	R	R	R	R	R	R	0.58
10	R	R	R	R	R	R	R	R	R	R	R	R	R	R	R	R	R	0.64
11	R	R	R	R	R	R	R	R	R	R	R	R	R	R	R	R	R	0.52
12	R	R	R	R	R	R	R	R	R	R	R	R	R	R	R	R	R	0.58
13	R	R	R	R	R	R	R	R	R	R	R	R	R	R	R	R	R	0.64
14	R	R	R	R	R	R	R	R	R	R	R	R	R	R	R	R	R	0.64
15	R	R	R	R	R	R	R	R	R	R	R	R	R	R	R	R	R	0.76
16	R	R	R	R	R	R	R	R	R	R	R	R	R	R	R	R	R	0.41
17	R	R	R	R	R	R	R	R	R	R	R	R	R	R	R	R	R	0.58
18	R	R	R	R	R	R	R	R	R	R	R	R	R	R	R	R	R	0.88
19	R	R	R	R	R	R	R	R	R	R	R	R	R	R	R	R	R	0.7
20	R	R	R	R	R	R	R	R	R	R	R	R	R	R	R	R	R	0.64
21	R	R	R	R	R	R	R	R	R	R	R	R	R	R	R	R	R	0.82
22	R	R	R	R	R	R	R	R	R	R	R	R	R	R	R	R	R	0.64
23	R	R	R	R	R	R	R	R	R	R	R	R	R	R	R	R	R	0.7
24	R	R	R	R	R	R	R	R	R	R	R	R	R	R	R	R	R	0.7
25	R	R	R	R	R	R	R	R	R	R	R	R	R	R	R	R	R	0.82
26	R	R	R	R	R	R	R	R	R	R	R	R	R	R	R	R	R	0.5
27	R	R	R	R	R	R	R	R	R	R	R	R	R	R	R	R	R	0.76
28	R	R	R	R	R	R	R	R	R	R	R	R	R	R	R	R	R	0.64
29	R	R	R	R	R	R	R	R	R	R	R	R	R	R	R	R	R	0.58
30	R	R	R	R	R	R	R	R	R	R	R	R	R	R	R	R	R	0.82
31	R	R	R	R	R	R	R	R	R	R	R	R	R	R	R	R	R	0.82
32	R	R	R	R	R	R	R	R	R	R	R	R	R	R	R	R	R	0.64
33	R	R	R	R	R	R	R	R	R	R	R	R	R	R	R	R	R	0.76
34	R	R	R	R	R	R	R	R	R	R	R	R	R	R	R	R	R	0.58
35	R	R	R	R	R	R	R	R	R	R	R	R	R	R	R	R	R	0.52
36	R	R	R	R	R	R	R	R	R	R	R	R	R	R	R	R	R	0.7
37	R	R	R	R	R	R	R	R	R	R	R	R	R	R	R	R	R	0.82
38	R	R	R	R	R	R	R	R	R	R	R	R	R	R	R	R	R	0.76
39	R	R	R	R	R	R	R	R	R	R	R	R	R	R	R	R	R	0.7
40	R	R	R	R	R	R	R	R	R	R	R	R	R	R	R	R	R	0.5
41	R	R	R	R	R	R	R	R	R	R	R	R	R	R	R	R	R	0.7
42	R	R	R	R	R	R	R	R	R	R	R	R	R	R	R	R	R	0.64
43	R	R	R	R	R	R	R	R	R	R	R	R	R	R	R	R	R	0.94
44	R	R	R	R	R	R	R	R	R	R	R	R	R	R	R	R	R	0.64

Table VI. Antibigram and MAR Index of the various *Staphylococcus* Isolates. The Blue band indicates MDR Strains.

Isolate	β-LACTAMS								POLYGLYCOLAMIDES				QUINOLONES				MAR Index
	IPM	MRP	CDR	CFZ	CTH	CTR	CTZ	CZE	PET	AK	GEN	TOR	NET	NA	AK	OP	
1	S	R	S	R	R	S	R	R	S	S	S	S	S	S	S	S	0.35
2	S	R	R	R	R	R	R	R	R	R	R	R	R	R	R	R	0.88
3	S	R	R	S	R	R	R	R	S	S	S	S	S	R	S	S	0.52
4	S	R	R	R	R	R	R	R	R	R	R	R	R	R	R	R	0.76
5	S	R	R	S	R	R	R	R	R	R	R	R	R	R	R	S	0.76
6	S	R	R	R	R	R	R	R	R	R	R	R	R	R	R	R	0.82
7	S	R	R	R	R	R	R	R	S	S	S	S	S	R	R	R	0.7
8	S	R	R	R	R	R	R	R	S	S	S	S	S	R	R	R	0.58
9	S	R	R	S	R	S	R	R	S	S	S	S	S	S	R	R	0.47
10	S	R	R	R	R	R	R	R	S	S	S	S	S	R	R	R	0.58
11	S	R	R	S	R	R	R	R	S	S	S	S	S	R	S	R	0.47
12	R	R	R	S	R	R	R	R	S	S	S	S	S	R	R	S	0.58
13	R	R	R	R	R	R	R	R	S	S	S	S	S	R	S	S	0.7
14	R	R	R	R	R	S	R	R	S	S	S	S	S	R	S	S	0.58
15	R	R	R	R	R	R	R	R	S	S	S	S	S	R	R	R	0.82
16	R	R	R	R	R	R	R	R	S	S	S	S	S	R	R	R	0.88
17	S	S	R	R	R	S	R	R	S	S	S	S	S	R	R	S	0.52
18	R	R	R	R	R	R	R	R	S	S	S	S	S	R	R	R	0.52
19	S	S	R	R	S	R	R	R	S	S	S	S	S	R	S	S	0.58
20	S	S	R	S	R	R	R	R	S	S	S	S	S	R	R	S	0.7
21	R	R	R	R	R	R	R	R	S	S	S	S	S	R	R	R	0.88
22	S	S	R	S	R	R	R	R	S	S	S	S	S	R	R	R	0.52

Table VII. Antibiogram and MAR Index of the various *Acinetobacter* Isolates.

REFERENCES

[1] Tenover, C. Fred. 2006. Mechanisms of Antimicrobial Resistance in Bacteria. The American Journal of Medicine, 119: S3-S10.

[2] Holt, J. G., Kreig, N. R., Sneath, P. H. A., Staley, J. T and Williams, S. T., 1994, In Bergey’s manual of determinative Bacteriology 9th edition, Williams and Wilkins, Maryland, USA.

[3] Tambekar D. H. Dhanorkar D. V., Gulhane S. R. Khandelwal V. K and Dudhane M. N., 2006, African Journal of Biotechnology, 5(17), 2006, 1562-1565.

[4] Dominic Hill, Barbara Rose, Aniko Pajkos, Michael Robinson, Peter Bye, Scott Bell, Mark Elkins, Barbara Thompson, Colin MacLeod, Shawn D. Arone and Colin Harbour, Journal of Clinical Microbiology, 43(10), 2005, 5085-5090.

[5] Thilo Kohler, Mehri Michea hamzhepour, Patrick Plesiat, Annie Lise Kahr and Jean Claude Pechere, 1997, Antimicrobial Agents and Cemothrapy, 41(11), 2540-2543.

[6] Azar Dokht Khosravi, Najmeh Parhizgari, Effat Abbasi Montazeri, Alireza Mozaffari and Fariba Abbasi, “The Prevalence of Bacteria Isolated From Endotracheal Tubes of Patients in Golestan Hospital, Ahvaz, Iran, and Determination of Their Antibiotic Susceptibility Patterns”, Journal of Microbiology, 6(1), 2013, 67-71.